INFORMATION TO USERS

This manuscript has been reproduced from the microfilm master. UMI films the text directly from the original or copy submitted. Thus, some thesis and dissertation copies are in typewriter face, while others may be from any type of computer printer.

The quality of this reproduction is dependent upon the quality of the copy submitted. Broken or indistinct print, colored or poor quality illustrations and photographs, print bleedthrough, substandard margins, and improper alignment can adversely affect reproduction.

In the unlikely event that the author did not send UMI a complete manuscript and there are missing pages, these will be noted. Also, if unauthorized copyright material had to be removed, a note will indicate the deletion.

Oversize materials (e.g., maps, drawings, charts) are reproduced by sectioning the original, beginning at the upper left-hand corner and continuing from left to right in equal sections with small overlaps. Each original is also photographed in one exposure and is included in reduced form at the back of the book.

Photographs included in the original manuscript have been reproduced xerographically in this copy. Higher quality 6" x 9" black and white photographic prints are available for any photographs or illustrations appearing in this copy for an additional charge. Contact UMI directly to order.

UMI

A Bell & Howell Information Company
300 North Zeeb Road, Ann Arbor MI 48106-1346 USA
313/761-4700 800/521-0600

Université d'Ottawa · University of Ottawa

MIGRATION OF OIL IN ARTIFICIAL ISLANDS AND BEHAVIOUR OF OIL CONTAMINATED SAND-STEEL INTERFACES

by

Alain-Claude Megnolo Mabia

A Thesis
submitted to the School of Graduate Studies and Research
under the supervision of

Dr. Erman Evgin

in partial fulfillment of the requirements for the degree of Master in Applied Sciences in Civil Engineering

Department of Civil Engineering
University of Ottawa
Ottawa, Ontario
Canada
March 1997

The Master in Applied Sciences in Civil Engineering is a joint program between Carleton University and the University of Ottawa, which is administered by the Ottawa-Carleton Institute for Civil Engineering

© 1997 Alain-Claude Megnolo Mabia, Ottawa, Ontario, Canada

National Library of Canada

Bibliothèque nationale du Canada

Acquisitions and Bibliographic Services

Acquisitions et services bibliographiques

395 Wellington Street
Ottawa ON K1A 0N4
Canada

395, rue Wellington
Ottawa ON K1A 0N4
Canada

Your file Votre référence

Our file Notre référence

The author has granted a non-exclusive licence allowing the National Library of Canada to reproduce, loan, distribute or sell copies of this thesis in microform, paper or electronic formats.

L'auteur a accordé une licence non exclusive permettant à la Bibliothèque nationale du Canada de reproduire, prêter, distribuer ou vendre des copies de cette thèse sous la forme de microfiche/film, de reproduction sur papier ou sur format électronique.

The author retains ownership of the copyright in this thesis. Neither the thesis nor substantial extracts from it may be printed or otherwise reproduced without the author's permission.

L'auteur conserve la propriété du droit d'auteur qui protège cette thèse. Ni la thèse ni des extraits substantiels de celle-ci ne doivent être imprimés ou autrement reproduits sans son autorisation.

0-612-26350-9

Canada

ACKNOWLEDGMENTS

I would like to express my sincere thanks to Dr. E. Evgin for his continuous encouragement and suggestions throughout this research.

DEDICATION

This thesis is dedicated to my parents. Mr. and Mrs. Mabia.

TABLE OF CONTENTS

LIST OF FIGURES

LIST OF TABLES

SUMMARY

Exploration wells have been drilled in the Canadian Beaufort Sea, using artificial islands. Basically, an artificial island consists of a caisson retained structure made of steel or concrete and filled with a sand core. These structures are often built on top of a sand berm overlying Sea bed soils. It has been acknowledged that during exploration of oil, it is possible that oil could spill on top of the sand filled core if a blowout occurs. During a blowout, oil will tend to migrate downward and thus contaminate the soil mass. The interface between the soil and the structural material would be contaminated as well. The oil industry claimed that the oil would be contained in the soil mass during a blowout. This lead to the motivation of the present study.

The first objective of this research is to investigate experimentally whether the oil would migrate downward in the soil mass and eventually continue upward and contaminate the water surrounding the artificial island. The second objective is to determine the response of the oil contaminated interface between the soil and the structural material to the applied load. For these reasons, this thesis is composed of two parts. Part I is dealing with an experimental investigation of oil migration in an artificial island and Part II is related to the mechanical behaviour of an oil contaminated interface between a steel plate and sand.

In part I, it was anticipated that if oil would migrate in the soil, the migration process would start from the sand filled core to the sand berm and eventually continue upward to the sea surface. In this process oil migration follows a J-shaped path. For this reason, laboratory experiments on soil columns were performed using three Plexiglass tubes assembled in a J-shaped appearance. The contaminant used in this experiment was Motormaster grade 50 oil because crude oil similar to the one at Beaufort Sea were not available. Since the soil properties of Ukalerk (Beaufort Sea) and Carp Airport were similar, Carp Airport sand was used for the purpose of this experiment. The acquisition

of the data included the date, the time, the location of oil front in the tube and the volume of oil and water displaced. This experiment showed that there was a possibility that oil would contaminate the Sea if a massive blowout occurs, since a portion of the contaminant was recovered at the other end of the J-tube. The time required for oil to travel in the J-tube was 3 months. But in real life with the dimensions of the full scale structure, with the same soil and the same contaminant, the time required for oil to contaminate the sea was evaluated to be 3 years and 10 months if 2 m of oil was left on top of the sand filled core.

Following the results of the oil migration in the artificial island, the mechanical behavior of the oil contaminated interface between the steel plate and sand was investigated in Part II. The newly developed C3DSSI (cyclic three-dimensional simple shear interface) testing machine, designed by Evgin and Fakharian, was used to perform a series of monotonic interface tests for both clean and oil contaminated sand. A medium crushed quartz sand (silica-24) was used. Four set of tests were carried out with clean dense sand, oil-contaminated dense sand, loose clean sand, and oil-contaminated loose sand. To prepare dense sand samples, the multiple sieving pluviation method (MSP) was used. Loose sand samples were obtained through the scooping method. Oil-contaminated samples were prepared by pouring a known volume of oil in the direct shear box, before placing the sand either in a dense or loose state. After placing the interface sample in the machine, a normal stress was applied. The normal stress ranged from 30-500 kPa. After application of the normal stress, the sample was subjected to horizontal shearing at a rate of 1.0 mm/ minute. From the test results obtained, it was found that the peak strength and the interface friction angle between the structural material and the soil would be reduced as a results of oil contamination. In addition the strain softening behavior of dense clean samples disappeared due to oil contamination. Oil-contaminated samples experienced a larger volume compression than clean samples, which were subjected to an important amount of dilation after a substantial initial compression. Because of these changes, the response of the caisson retained structure to the applied load would change due to oil contamination of interfaces between the soil and the structural materials.

CHAPTER 1

INTRODUCTION

1.1 Statement of Problem

For the last two decades, exploration wells have been drilled in the Canadian offshore. The oil potential in the Labrador sea for instance, has been evaluated to be twenty-six billion barrels. At $ 15/barrel, the value of this resource would be $390 billion. The existence of oil in the offshore has been known to the Canadian oil industry for several decades and the increase in demand have encouraged oil companies and government officials to develop this source of energy. It is anticipated that economic benefit would be overwhelming if oil production becomes a reality. To explore for oil, various drilling platforms have been used in the Canadian offshore, such as drillships and artificial islands. It has been recognised that during exploration and production of oil, there should be prudent regard for possible oil spills. Inspite of extreme care, serious blowouts from both exploration and production wells have occurred (Environment Canada, 1979).

The present investigation is concerned with oil migration in soils and the mechanical behaviour of oil contaminated interfaces. The possibility of contamination of hydraulic fills will also be evaluated. Very little is known about the response of piles in the case of contaminated interfaces. Since most of offshore oil structures are supported on piles (Chan and Hanna, 1980), the need to study the behaviour of contaminated interfaces is therefore important. What would happen in a caisson retained island if a massive oil spill occurred? Would there be any contamination of the water surrounding the artificial island? What would be the response of soil-structure systems such as axially loaded piles in case of oil contamination of interface and the soil mass?

Oil migration through unsaturated soils have been investigated in the past. Recent experiments were conducted at Utah State University by Ajit et al. (1994) to determine the mobility of oil through the unsaturated zone of a soil. Their studies have provided information on the influence of parameters governing the oil migration process in the subsurface environment, such as viscous gravitational (including buoyancy) and capillary forces, oil saturation, percolation rates, hydraulic conductivities, moisture content of soil, and pressure distribution. Various graduate students at the University of Ottawa including Ben Amor (1990) and Farah (1992) have presented data concerning oil contamination of sand. Additional studies on the topic was provided by Evgin et al. (1995). These studies have concluded that some strength parameters of sand were influenced by oil contamination. Thus, the effect of oil should be considered in the design of soil-structure systems such as shallow and deep foundations, retaining walls, tunnels and cavities, short dams-abutment junctions, axially loaded piles, and anchors in sea beds.

In the design of foundations, or other structures that are in direct contact with soil, there is always an interaction between the soil and solid face where the forces are transmitted through a layer of soil next to the contact surface, which is called the interface. At the interface many activities can take place, namely relative motions, stress concentrations and drastic changes in displacement gradients. In the past, various devices were used in two- and three-dimensional monotonic tests, to study experimentally the behaviour of contact surfaces between two dissimilar materials such as soil and a structural material.

A simple shear apparatus was developed recently by Evgin and Fakharian (1996) to study the behaviour of interfaces. The simple shear apparatus is capable of measuring the sliding displacement between the soil and the structural material in addition to measuring the tangential displacements resulting from the deformation of the soil mass.

Fakharian and Evgin (1996) also used a direct shear apparatus. The displacements measured by the direct shear device do not separate the displacements due to the deformation of the sand mass and the displacement at the interface.

Yoshimi and Kishida (1981) used a ring torsion type device which has the ability to eliminate and to avoid non-uniformity of normal and shear stresses in the sample.

All these aforementioned experimental studies have provided the required information for a better understanding of the load-deformation behaviour of interfaces. Properties such as relative density, moisture content, roughness of the structural material, roundness of the sand particles, and rate of shearing are known to influence the response of an interface to loading.

1.2 Objectives

The main objectives of this dissertation are as follows:

1. To investigate experimentally the migration of oil in sand.

2. To determine whether the oil would contaminate the water surrounding the caisson retained artificial islands in the event of a massive blowout.

3. To determine the differences in the behavior of clean and oil contaminated interfaces between sand and a steel plate under constant normal loading conditions in two-dimensional monotonic tests.

1.3 Scope of Research

To achieve the objectives, the steps listed below are followed.

1. Review the literature for multiphase flow in porous media to understand the mechanisms of oil migration in soils.

2. Conduct a laboratory experiment with scaled Plexiglas columns to collect data on oil migration. Use Carp Airport (Ottawa) sand and Motomaster oil grade 50.

3. Conduct a series of monotonic two-dimensional interface tests under constant normal stress conditions using a crushed silica (clean and oil contaminated) sand and a structural material (sand-blasted steel). The need to study two-dimensional monotonic tests stems from the fact that the working piles supporting the artificial island may be subjected to constant loading.

1.4 Outline of Thesis

Chapter 2 discusses the types of drilling platforms used in the Canadian offshore including causes of blowout during exploration of oil and sources of oil contamination in the subsurface environment.

Chapter 3 presents a review of multiphase flow in porous media.

Chapter 4 presents the description of the laboratory experiment of oil migration in Plexiglas columns and provides the data base.

Chapter 5 describes the interface tests including the sample preparation and test apparatus. The results of two-dimensional monotonic interface tests under various constant normal stresses are discussed in this chapter.

Chapter 6 presents a discussion and concluding remarks

CHAPTER 2

DRILLING SYSTEMS AND BLOWOUTS

2.1 Introduction

Exploration of oil in the Canadian Sea is usually done through drilling systems such as artificial islands and drillships. In general the technology, procedures, and development methods employed by both drilling systems are basically the same. Irrespective of the drilling system used, it has been acknowledged that blowouts have occurred and unfortunately will continue to occur during the production and exploration of oil. In this chapter, artificial islands and drillships systems will be briefly presented. Also, sources of oil contamination will be discussed.

2.2 Artificial Islands

In the Canadian Sea, most artificial islands are built using a flat-sided (1:6-1:8) subsea sand berm on which a steel or concrete caisson is placed. Various methods have been used to place the hydraulic sand fills. The most common techniques used to place hydraulic sand fills in the Beaufort Sea were bottom dumping and pipeline placements.

Clark and Jordaan (1987) reported that 25 % of arctic offshore islands have experienced unexpected geotechnical problems. It has been acknowledged that the placement technique has a great impact on the in situ density. Over the past years several cases of failure of artificial islands have been reported and in the majority of these failure. liquefaction was the cause. In 1988, it was reported that liquefaction occurred in some parts of the fill material in the case of Molikpaq. an offshore platform located in the Canadian Beaufort Sea. To provide assurance against liquefaction. Sladen and Hewitt (1989) stated that the sand berm of the artificial must meet rigorous gradation and in situ density specifications. Figure 2.1 shows the schematic representation of an artificial island in the Beaufort Sea.

The results obtained by (Sladen and Hewitt, 1989) from many artificial islands constructed in the Canadian Beaufort sea have concluded that the relative densities of materials placed by dumping were 20-30 % higher than pipelines placed materials. Hence the performance of platforms constructed with material placed by bottom dumping are more reliable. But in an event of a blowout, the strength and deformation properties of these materials has to be re-investigated because the soils would be oil contaminated.

2.3 Drillships

Drillship systems consist of a drillship and ice-class towing vessels. During the exploration of oil. the main problem experienced by drillships is the iceberg threat. To avoid iceberg threats, ice-class towing vessels accompany drillships. These ice-class vessels have towing equipment on board to divert iceberg from a safety region around the drilling operation. Drillships are capable of drilling in water depth up to 350 m. with wells as deep as 8000 m. Figure 2.2 shows the schematic representation of the dynamic positioning of drillingship offshore Labrador.

2.4 Blowouts

Offshore blowout can occur during either exploration or production of oil. A study conducted by Environment Canada (1979) in the Labrador Sea concluded that blowouts can occur if the blowout preventor (BOP) valves (see Figure 2.2) fails to operate properly, due to mechanical problems for instance. A blowout can be controlled by either closing the cap of the well head or by simply drilling a relief well. A relief well is usually used to contain an original well proven to be uncontrollable. Figure 2.3 shows a relief well drilling. During a blowout fluid may migrate toward the sea water surface, or under water, either in the reservoir pipe or at the sea floor itself. If the fluid come out of the ground from the outside of the casing pipe lining the well, this phenomenon is known as cratered blowout. During a cratered blowout a significant amount of oil can be lost if the problem is not solved immediately. This was the case in Santa Barbara, California spill of 1969 (Environment Canada, 1979), where an estimated 13000 tones of oil was lost into the sea over a period of three months. Apart from blowouts occurring in drilling systems there are other sources of oil contamination.

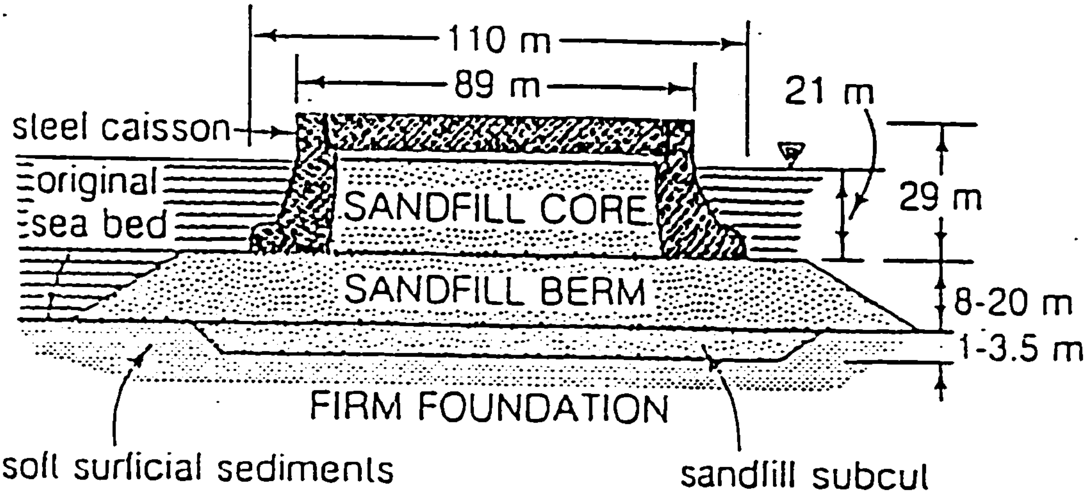

Figure 2.1 Schematic representation of the Molikpaq structure. (After Sanderson, 1988)

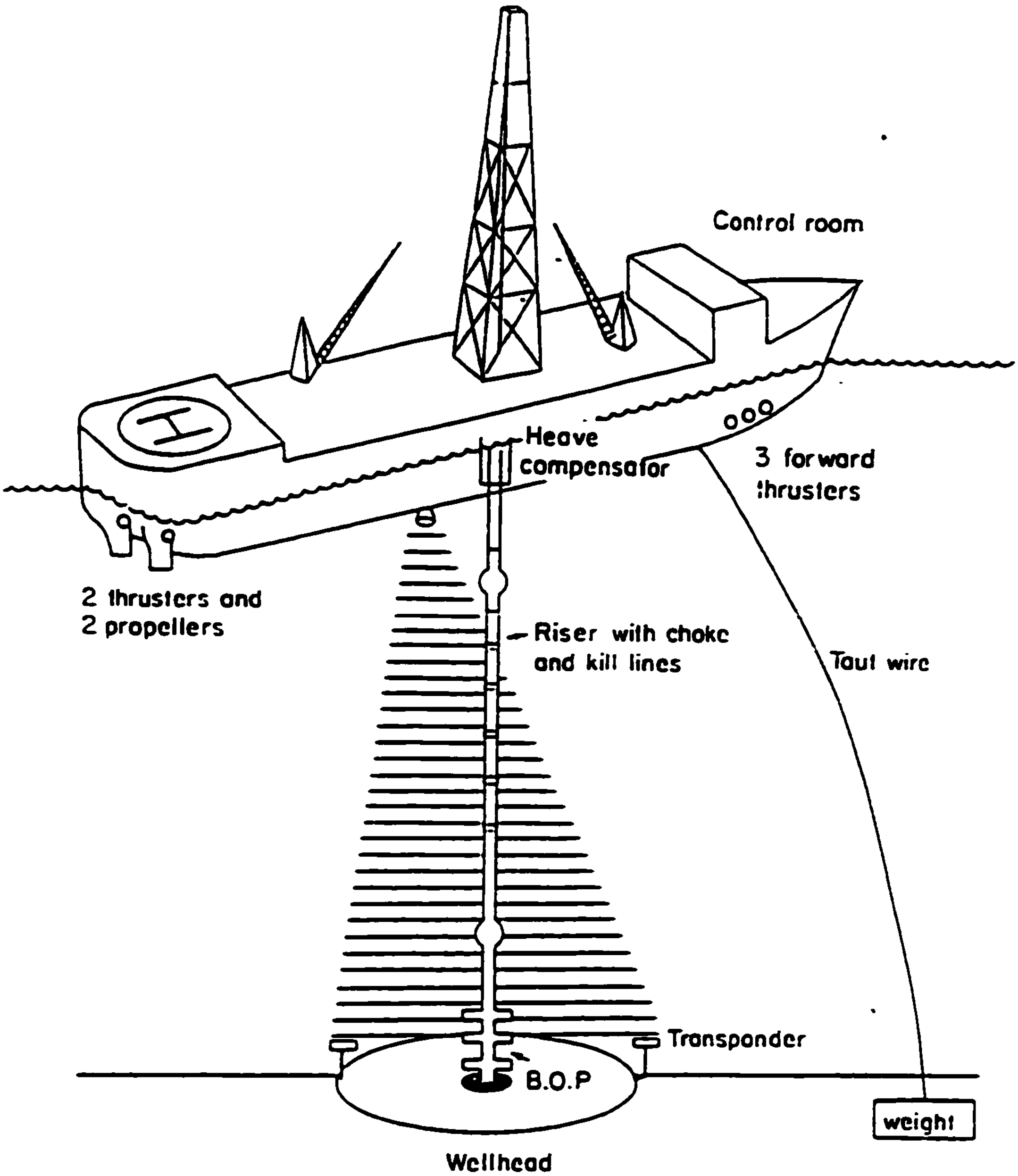

Figure 2.2 Schematic representation of the dynamic positioning of drillship offshore Labrador. (Environment Canada, 1979).

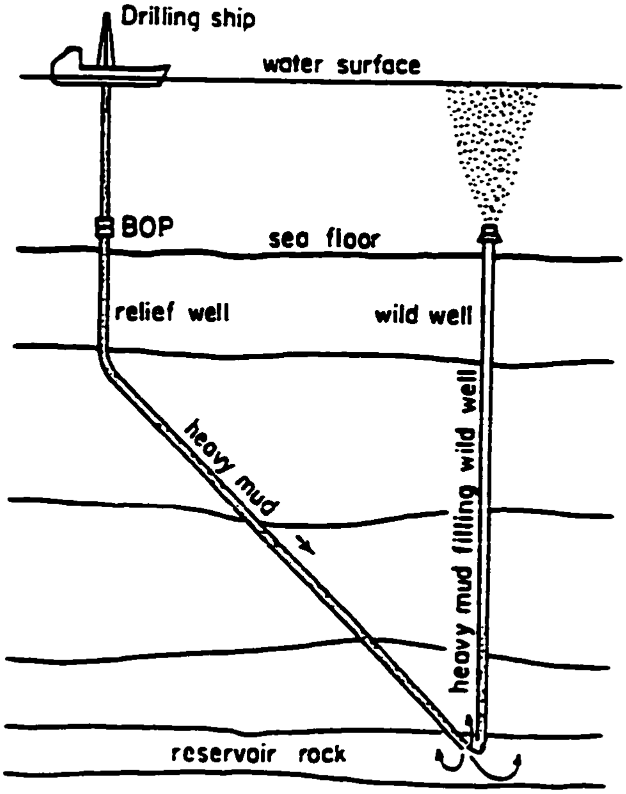

Figure 2.3 Relief well drilling. (Environment Canada, 1979)

2.5 Sources of Oil Contamination

The source of oil contamination is diverse. The common sources of oil contamination are: leaking underground storage tanks, pipelines, landfill sites and dumps, periodic spillage at industrial and refuelling facilities, accidental spills during transportation, and spillage during exploration of oil in offshore. Several factors render the situation of this contaminant very difficult to investigate including: (1) accessibility of the subsurface environment, (2) the mechanisms and rate of hydrocarbon movements in soils, (3) the fate of degradation of petroleum products, and (4) the complexity of crude oils and petroleum products. In order to determine the bulk properties of solubility of oil it is important to examine the oil chemistry.

2.5.1 Oil Chemistry

Petroleum products are a mixture of hydrocarbons. Depending on the type of hydrocarbons present in the subsurface environment, there is a variation in properties extending over many order of magnitude. Mackay et al. (1985) conducted a study on a diesel fuel and found that hydrocarbon tends to migrate through water if an appreciable fraction of it can partition into water. Table 2.1 gives some illustrative properties of selected hydrocarbons such as the coefficient of solubility and vapour pressure of a diesel fuel. In order to obtain the solubility of a mixture of hydrocarbons say diesel fuel, the solubility of each component in the fuel, weighted in proportions of their amount in the mixture are added to determine the solubility of the fuel. If the components of a mixture of hydrocarbons are not known, a gas chromatograph (CG) is often used.

A gas chromatograph is a device used to separate the components of a sample and determine the percentage of each component present in the mixture. In this study I did not have access to a gas chromatograph, therefore I did not know the components of the hydrocarbons present in the oil used in this experimental work. In general hydrocarbons present in petroleum products are classified in three groups:

1. Alkanes: Which are any class of hydrocarbons with each carbon atom bounded to four other atoms. Alkanes have well-defined properties and degrade rapidly.

General formula: C_NH_{2N+2}, where N is the number of carbon atoms.

Example: Methane (C_2H_6).

2. Alkenes: Any class of hydrocarbons characterised by the presence of a carbon-carbon double bond. They are difficult to identify.

General formula: C_NH_{2N}, N is the same as defined above.

Example: Ethylene (C_2H_4)

3. Aromatics: Any class of hydrocarbons characterised by the presence of a benzene ring or related structure. Aromatics are fairly well identified and more soluble in water than other hydrocarbons.

General formula: C_NH_{2N-6} . N is the same as defined above. Example: Benzene (C_6H_6).

Table 2.1 Illustrative Properties of Selected Hydrocarbons at 25°C. (After, Calabrese et al., 1988)

Hydrocarbon	Formula	Water Solubility (g/m)	Vapor Pressure (P_a)
n-Hexane	C_6H_{14}	9.5	20,000
n-Octane	C_8H_{18}	0.6	1,900
n-Decane	$C_{10}H_{22}$	0.05	175
Benzene	C_6H_6	1,780	12,700
Toluene	C_7H_8	525	3,800
p-Xylene	C_8H_{10}	185	1,170
Naphthalene	$C_{10}H_8$	31	11
Biphenyl	$C_{12}H_{10}$	7	1.3
Anthracene	$C_{14}H_{10}$	0.04	0.001
Pyrene	$C_{16}H_{10}$	0.14	0.0009
3.4 Benzpyrene	$C_{20}H_{12}$	0.001	Negligible

CHAPTER 3

MULTIPHASE FLOW IN POROUS MEDIA

3.1 Introduction

Flow of immiscible fluids in porous media has caught the attention of many researchers including, Collins (1961), Philip (1963), Bear (1972), and Greenkorn (1983). Among a large number of monographs written on the subject, the report published in 1856 by Henry Darcy on the water supply of the city of Dijon, France which describes the theory of flow of water through sand in particular and fluids through soils in general, was the most acclaimed. Before discussing multiphase flow in porous media, let us first limit ourselves to the analysis of a single fluid (water) through soil (sand). Darcy's law is reviewed to provide a basis of understanding of a single phase flow in porous medium.

3.2 Darcy's Law

Darcy's report described a laboratory experiment analyzing the flow of water through sand. The apparatus consisted of :

- a circular cylinder of cross section A, filled with sand,
- inflow and outflow tubes and a pair of manometers attached to the cylinder.

A schematic representation of Darcy's experimental apparatus is illustrated in Figure 3.1.

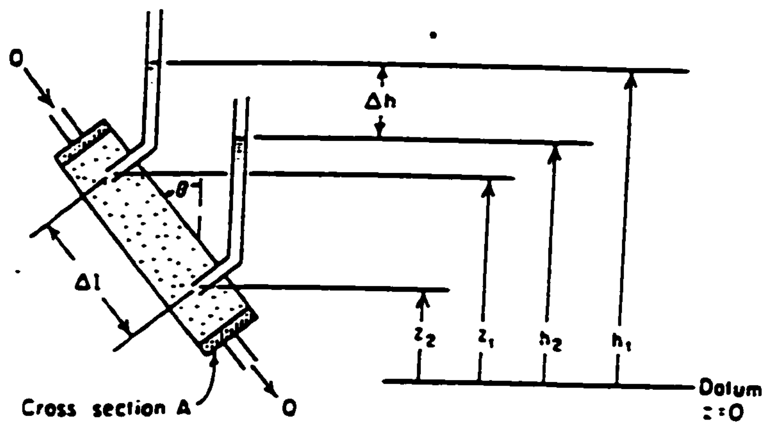

Figure 3.1 Experimental apparatus for the illustration of Darcy's law. (After Freeze and Cherry, 1979).

3.1 Description of Darcy's Experiment

Water was introduced and allowed to flow at a constant rate Q through the cylinder. hence saturating the entire sand sample. After a series of experiments. Darcy observed that the water flow rate was proportional to the water level difference in the manometers at the entrance and exit of the cylinder. Thus he concluded that the specific discharge (which is the ratio of the flow rate divided by the cross section) was directly proportional to the hydraulic head difference $\Delta h = (h_1 - h_2)$ between points 1 and 2 (points where the hydraulic heads were measured) when ΔL (which is the length of the sample in the macroscopic flow direction) was held constant and inversely proportional to ΔL when the head difference (Δh) was held constant. Using mathematical notations Darcy's observations can be summarized as follows:

$$\frac{Q}{A} \propto \frac{\Delta h}{\Delta l} \qquad (3.1)$$

where: Q = volumetric flow rate $[L_w^3 T^{-1}]$

A = cross-sectional area of sand column $[L_t^2]$

Δh = drop in water level between the manometers $[L_w]$

Δl = distance between the manometers $[L_t]$

If we introduce a proportionality constant known as the hydraulic conductivity. Darcy's Law becomes:

$$q = \frac{Q}{A} = -K\frac{\Delta h}{\Delta l} \qquad (3.2)$$

where: q = specific discharge $[L\ T^{-1}]$

= Darcy flux

= Darcy velocity

K = hydraulic conductivity [L T^{-1}]

Darcy's Law in differential vector form in one-dimension can be written:

$$q = -K \frac{dh}{dx} \tag{3.3}$$

Darcy's law in differential vector form, in three dimensions is given by:

$$\bar{q} = -[K]\left(\bar{i}\ \frac{\partial h}{\partial x} + \bar{j}\ \frac{\partial h}{\partial y} + \bar{k}\ \frac{\partial h}{\partial z} \right) = -[K]\ \nabla h = -[K]\ \text{grad}\ (h) \tag{3.4}$$

in matrix form this equation becomes:

$$\bar{q} = - \begin{Bmatrix} \bar{q}_x \\ \bar{q}_y \\ \bar{q}_z \end{Bmatrix} \tag{3.5}$$

$$= - \begin{bmatrix} K_{xx} & K_{xy} & K_{xz} \\ K_{yx} & K_{yy} & K_{yz} \\ K_{zx} & K_{zy} & K_{zz} \end{bmatrix} \begin{bmatrix} \frac{\partial h}{\partial x} \\ \frac{\partial h}{\partial y} \\ \frac{\partial h}{\partial z} \end{bmatrix} \tag{3.6}$$

$$= -\left\{\begin{matrix} K_{xx}\dfrac{\partial h}{\partial x} + & K_{xy}\dfrac{\partial h}{\partial y} + & K_{xz}\dfrac{\partial h}{\partial z} \\ K_{yx}\dfrac{\partial h}{\partial x} + & K_{yy}\dfrac{\partial h}{\partial y} + & K_{yz}\dfrac{\partial h}{\partial z} \\ K_{zx}\dfrac{\partial h}{\partial x} + & K_{zy}\dfrac{\partial h}{\partial y} + & K_{zz}\dfrac{\partial h}{\partial z} \end{matrix}\right\} \quad (3.7)$$

The coefficient K is also called the permeability. Its magnitude depends on the properties of the porous media and the fluid flowing through it. In fact K is the constant of proportionality relating Darcy's flux to the hydraulic gradient. According to Darcy's phenomenological law, the gradient of potential energy is the driving force responsible for the water movement in the soil.

Darcy's empirical law which describes the flow of a single fluid (water) in the soil (sand) has been modified by many researchers to account for the presence of more than one fluid in the soil. Since Darcy's equation incorporates the hydraulic gradient between two points in the same fluid, one must be careful in keeping track of the potential energy if more than one fluid is involved in the porous medium. Nevertheless it is possible to represent the potential energy of any fluid in the porous medium in terms of the others.

Consider that water and oil are both present in a cylinder and assuming that both fluids do not mix. The potential of oil in the cylinder as an equivalent head of water is given by the following equation:

$$h_e = \left(\frac{\rho_{fluid}}{\rho_{water}}\right) h_a \quad (3.8)$$

where:

h_e = equivalent head of water in the cylinder, [m H_2O]

h_a = actual head of oil in the cylinder, [m H_2O]

ρ_{fluid} = density of the fluid, [g/cm^3]

ρ_{water} = density of water, [g/cm^3].

Macroscopic equations describing multiphase flow in porous media, are thus generated from Darcy's law of single-phase flow in porous media. However the validity of Darcy's law is limited to some conditions:

1. The flow in the flow field must be viscous (or creeping), viz., with Reynolds number less than 1.

2. Newtonian fluids (i.e., the viscosity is constant).

Under steady-state conditions, the following analogous equation has been derived for two-phase flow in porous media:

$$Q_i = \left(\frac{K_{ri}}{\mu_i} A \right) \left(\frac{\Delta p_i}{l} \right) \quad (i = 1, 2) \tag{3.9}$$

where:

Q_i = volumetric flow rate, [m^3/s]

Δp_i = pressure drop of fluid i, [m of H_2O]

A = cross-sectional area, [m^2]

μ_i = viscosity of fluid i, [Ns/ m^2]

l = length of the soil mass, [m]

K_{ri} = effective permeability or phase permeability of the porous medium to fluid i, [m/s]

Further extensions of Darcy's law have been suggested by Muskat et al. (1937). They introduced the relative permeability k_{ri}, which depends on the porosity of each fluid in the soil.

$$Q_i = \left(\frac{k * k_{ri}}{\mu_i} A\right)\left(\frac{\Delta p_i}{l}\right) (i = 1, 2) \qquad (3.10)$$

Further generalization of Darcy's law was made by Marle (1981). He derived the velocity of phase i in each fluid as:

$$v_i = \left(\frac{k * k_{ri}}{\mu_i}\right)\left(\nabla p_i - \rho_i * g\right) \qquad (3.11)$$

where: $v_i = \left(\frac{\delta Q_i}{\delta A}\right) n$ (3.12)

k = hydraulic conductivity of the porous medium [m/s]

k_i = permeability of phase i [m/s]

k_{ri} = relative or effective permeability of phase i [m/s]

n = unit vector of the surface (partial derivative) A.

g = gravitational acceleration vector, [m/s^2] and

ρ_i = density of fluid i. [kg/m^3]

Δp_i = pressure drop of fluid i, [m of H_2O]

μ_i = viscosity of fluid i, [Ns/m^2]

These generalizations of Darcy's law lies on the assumption that the porous medium is subdivided into small blocks allowing the use of approximately constant values of v_i, P_i,

k^*k_{ri}, ρ_i, and μ_i for each fluid within each block. It is also assumed that the pressure P_i in any two phases at any point in the porous medium are related to each other via the capillary pressure P_c. It was shown by Leverett (1941) that two pressure gradients are related to each other by the gradient of the capillary pressure:

$$\nabla P_2 - \nabla P_1 = \nabla P_c \qquad (3.13)$$

3.3 Forces Acting on a Fluid Particle

During flow in porous media the following forces act on a fluid particle:

- pressure forces, exerted by the surrounding fluid
- viscous friction forces exerted by the surrounding fluid and the solid
- gravitational forces
- inertia forces
- surface forces, acting on the interface between the two fluids and on the line where the latter meets the solid.

The evaluation of the importance of these forces at the macroscopic level indicated that inertia forces are almost negligible. Pressure forces and viscous forces are approximately proportional to the flow rate, therefore they are important. Capillary and gravitational forces are independent of the flow rate, hence they are relatively more important when the flow rate is slower.

To illustrate the importance of these forces, consider the following example: Two capillary tubes with different diameters branching from a common stem, diverging and come together again (see Fig. 3.2).

Assuming that the two capillaries are filled with oil first. If water is pumped from the bottom stem of the capillaries, the meniscus formed at the intersection of the two fluids will move. When this meniscus reaches the bottom fork it will separate into two new meniscuses. each advancing into one of the tubes. If the two tubes are slightly constricted at the point where they come together. water may reach the fork in the right tube first. while oil still remains in the left tube. If this happens a portion of oil phase will be trapped in the left tube. Assuming that the pressure drop ΔP in the system is kept constant, the driving pressure drop in each tube is obtained by adding to the later the pressure difference ΔP:

$$\Delta P = \frac{2T*\cos\alpha_1}{r_1} \text{ for the first tube} \tag{3.14}$$

$$\Delta P = \frac{2T*\cos\alpha_2}{r_2} \text{ for the second tube} \tag{3.15}$$

where: T = interfacial tension, [N/m]

α_1 = wetting angle of fluid 1, [°]

α_2 = wetting angle of fluid 2, [°]

r_1 = radius of tube 1, [m]

r_2 = radius of tube 2, [m]

Marle (1981) stated that if a slight pressure drop occurs in the system. the smaller tube will be relatively favored over the larger one in reaching the upper fork. while a greater increase in the pressure drop will favor the larger tube. Thus the ratio of speed of advance of the meniscuses in the two tubes is a function of the pressure drop. consequently the quantity of oil which remained trapped depends upon the applied pressure drop. The aforementioned example allows us to understand why residual oil saturation in a porous medium may depend on the flow rate of water.

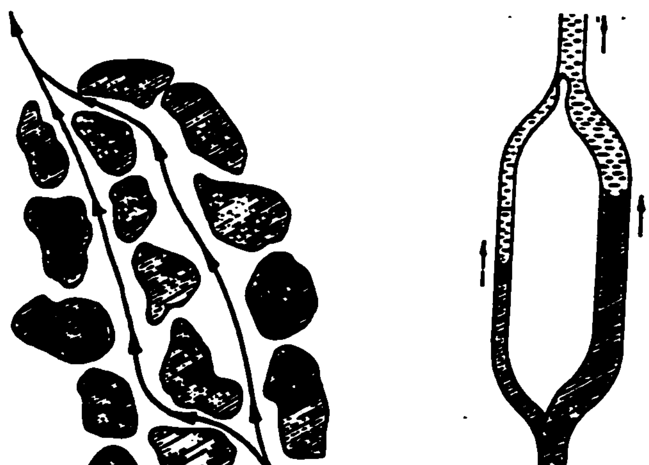

Figure 3.2 Illustration of two fluids flowing in two different capillary tubes with two common stems. (After Marle, 1981).

3.4 Distribution of Fluids in the Pores

In a porous media one can distinguish a few possibilities as far as the distribution of two fluids in the pores is concerned:

Co-current flow, which occurs when each phase flow in the same direction.

Countercurrent flow, occurring when different phases flow in opposite directions. A countercurrent flow may take place when a system saturated with a nonwetting phase is brought in contact with a wetting fluid. Another example is when capillary forces are small compared with gravitational and viscous forces, which is the case when heavy oil drains from a formation in counter-current flow.

Drainage, which is a process describing the displacement of a wetting fluid (i.e., water) by a nonwetting fluid (i.e., oil). A wetting phase is drained out of the pores under the influence of gravity or by forcing of a nonwetting phase under pressure. Drainage is often called "desaturation", "dewetting", or "desorption". When water is being displaced by oil at a constant rate under a pressure exceeding the capillary pressure required for penetration into the system, it is called "oil flooding".

The displacement of a nonwetting phase by a wetting phase is known as imbibition or "spontaneous imbibition". Spontaneous imbibition occurs when a porous medium containing a nonwetting phase is brought in contact with a wetting phase. The wetting phase spontaneously displaces a portion of the nonwetting phase. Spontaneous imbibition may be controlled by means of regulating externally the capillary pressure. The process of controlling spontaneous imbibition is sometimes referred to as "forced" imbibition, while the process of penetration of a wetting phase in a nonwetting phase is termed " wetting", "saturation", or "adsorption". If a nonwetting phase (oil) is being displaced by a wetting phase (water) at a constant rate, under pressure in excess of capillary pressure, this process is known as "water flooding".

In general, regardless of the type of forces that are responsible for the displacement of any phase by another, immiscible displacement can be referred to as "infiltration".

3.5 Mechanisms of Infiltration of Water through Sand

Infiltration of water through the soil surface generally takes place over small period of time. During the infiltration process, liquids usually enters the porous material under the influence of capillary and gravity forces. For soils, the infiltration usually amounts to the displacement of air by water. It has been shown experimentally that at the early stage of the infiltration process, the infiltration rate is very large, then this rate decreases to a limiting value at larger times. The high initial rate is due to the fact that at the early stages of the infiltration process the capillary forces are greater than the gravitational forces. As the infiltration proceeds, the gravitational force coupled with the resistance of air will eventually overcome the capillary forces, thus reducing the infiltration rate. According to experiments conducted by Sherman et al.(1967), the infiltration rate will decrease asymptotically to a constant value, mainly due to the influence of the water content in the soil. Horton (1969) pointed out that for a given soil there is a limiting curve that defines the maximum possible rate of infiltration as a function of time. Horton called this limiting curve, the curve of infiltration capacity of soil. Rubin and coworkers (1973) showed that the final constant infiltration rate in the Horton curve is numerically equivalent to the saturated hydraulic conductivity of the soil. After a series of experiments. Rubin et al. (1973) concluded that the decline of the infiltration rate in the sand was mainly caused by the filling of the pores by water. On the basis of experiments conducted by Naal (1976). an analytical form of the infiltration curve from the Norton equation was expressed as follows:

$$f(t) = f_c + (f_0 - f_c) * e^{-\delta t} \quad (3.16)$$

where:

f = infiltration rate at time t

f_0 = initial rate in the case of air-dry soil

f_c = value of the infiltration with decreasing intensity asymptotically to a constant number.

δ is a parameter which depends on the type of soils. For wet soil δ is equal to 0.63 and for dry soil δ is taken as 0.35. As a mean value. 0.43 is often used for δ in the case of artificial sprinkling on different soils.

3.6 Surface Tension and Contact Angle

The interface geometry within a given porous medium is governed by three parameters (the pore geometry. the surface tension, and the contact angle). When two fluids are in contact with a solid surface, the two will meet at an angle called the contact angle θ. If these fluids are in equilibrium, the vector sum of the three forces arising from the three surface tensions will be zero.(See Fig. 3.3)

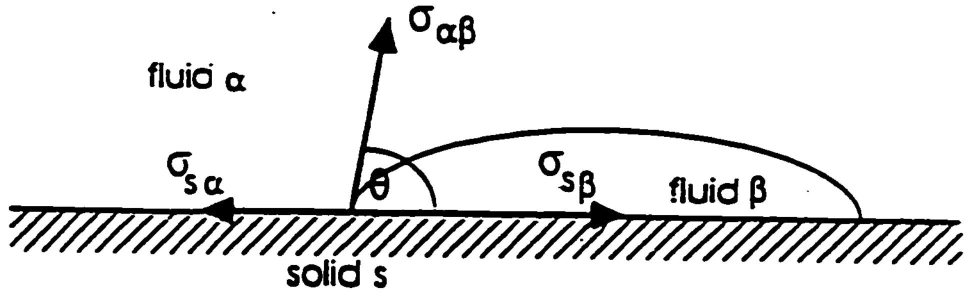

Figure 3.3 Surface tension stresses between two fluids and a solid surface (after Dullien, 1979).

At equilibrium the summation of forces acting on the solid surface and fluid interface must be zero. Replacing the stresses in Fig. 3.3 by their corresponding forces in the equilibrium equation we have the following relation:

$$F_{s\alpha} = F_{s\beta} - F_{\alpha\beta} \cos\theta \tag{3.17}$$

where:

θ is the contact angle measured on the side of the denser fluid. A fluid whose contact angle is less than 90 ° is said to the wetting. If the contact angle is greater than 90 ° the fluid is said to be nonwetting. When the contact angle is equal to 90 °, one speaks of intermediate or neutral wettability.

$F_{s\alpha}$ is the surface tension between the solid and fluid α

$F_{s\beta}$ is the surface tension between the solid and fluid β

$F_{\alpha\beta}$ is the surface tension between the solid and the two fluids. In the case of oil and water, the contact angle will be measured on the side of water.

3.7 Mechanisms of Trapping of Nonwetting Phase in a Porous Media

The mechanisms determining the microscopic trapping of a residual nonwetting fluid (oil) in a porous media are governed by the following factors:

- geometry of the pore network,
- fluid-fluid properties such as interfacial tension,
- density difference of the two phases (oil and water),
- viscosity ratio,
- nonwetting phase behavior,
- fluid-material interfacial properties determining the wetting fluid (water) behavior, and
- the applied pressure and gravity.

The trapping of residual nonwetting phase is usually expressed in terms of dimensionless numbers, namely the capillary number (ratio of the viscous to capillary forces) and Bond number (ratio of gravity to capillary forces).

The following equations describes mathematically the Bond number (N_B) and capillary number (N_{CA}).

$$N_B = \frac{\Delta\rho * g * R^2}{\sigma} \qquad (3.18)$$

$$N_{CA} = \frac{v\ \mu}{\sigma} \qquad (3.19)$$

where:

$\Delta\rho$ = fluid density difference [g/cm^3]

g = acceleration due to gravity [cm/sec^2]

R = particle effective grain size radius [cm]

σ = interfacial tension [dyne/cm]

v = displacing fluid velocity [cm/sec]

μ = displacing fluid viscosity [poise- g/cm-sec]

In an experimental study on the effect of viscosity and buoyancy forces on the trapping of oil in sand, Morrow et al. (1981), stated that for vertical displacement, residual oil saturations varied from normal values of about 14.3 % (See Fig. 3.4) when the Bond number was less than 0.000667 and the capillary number was less than $3x10^{-6}$, down to near zero when either the Bond number exceeded 0.35 or the capillary number exceeded $7x10^{-7}$. Their study also showed that, the effects of the Bond and the capillary numbers on the residual recovery were superimposed. In addition, the mobilization of trapped blobs was about five times more difficult to achieve than from prevention of trapping. Furthermore, a significant influence of the buoyancy forces on the microscopic displacement of the blobs was observed at low interfacial tension systems.

Capillary forces were dominant for any combination of capillary number less than 10^{-6} and Bond number less than 0.0067. This resulted in an isolation of blobs once an imbibition event occurred. An increase in the Bond number, had a tendency to activate the imbibition process into the lower region of the blob before the upper region was increased, since the hydrostatic pressure between the regions was increased. Morrow et al. (1981) laboratory investigations showed that trapped residual oil can be recovered if there is sufficient pressure difference due to viscous flow, so that a significant portion of blobs are mobilized. Morrow et al. (1981) results for the effects of gravity and viscous forces on trapping are given in Table 3.1.

Taber (1969) showed that, at low interfacial tensions of the order of 1/100 dyne/cm, mobilization of a significant quantity of residual oil was possible. He concluded that at normal oil-water interfacial tensions (i.e., no surfactant added in the porous medium), capillary forces which retain residual oil far exceeded buoyancy forces. But when surfactant are introduced in the system, interfacial tensions are lowered, consequently viscous forces can overcome capillary forces, hence buoyancy forces may also have significant effect on both trapping and mobilization.

Figure 3.4 Effect of capillary number on trapping of residual saturation at Bond numbers greater than 0.00667. (After Morrow et al., 1981).

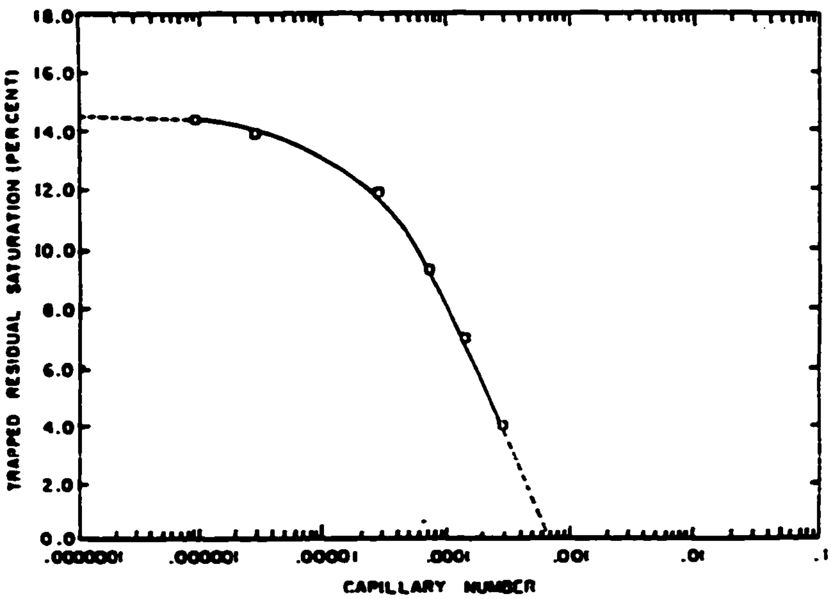

3.7.1 Calculation of the Capillary and Bond Numbers utilized for Carp Airport Soil

Given:

Density of water, $\rho_{WATER} = 1.0$ g/cm^3

Density of oil, $\rho_{oil} = 0.927$ g/cm^3

Acceleration of gravity, $g = 981$ cm/sec^2

Oil viscosity, $\mu = 455$ mPa.s

Effective grain size $D_{10} = 0.30$ mm

Surface tension $\sigma = 0.035$ N/m

The properties of oil and water are given at 20 °C and standard atmospheric pressure (Streeter et al., 1985).

Required

1) Determine the Bond number N_B and the capillary number N_{CA} of Carp Airport soil.

Solution

Step 1: determination of the density difference

$\Delta\rho = 1 - 0.927 = 0.073$ g/cm^3

Step 2: converting the oil viscosity into appropriate units

$\mu = 455$ mPa.s $= 455 * 10^{-3} * 10$ poise or $455 * 10^{-2}$ p

Step 3: determination of the mean particle radius

$$R = \frac{d}{2}$$

Assuming that the effective pore diameter is:

$$d = 0.2\ D_{10}$$

$$d = 0.2*0.19\ mm$$
$$= 0.038\ mm$$

thus

$$R = \frac{0.038}{2}$$

$$= 0.019\ mm$$

$$= 19*10^{-6}\ m$$

Step 4: Converting the surface tension into appropriate units

$1 N/m = 10^3$ dyne/cm
thus, $\sigma = 0.035*10^3$ dyne/cm

Step 5: Evaluation of the average velocity of oil migration

It took approximately 100 days for the contaminant to travel through the entire 241.8 cm of soil length in the J-tube,
hence the average velocity is:

$$v = \frac{241.8}{100*3600*24} = 2.80*10^{-5}\ cm/sec$$

Substituting the appropriate values in (3.18) and (3.19), we obtain the Bond number and capillary number as follow:

$$N_B = \frac{0.073 * 981 * \left(19 * 10^{-4}\right)^2}{0.035 * 10^3}$$

$$= 7386 * 10^{-9}$$

$$N_{CA} = \frac{2.8 * 10^{-5} * 4.55}{0.035 * 10^3}$$

$$= 364 * 10^{-8}$$

Table 3.1 Nonwetting Phase Saturations trapped in random packings of equal spheres at various Bond and Capillary numbers. ($\Delta\rho = 0.748$, $\rho = 23.19$ dyne/cm). (After Morrow et al., 1981)

Mesh Size	Mean Dia. (mm)	Bond Number	Inverse Bond Number	% S_{nw} at Capillary Number				
				2.82×10^{-6}	2.82×10^{-5}	7.07×10^{-5}	1.41×10^{-4}	2.82×10^{-4}
12–14	1.55	0.1895	5.277	2.97	2.56	1.90	1.62	1.21
14–16	1.29	0.1313	7.619	4.83	4.28	3.41	2.76	—
16–18	1.09	0.0937	10.671	6.31	5.22	4.35	3.37	—
18–20	0.925	0.0675	14.818	7.79	6.68	5.45	3.74	—
25–28	0.655	0.0338	29.551	10.30	9.19	6.65	4.78	2.11
32–35	0.462	0.0168	59.399	12.36	10.60	8.19	5.14	2.64
42–48	0.327	0.00843	118.568	13.95	11.72	8.51	6.14	3.07
48–60	0.275	0.00596	167.647	14.03	11.94	9.27	6.54	3.68
65–80	0.191	0.00288	347.532	14.06	11.92	9.21	6.92	4.07
80–100	0.165	0.00215	465.685	13.99	11.90	9.39	6.94	4.05
100–115	0.137	0.00148	675.492	14.06	11.88	9.28	6.96	4.06

3.8 Immiscible Flow in Porous Media

Flow of immiscible fluids in porous media can occur during steady-state or transient states.

3.8.1 Fluid Flow under Steady-State Conditions

At steady-state, all macroscopic properties of the system are time invariant at all points. Steady state flow occurs when at any point in a flow field, the magnitude and direction of the flow velocity are constant with time and the saturation of the medium with respect to all fluids contained in the system is also constant. Two conceptions of the microscopic picture of simultaneous flow of two immiscible fluids in porous media have been acknowledged during steady-state conditions.

One of these conceptions is based on the funicular flow regime described by Scheidegger (1974). In a funicular flow regime both the wetting and nonwetting phase flow simultaneously in all capillary, the wetting phase on the outside surrounding the nonwetting phase, which is on the inside and occupies the central portion of each capillary. The funicular flow regime is the result of the distribution of two continuous phases at high nonwetting phase saturation when the flow channels in the medium have irregular cross sections. An increase in the saturation of the nonwetting phase implies an increase in the average diameter of the funicular entities of this phase.

The other conception of the microscopic picture is based on Craig's (1971) direct visual observations of two-phase flow using photomicrographs in synthetic porous matrices. His observations are based on the channel flow concept of fluid. The photomicrographs shoved that each fluid moved through its own separate network of interconnecting channels. As a result of the increase of the nonwetting saturation, the number of channels carrying nonwetting phase increased and a corresponding decrease of channels carrying only the wetting phase. Craig's studies concluded that there was some wetting fluid in the pores carrying nonwetting fluid, which corresponds to the funicular concept. The nonwetting phase will tend to occupy the larger pores and the wetting phase the finer ones for a combination of the following factors:

- at least one phase has a strong wetting preference for the solid.
- the viscosity of neither fluid is very great.
- the interfacial tension between the two fluids is not very low.
- the saturation of neither phase is very low.
- the pores are not identical.

Greffen et al. (1951) stated that the nonwetting phase is capable of contributing to flow at much lower saturations (i.e., 10% less than the breakthrough) value. According to Chatzis and Dullien (1985) this breakthrough value corresponds to nonwetting phase saturation of about 10% of the pore volume in sandstone. Greffen et al. (1951) added that there may be a continuous network of a fluid at such low saturations and, therefore, the flow of the nonwetting phase probably takes place by a "blob" or "slug"-flow mechanism, under the influence of the viscous forces exerted on it by the wetting phase. In steady co-current flow, the fluid pressures are constant at any point in the flow field. At a particular point in the system the pressure difference is equal to the capillary pressure given by the Laplace equation at the point of interest. The stable position of a meniscus anywhere in the flow field is determined by the difference between the steady state pressures in the two phases and the pore geometry. Because of this stability of the meniscus, there is no displacement of any phase by the other during steady states conditions.

Greffen et al. (1951), Fatt (1961, 1966), and El-Sayed and Dullien (1977) showed experimentally that at relatively low saturations of the nonwetting phase, corresponding to conditions just after breakthrough (about 50% by volume of the nonwetting phase is prevented from flow in a drainage process). This condition of immobile, but continuous, nonwetting phase is sometimes called " dendritic" because of its treelike appearance.

3.8.2 Fluid Flow under Transient Conditions

During transient or unsteady state conditions, all macroscopic properties of the system change with time. Transient flow occurs when at any point in a flow field, the magnitude or direction of the flow velocity changes with time. The saturation in transient state at any point in the system will change with time as well.

If a nonwetting fluid (oil) is pumped into a system at an increased rate, while the flow rate of the wetting fluid (water) is kept unchanged, a temporary transient state will result, while the menisci separating the two phases moves to new equilibrium positions thus, the nonwetting phase will penetrate some smaller pores from which it displaces the wetting phase. During the displacement process there is no capillary equilibrium in the system, but the pressure difference between the two sides of a meniscus at any microscopic point in the system has been assumed to be equal to the capillary pressure predicted by Laplace's equation. For the conditions existing at that point. Calvo et al. (1990) reported that dynamic capillary (P_c^d) will take place in the flow field.

Calvo et al. (1990) calculated dynamic pressure from measurements as a function of time of the position x of the interface between two immiscible fluids 1 and 2, in the process of fluid 1 displacing fluid 2 in a uniform capillary tube, with a constant pressure differential ΔP maintained between the two extremities of the tube. Their equation is derived from an integrated form of the Washburn equation applied to horizontal displacement where both fluids have nonnegligible viscosities.

In imbibition: $$\int_0^t P_c^d dt = \frac{32}{D^2}\left[\frac{\mu_1-\mu_2}{2}x^2+\mu_2 L*x\right]-\Delta P*t \qquad (3.20)$$

In drainage: $$\int_0^t P_c^d dt = -\frac{32}{D^2}\left[\frac{\mu_1-\mu_2}{2}x^2+\mu_2 L*x\right]+\Delta P*t \qquad (3.21)$$

where μ_1 and μ_2 are the viscosities of fluid 1 and fluid 2 respectively, and D is the diameter of the tube.

During transient states, the morphology of the pore space allows, the displacing phase to surround and cut off portions of the phase originally present in the pore space. An approximate schematic description of the pore geometry of the pore system is given in Fig. 3.5

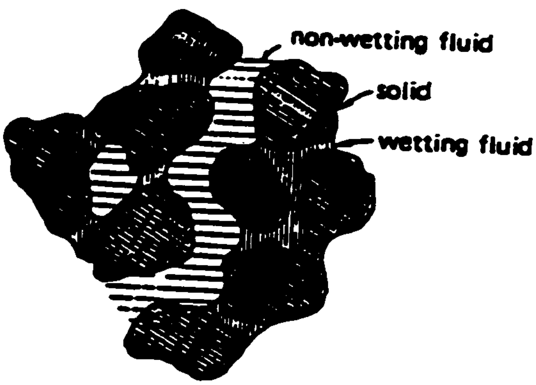

Figure 3.5 Schematic description of the pore geometry of the porous medium.(After Marle, 1981).

These cut off portions, which are called blobs or ganglia, of the displaced phase are usually stationary since the presence of interfacial forces are too great in comparison to viscous or gravitational forces. An increase of the flow rate of the displacing phase and/or a decrease of the interfacial tension between the two phases may result in the flow of the ganglia or blobs along with the displacing phase. Usually under normal conditions, all the residuals displaced phase in the pores remain immobile, consequently the two-phase flow degenerates into one-phase flow in a pore network, containing obstacles in the form of blobs or ganglia of the displaced phase. The solid grains constituting a porous media leave interconnected and irregularly sized spaces between them resulting in an irregular cross sections and a rough surface, that is why some of the wetting phase remains trapped along the surfaces of grooves, edges, and wedges.

When water and oil flow together in a porous media, their vertical migration can be predicted using the generalized form of Darcy's law in one direction given below (Cary et al., 1989):

$$V_o = \frac{\partial F_o}{\partial t} = -k_o\left[\frac{\partial P_o}{\partial z} + \rho_o\right] \tag{3.22}$$

$$V_w = \frac{\partial F_w}{\partial t} = -k_w\left[\frac{\partial P_w}{\partial z} + \rho_w\right] \tag{3.23}$$

where:

V_w = water phase Darcian velocity, [m/s]

V_o = oil phase Darcian velocity, [m/s]

F_w = net water phase flow . [m]

F_o = net oil phase flow. [m]

P_w = pressure in the water phase, [m of H_2O]

P_o = pressure in oil phase. [m of H_2O]

k_w = water phase hydraulic conductivity, [m/s]

k_o = oil phase hydraulic conductivity, [m/s]

ρ_w = specific gravity of water

ρ_o = specific gravity of oil

z = migration depth. [m]

t = time. [s]

CHAPTER 4

LABORATORY EXPERIMENTS OF OIL MIGRATION

4.1 Experimental Design

A laboratory experiment was carried out to determine the fate of oil migration in caisson retained islands in the case of a blowout. It was necessary to know whether the oil would be confined within the sand or would flow through and contaminate the sea. It was anticipated that if oil was to migrate in the soil, one of the possibilities was that the migration process could start from the sand-filled core to the sand berm and eventually continue upward toward the sea surface. Such a migration process follows the path of a "J-tube". For this reason three Plexiglas tubes with an inner diameter of 5.022 cm were assembled in a J-shape appearance. Such a diameter was chosen in order to minimize the problem of uneven flow like "viscous fingering" which can occur in the case of water and oil migration.

The tubes were 194, 134.6, and 61 cm in length.. with the 194 and 134.6 cm long tubes as the vertical columns and the 61 cm tube as the horizontal piece. The two vertical columns were connected to the horizontal tube by means of two elbows averaging 10.4 cm in length with an inner diameter of about 5.025 cm. A comparison between this experimental setup and the conditions in the field associates the 194 cm long column to the sand-filled core, the 136.4 cm column to the sand berm. and the 61 cm column as a portion of the open sea. Figures 4.1 and 4.2 are respectively schematic representations of the field conditions and a typical flow path of oil migration. Figure 4.3 shows the schematic representation of the experimental setup.

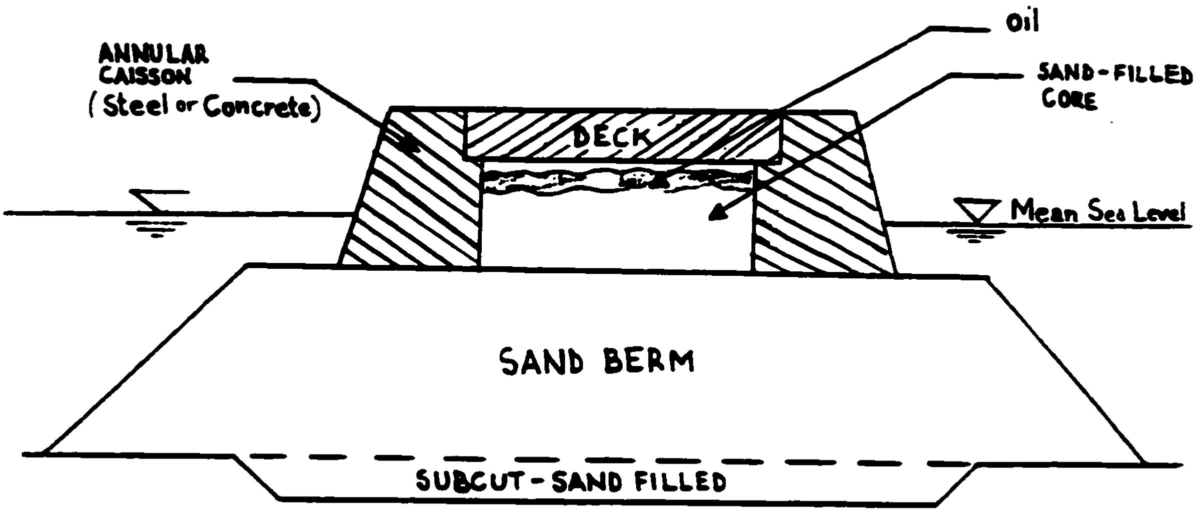

Figure 4.1 Schematic representation of a caisson retained Island.

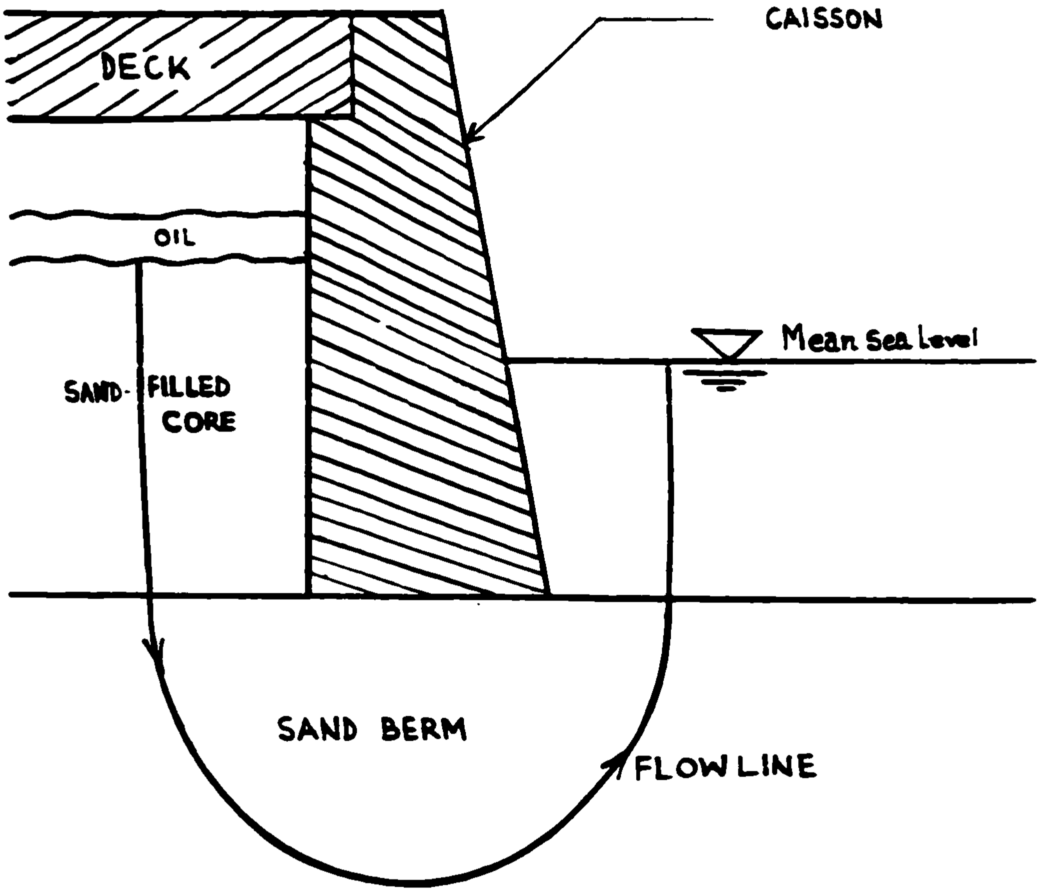

Figure 4.2 Typical flow path of oil migration.

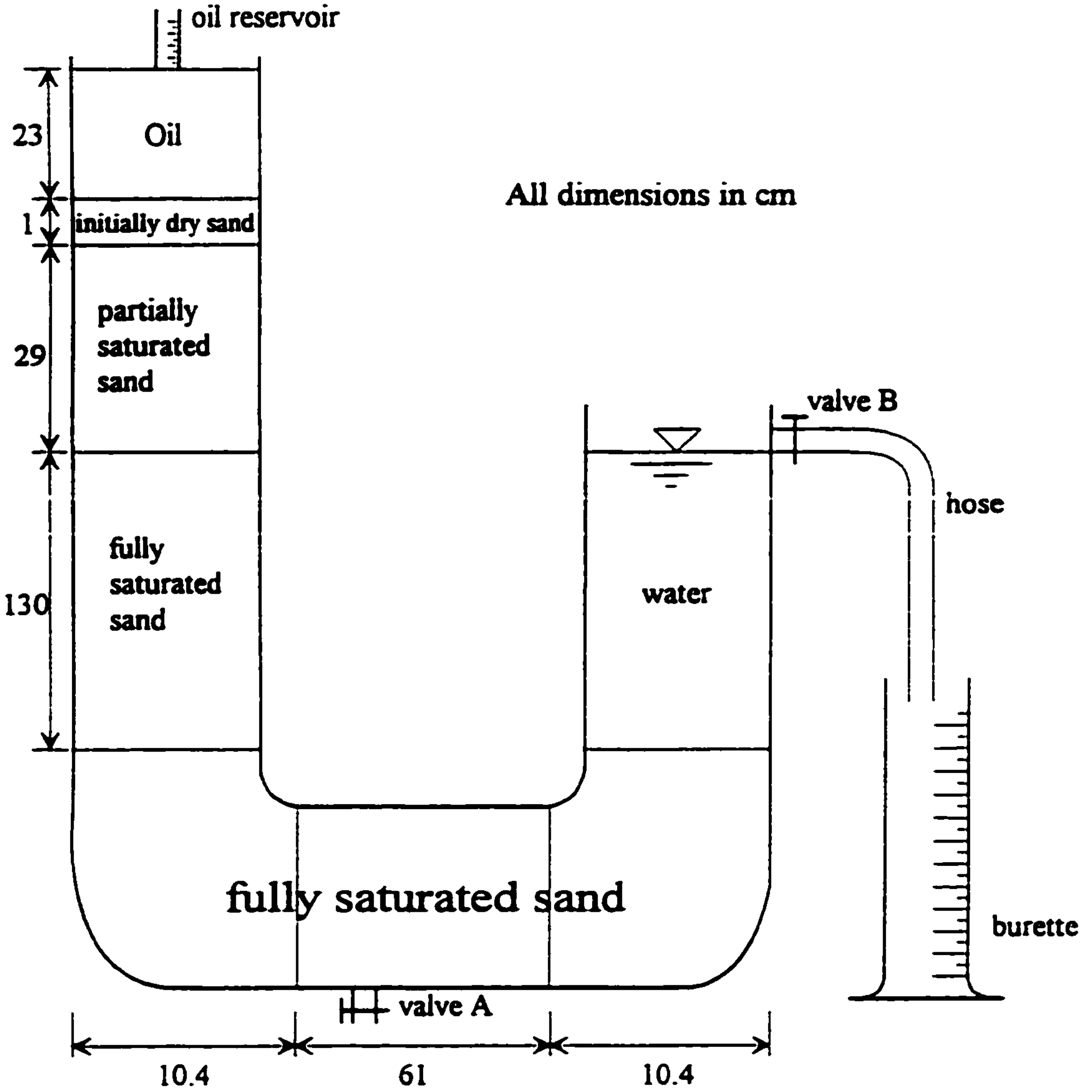

Figure 4.3 J-Tube illustrating the Schematic representation of the experimental setup.

4.2 Description of the Experiment

The type of soil used for this study consist of natural sand from Carp Airport (Kanata). This sand was considered because of its similar properties with Ukalerk sand (Beaufort Sea). The descriptions of these soils are summarized in terms of grain size distribution in Table 4.2. The oil used in this research is Motomaster grade 50 oil. This oil was chosen because, crude oil at its brute stage such as the one at Beaufort sea, was not commercially available. Motormaster grade 50 oil, is a light, non-volatile petroleum oil with a viscosity of 455 mPa.s. With such a light oil, it was anticipated that a reasonable migration would be possible in the soil columns.

In this experiment two of the three glass columns sections were filled with sand and the third with water. A dense sand was placed in the horizontal tube. The sand was placed in a dense state to reduce the amount of volume reduction during saturation and to avoid air being trapped in the tube. Subsequently the sand in this portion of the apparatus was fully saturated. The saturation was achieved by supplying water through a valve which was installed at the bottom of the tube. To complete the saturation, the two vertical columns connected to the horizontal tube were filled with water. This additional step was taken to make sure that the sand in the horizontal tube was fully saturated. To prevent the sand from escaping the horizontal tube, a screen was placed on each elbow. Before pouring the sand in the left vertical column, a permeability test was conducted on the horizontal column. The results of the permeability test were also analyzed.

A raining technique was used to place the sand in the left vertical column. The sand was rained at a constant rate from a given height to ensure full saturation. With this raining technique, the sand became uniform and had less air trapped. The depth of fully saturated soil was about 130 cm, which was the same depth as the water in the right column. On top of this saturated sand, a layer of 30 cm dry sand was rained. Capillary rise took place to about 29 cm above the water table, thus leaving only 1 cm of dry sand. To allow the contamination of the soil system, a clearance of 30 cm remained at the top of the dry sand layer.

A constant supply of oil was fed to the system as required to maintain the total head constant at 23 cm above the dry sand layer. This was done by passing oil through a reservoir. The reservoir consisted of a 65 cm long glass tube, with a 2.54 cm inner diameter. Two valves attached at each end of the reservoir were used to release oil into the porous medium. To fill the reservoir, the valve at the top end was opened while the bottom valve was closed. A similar exercise was performed to release oil from the reservoir to the soil system. This was accomplished by opening the bottom valve while keeping the valve at the top end closed. To ensure that the oil supply was constant, the interface between the bottom end of the reservoir and the oil surface in the left vertical column was brought to a permanent equilibrium position. The permanent contact position was obtained by placing the bottom end of the reservoir in such a way that it barely touched the oil surface of the left vertical column. With this setup it was assumed that the amount of oil seeping through the soil was equal to the amount of oil draining from the reservoir, since there was no oil leakage from the tubes throughout the experiment.

To simulate the field conditions, the water table level in the right vertical column was kept at a height of 130 cm. To maintain the water table constant, a valve was connected to the right vertical column at 130 cm level. Through this valve, displaced water and/ or oil from the porous medium was collected in a burette.

In summary, 5530 g of soil mass was used in the vertical column of which 4405 g was fully saturated to a height of 130 cm. The remaining 1125 g of soil consisted of a layer of 1 cm of initially dry sand and a layer of sand which later became a confined partially saturated sand layer. In addition, 3000 g of fully saturated sand was placed in the horizontal tube while no sand was contained in the right column which was filled with 130 cm of water. The densities of the soils in the J-tube are summarized in Table 4.1.

Table 4.1. Densities of the soils in the J-tube.

Soil	Mass (g)	Volume (cm^3)	Density (g/cm^3)
Initially dry sand	37	19.8	1.87
Partially saturated sand	1088	574.2	1.89
Fully saturated sand	4450	2573.8	1.73
Highly packed fully saturated sand	3000	1619.5	1.85

4.3 Acquisition of Data

The procedure for collecting the data was very simple. The measurements of the database included the date, the time, the reservoir level, and the amount of water and/or oil displaced. At the beginning of the experiment the location of oil in the soil was measured frequently since at that time the oil was migrating very fast. After a while the measurements were taken on selected days of the week.

4.4 Characteristics of Carp Airport Sand

Offshore sands available for use in hydraulic constructions are typically fine grained and uniform. Carp Airport sand is a natural sand and basically fits this description. A sieve analysis was performed and the results correlated reasonably well with the typical grain size distribution of Ukalerk and Nerlerk sands. Figures 4.4 and 4.5 show the grain size distributions of each of the aforementioned soils.

4.4.1 Relative Density Test of Carp Airport sand.

Date of test: June 10 1994

Tested by: Megnolo

Location: CBY Geotechnical Lab Room D113

4.4.1.a Minimum Density

Table 4.2 Minimum density parameters

Trial No	Weight of mold (g)	Weight of sand + mold (g)	Mass of sand (g)	Height of mold (cm)	diameter of mold (cm)	Volume of mold (cm ^{3})	Min density (g/cm ^{3})
1	3625	8195	4570	15.55	15.34	2872.4	1.59
2	3625	8247.5	4622.5	15.55	15.34	2872.4	1.61

hence the average minimum density is :

$$\rho_{min} = \left(\frac{1.59 + 1.61}{2}\right) = 1.60 \text{ g/cm}^3$$

4.4.1.b Maximum Density

After shaking the mold and sand of trial 2 on the electric shaker, the following parameters were determined:

Plate thickness = 1.26 cm

Distance from the top of the mod to the plate = 13.26 cm

Height of sand in the mold = 15.55-(1.03+1.26) = 13.26 cm

Volume of the sand in the mold = $\left(\frac{3.14 * 15.34}{4}\right)13.26 = 2449.4\ cm^3$

hence,

$$\rho_{max} = \frac{4622.5}{2449.4} = 1.89\ g/cm^3$$

4.4.1.c Specific Gravity and Density of Sand

The specific gravity of the sand was determined by submerging a known mass (M) of sand into water. Using a laboratory scale, the submerged mass (M*) of sand was recorded. The specific gravity was then calculated using the following formula:

$$G_S = M^*/(M-M^*) \tag{4.1}$$

experimental values of M and M* were 110.5 g and 80.5 g respectively, thus

$$G_S = 80.5/(110.5-80.5) = 2.68$$

The density of soil was calculated using the following formula:

$$\rho_S = G_S * \rho_w \tag{4.2}$$

where ρ_w = 1 g/cm^3 is the density of water at the ambient temperature, in this case 20° C, hence,

$\rho_S = 2.68*1 = 2.68$ g/cm^3

4.4.1.d Maximum and Minimum Void Ratios

$$e_{min} = \rho_s / \rho_{max} - 1 \qquad (4.3)$$
$$= 2.68/1.89 - 1$$
$$= 0.42$$

$$e_{max} = \rho_s / \rho_{min} - 1 \qquad (4.4)$$
$$= 2.68/1.60 - 1$$
$$= 0.68$$

4.4.5 Sieve Analysis

A summary of the grain size analysis of Carp Airport soil is given on Table 4.3. The results obtained form the sieve analysis helped to determine the following parameters:

D_{60} = 0.34 mm,

D_{10} = 0.19 mm.

The coefficient of uniformity which is given by:

$$C_u = \frac{D60}{D10} = \frac{0.34}{0.19} = 1.79$$

A comparative study of the sand properties at Carp Airport and Ukalerk is summarized in Table 4.3 below.

Table 4. 3 Typical properties of Ukalerk (Beaufort sea) and Carp Airport sands

Property	Ukalerk	Carp Airport
Uniformity coefficient (C_u)	1.5-1.80	1.79
Maximum void ratio (e_{max})	0.80	0.68
Minimum void ratio (e_{min})	0.50	0.42
Specific gravity (G_s)	2.66	2.68

Table 4.3 Grain Size Analysis of Carp Airport Soil.

Project Sieve analysis Job No.

Location of Project Geotechnical Lab D113 Boring No. Sample No.

Description of Soil Depth of Sample

Tested By MEGNOLO Date of Testing 27/05/1994

Soil Sample Size (ASTM D1140-54)

Nominal diameter of largest particle	Approximate minimum mass of sample, g
No. 10 sieve	200
No. 4 sieve	500
3/4 in.	1500

Mass of dry sample + dish	641
Mass of dish	390.6
Mass of dry sample, M_s	250.4

Sieve analysis and grain shape

Sieve no.	Diam. (mm)	Mass retained	% retained	% passing
10	2.00	0.7	0.3	99.7
20	0.850	10.8	4.3	95.4
40	0.425	62.8	25.1	70.3
50	0.300	80.1	31.9	38.4
80	0.180	79.1	31.6	6.8
100	0.150	8.7	3.5	3.3
200	0.075	7.0	2.8	0.5
Pan	—	0.8	–	–
		$\Sigma = 250.0$		

% passing = 100 − Σ % retained.

Figure 4.4 Grain size distribution of Carp Airport soil.

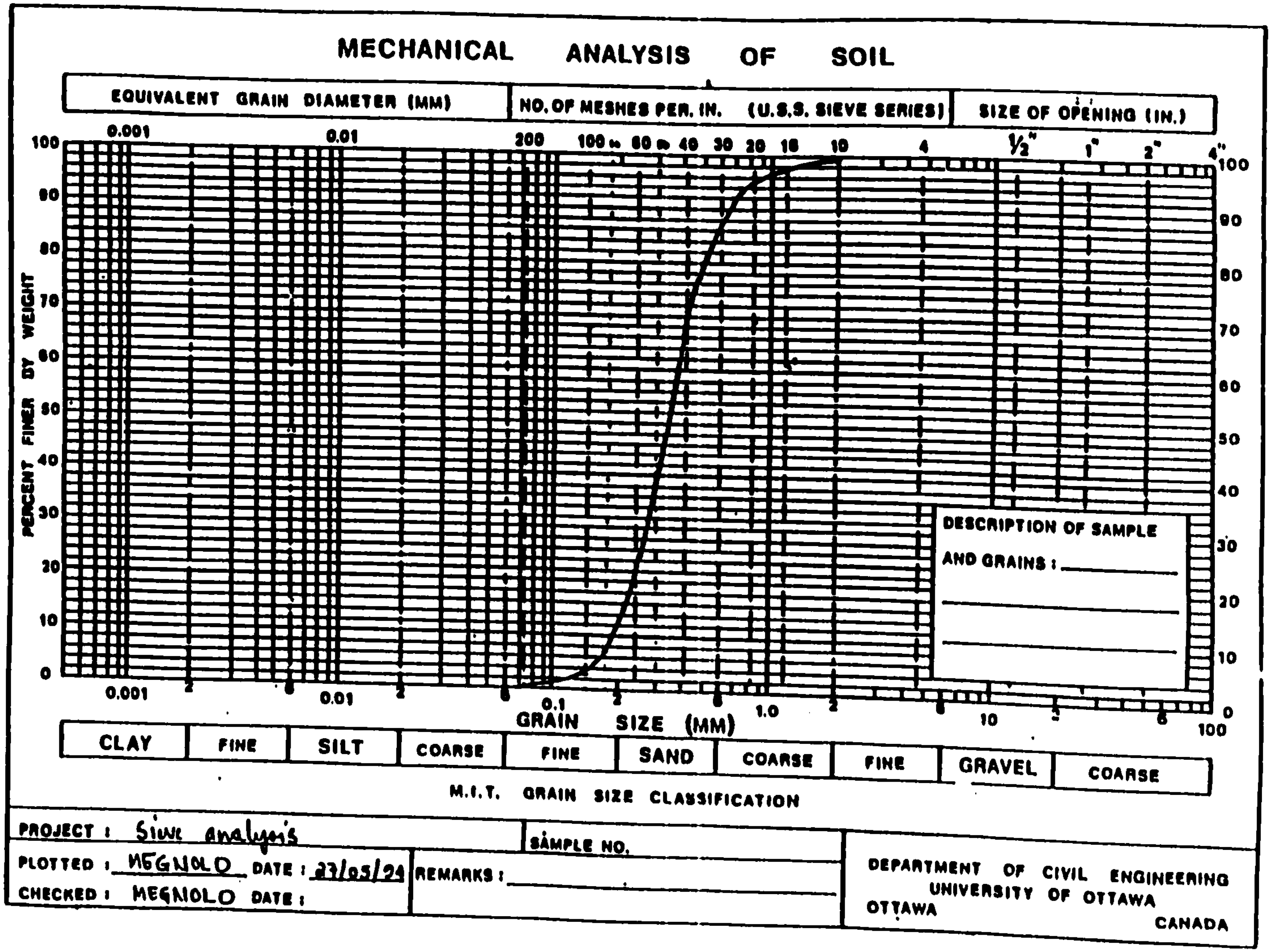

Figure 4.5 Grain size distribution of Carp Airport and Beaufort Sea soils.

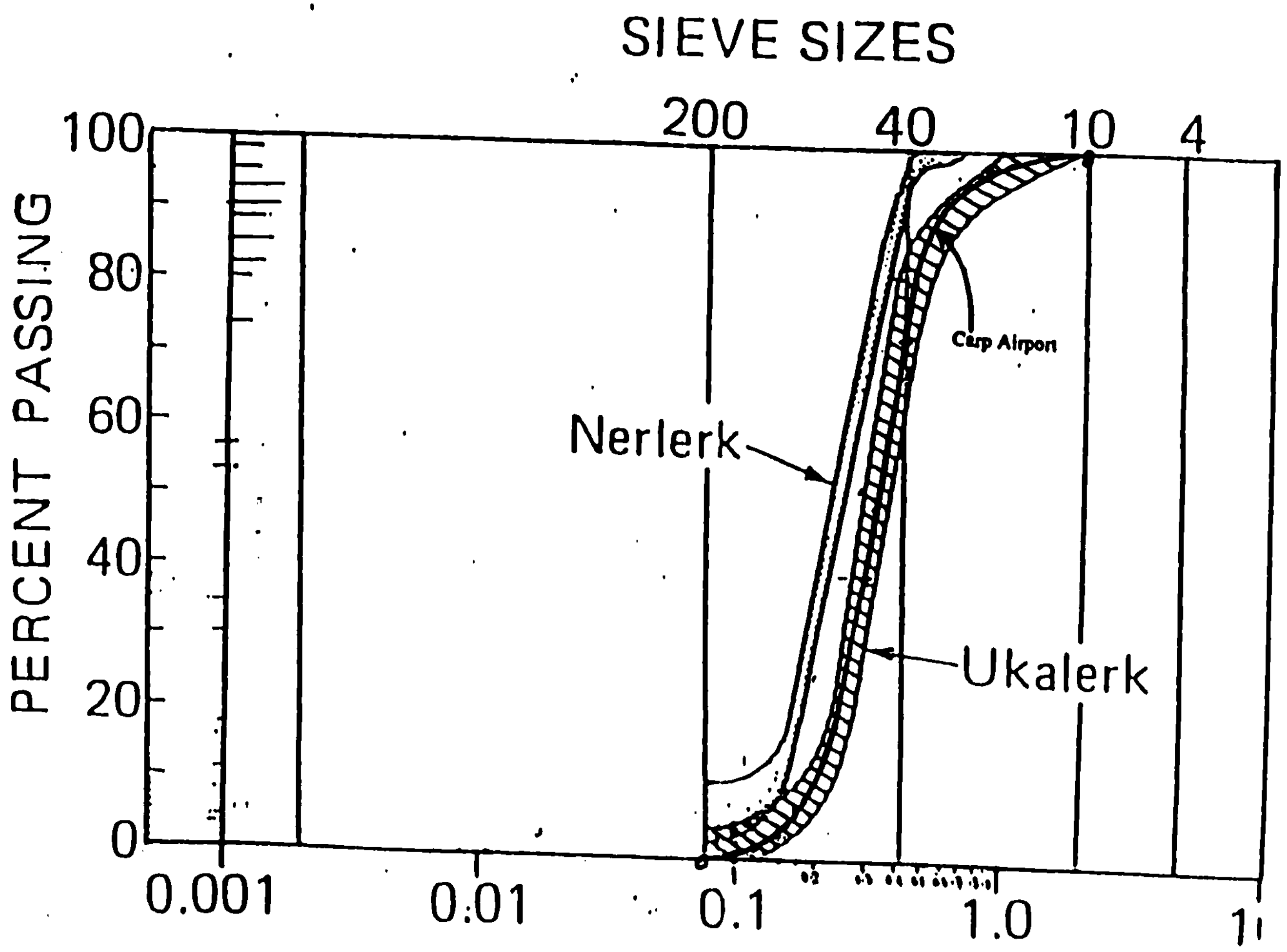

4.5 Determination of Hydraulic Conductivities

The constant head method was used to conduct a series of 4 permeability tests in order to determine the hydraulic conductivites in every layer composing the soil system. The first test was carried out to determine the conductivity in the horizontal tube. This test was performed before any sample was placed in the left vertical column. The second test was done for an equivalent system consisting of the saturated soil in the vertical column and the sand in the horizontal tube. From the equivalent hydraulic conductivity concept, an expression was derived to obtain the hydraulic conductivity of the saturated layer of sand in the vertical column. Similar tests were done to determine the coefficients of permeability of the soil in the capillary zone and the sand layer which was initially dry. The soil in the capillary zone was partially saturated. Since these tests were performed at 20 ° C, no correction was necessary to account for the effects of viscosity.

Using the constant head method the coefficient of permeability of soil is given by:

$$K_1 = \frac{Q * L_1}{A * h * t_1} \text{ for soil 1} \tag{4.5}$$

or

$$t_1 = \frac{Q * L_1}{A * h * K_1} \tag{4.6}$$

Similarly for soil 2

$$t_2 = \frac{Q * L_2}{A * h * K_2} \tag{4.7}$$

for the equivalent system

$$t = \frac{Q * L}{A * h * K} \qquad (4.8)$$

where:

t_1, t_2 are respectively the time required by water to travel in soil 1 (horizontal tube) and soil 2 (vertical glass column).

t is the equivalent time required to travel through the system encompassing both soils.

K_1, K_2, and K are respectively the hydraulic conductivity in soil 1, soil 2, and the equivalent corresponding soil system.

Q is the flow rate flowing through the soil: A is the cross section of the glass column:

L_1 and L_2 are the lengths of the sand masses in the horizontal tube and in the vertical column:

L is the total length of the sand mass consisting of soil 1 and soil 2.

The equivalent time t is the summation of t_1 and t_2. Substitutions of (4.6) and (4.7) into (4.8) gives:

$$t = \frac{Q * L_1}{A * h * K_1} + \frac{Q * L_2}{A * h * K_2} \qquad (4.9)$$

Equating equations (4.8) and (4.9) gives:

$$\frac{Q * L}{A * h * K} = \frac{Q * L_1}{A * h * K_1} + \frac{Q * L_2}{A * h * K_2} \qquad (4.10)$$

Solving for K_2 we get:

$$K_2 = \frac{L_2}{\left(\frac{L}{K} - \frac{L_1}{K_1}\right)} \tag{4.11}$$

K = 0.0280 cm/s.

K_1 = 0.0189 cm/s,

L_1 = 81.8 cm.

L_2 = 130 cm

L= 211.8 cm

The value of K were obtained experimentally. The results of the permeability tests which helped to determine K and K_1 are shown on Tables 4.4 and 4.5.

Substituting the numerical values in equation (4.11) yields:

$$K_2 = \frac{130}{\left(\frac{211.8}{0.0280} - \frac{81.8}{0.0189}\right)}$$

$$= 0.0402 \text{ cm/s}$$

Similarly using the derivation of equation (4.11), the hydraulic conductivities of the soils in the capillary zone and the sand layer which was initially dry were obtained.

The results of the third and fourth permeability tests for the partially saturated and initially dry sand layers gave the following:

K_{r1} = 0.0240 cm/s

$K_{r2} = 0.0233$ cm/s

with

$L_{r1} = 240.8$ cm

$L_{r2} = 241.8$ cm

where:

K_{r1} is the equivalent hydraulic conductivity of the system consisting of the partially saturated sand, the fully saturated sand in the vertical column, and the highly packed fully saturated sand in the horizontal tube.

k_{r2} is the equivalent hydraulic conductivity consisting of the entire four soil layers in the J-tube.

L_{r1} is the length of the soil system composed of the highly packed fully saturated sand in the horizontal tube, the fully saturated sand, and the partially saturated sand in the vertical column..

L_{r2} is the total length of the four layers of soils in the J-tube.

using the derivation of equation (4.11), K_3 and K_4 were obtained as follows:

$$K_3 = \frac{L_3}{\left(\frac{L_{r1}}{K_{r1}} - \frac{L}{K}\right)} \tag{4.12}$$

$$K_4 = \frac{L_4}{\left(\frac{L_{r2}}{K_{r12}} - \frac{L_{r1}}{K_{r1}}\right)} \tag{4.13}$$

where:

K_3 = hydraulic conductivity of the partially saturated sand

K_4 = hydraulic conductivity of the initially dry sand layer

L_3 = length of the partially saturated sand

L_4 = length of the initially dry sand

L_3 = 29 cm and L_4 = 1 cm

Substituting the numerical values in equations (4.12) and (4.13) gives:

$$k_3 = \frac{29}{\left(\frac{240.8}{0.0240} - \frac{211.8}{0.0280}\right)} = 0.0117 \text{ cm/s}$$

and

$$k_4 = \frac{1}{\left(\frac{241.8}{0.0233} - \frac{240.8}{0.0240}\right)} = 0.029 \text{ cm/s}$$

The results of the hydraulic conductivities of the soil system are summarized on Table 4. 6

Table 4.4 Coefficient of permeability results for the fully saturated sand in the horizontal tube.

Project: K for the horizontal tube Job No. ______

Location of Project: CBY laboratory D113

Description of Soil: Natural sand

Tested by: MEGNOLO Date of Testing: August 17th, 1994

Sample Dimensions: Diam. 5.022 cm; Area 19.80 cm²

Mass soil + pan Init. 7587.5 g; Ht. 81.80 cm

Mass soil + pan Final 4587.5 g; Vol. 4620.46 cm³

Mass of Sample 3000 g; Density, ρ 1.85 g/cm³

Constant Head

h = 42 cm

Test data / *Test data cont'd*

Test No.	t, s	Q, cm³	T, °C	Test No.	t, s	Q, cm³	T, °C
1	300	60	20°	1	300	60	20°
2	300	55	20°	2	300	55	20°
3	300	60	20°	3	300	60	20°
4	300	55	20°	4	300	55	20°
				Average	300	57.50	20°

$k_T = \frac{QL}{Aht} = \frac{57.50 \times 81.80}{19.80 \times 42 \times 300}$ = 0.0189 cm/s

$\alpha = \eta_T/\eta_{20}$ = 1

$k_{20} = \alpha k_T$ = 0.0189 cm/s

Table 4.5 Coefficient of permeability results for the equivalent system consisting of the sand in the vertical left column and the sand in the horizontal tube.

Project K for both the vertical & horizontal tubes Job No. ____

Location of Project CBY Geotechnical lab 1113

Description of Soil Natural sand

Tested by MEGNOLO Date of Testing June 9th 1994

Sample Dimensions: Diam. 5.022 cm; Area 19.80 cm^2

Mass soil + pan Init. ____ g Ht. 130 + 81.8 = 211.8 cm

Mass soil + pan Final ____ g Vol. 4193.64 cm^3

Mass of Sample ____ g Density, ρ ____ g/cm^3

Constant Head

h = 42 cm

Test data / *Test data cont*

Test No.	t, s	Q, cm^3	T, °C	Test No.	t, s	Q, cm^3	T, °C
1	300	35	20°	1	300	35	20
2	300	35	20	2	300	35	20
3	300	30	20	3	300	30	20
4	300	32	20	4	300	32	20
				Average	300	33	20°

$k_T = \frac{QL}{Aht} = \frac{33 \times 211.8}{19.80 \times 42 \times 300}$ = 0.0280 cm/s

$\alpha = \eta_T/\eta_{20}$ = 1

$k_{20} = \alpha k_T$ = 0.0280 cm/s

Table 4. 6 Summary of the hydraulic conductivity results in the soil.

Layer	Hydraulic conductivity (cm/s)
Initially dry sand	0.0290
Partially saturated sand	0.0117
Saturated sand in the vertical column	0.0402
Saturated sand in the horizontal column	0.0189
Entire soil system	0.0223

4.6 Finite Element Analysis of Potential Distribution in the J-Tube

4.6.1 Introduction

The analysis of a physical process that involve flow in a porous media usually requires the distribution of the potential gradient. Due to lack of adequate equipment in the lab. it was difficult to measure the distribution of air and liquid pressures in the soil system. One option was to use a commercially available finite element program written in FORTRAN to simulate the distribution of the pressure in the soil. The model used herein called FLUID (Logan, 1992) is simple and make it easy to incorporate a wide variety of physical conditions in the soil system. In addition, the input data required are minimal and fairly easy to input. The J-tube was discretized with triangular elements. Figure 4.6 shows the discretization of the tube. The results of the model simulation are listed in appendix D.

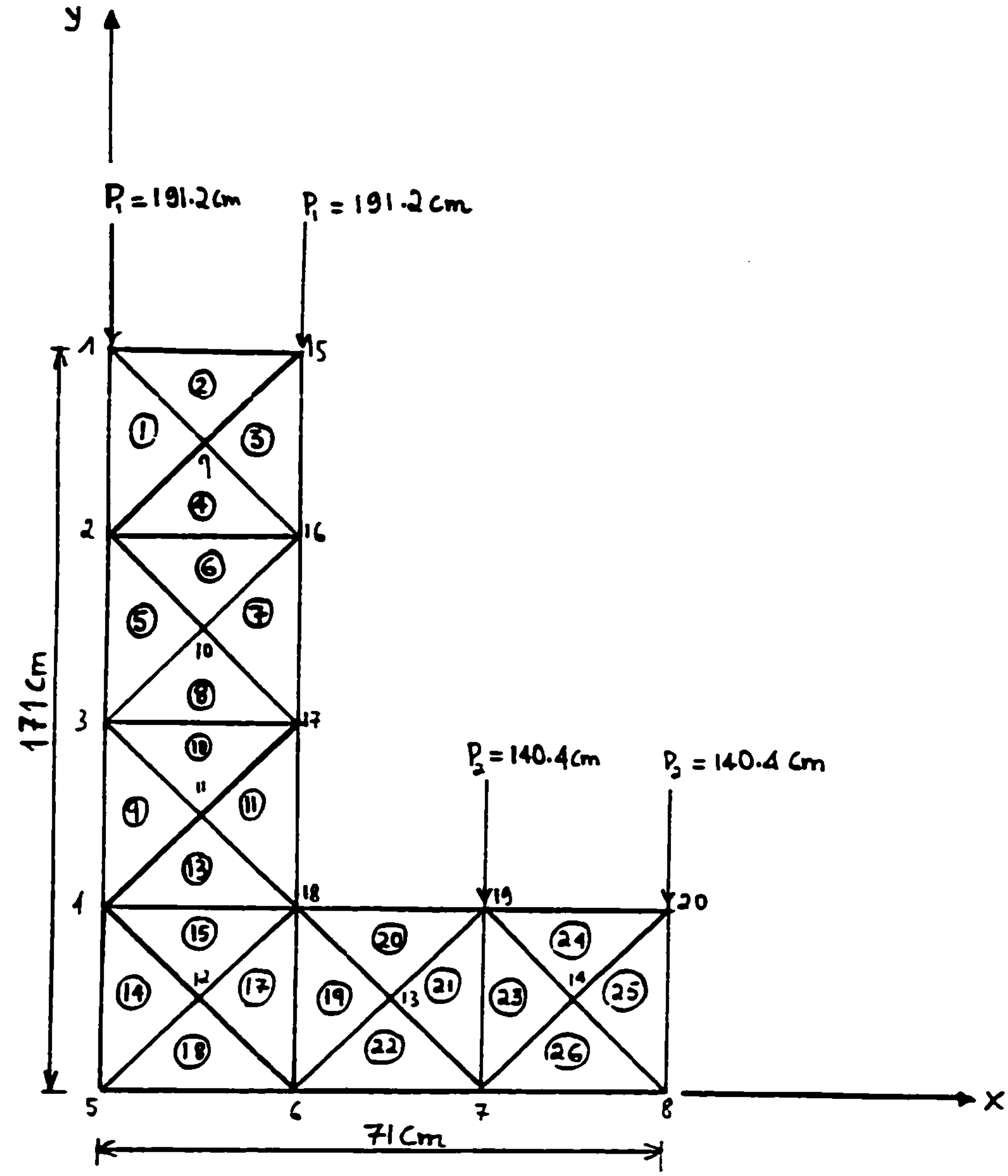

Figure 4. 6 Discretization of the J-tube.

4.6.2 Input Data

The specified nodal flow data were obtained from the potential equation:

$$P = h - z \qquad (4.14)$$

where:

P = total head

h = pressure head

z = elevation head

On the left vertical tube, the total head $P_1 = h_1 + z_1$ (4.15)

The pressure head on the right vertical tube. $P_2 = h_2 - z_2$ (4.16)

Given:

z_1 = 170.4 cm

z_2 = 10.40 cm

h_1 = 21.32 cm

h_2 = 130.0 cm

Therefore.

$P_1 = 21.32 + 170.4 = 191.72$ cm or 1.9172 m

$P_2 = 130 - 10.4 = 140.40$ cm or 1.4040 m

Program FLUID only deals with isotropic soils. For that reason the hydraulic conductivity used here is that of the entire soil system.

$k_{xx} = k_{yy} = 2.0 * 10^{-2}$ cm/sec

The variation of the total head distribution along the J-Tube is given on Figure 4.8

4.7 Determination of the pressure distribution using Darcy's law

Alternatively, Darcy's law was used to determine the total head at the top and bottom of each layer composing the soil system in the J-tube just at the beginning of the migration of oil in the soil. It was assumed that the pressure distribution within each layer was linear. For this analysis the points at which the total heads are sought are given in the figure below.

For soil 1, Darcy's law is given by:

$$Q_1 = K_1 * \left(\frac{(H_A - H_B)}{L_1} \right) * A \tag{4.17}$$

Where:

Q_1 is the flow per unit time

H_A and H_B are the total heads at points A and B,

K_1 is the hydraulic conductivity in soil 1 (initially dry sand).

L_1 is the length of soil 1.

A is the cross sectional area of the J-tube.

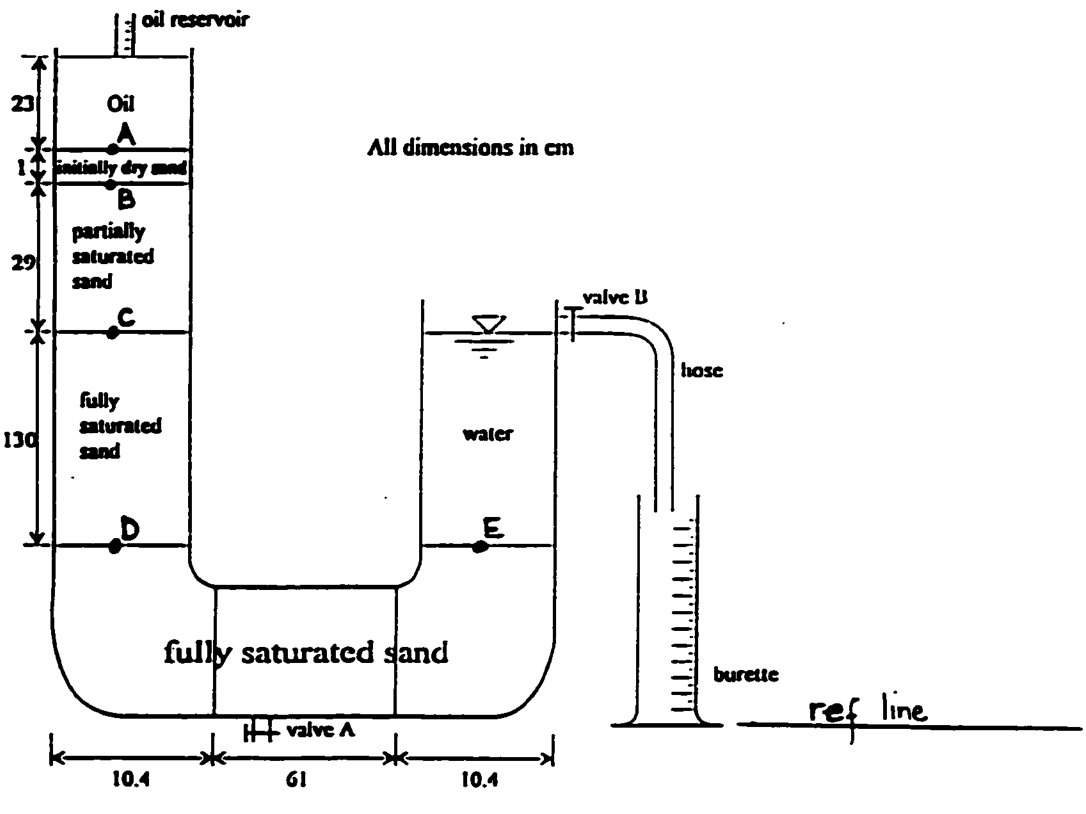

Figure 4.7 Points where Darcy's law is applied.

Similarly for soil 2, the partially saturated sand:

$$Q_2 = K_2 * \left(\frac{(H_B - H_C)}{L_2} \right) * A \tag{4.18}$$

For soil 3, the fully saturated sand:

$$Q_3 = K_3 * \left(\frac{(H_C - H_D)}{L_3} \right) * A \tag{4.19}$$

For soil 4, the highly packed fully saturated sand:

$$Q_4 = K_4 * \left(\frac{(H_D - H_E)}{L_4} \right) * A \tag{4.20}$$

The flow coming in and out of the tube is the same, therefore we have the following relations:

$$Q_1 = Q_4 \tag{4.21}$$

$$K_1 * \left(\frac{(H_A - H_B)}{L_1} \right) * A = K_4 * \left(\frac{(H_D - H_E)}{L_4} \right) * A \tag{4.22}$$

Solving for H_D, we get:

$$H_D = \frac{\frac{K_1}{L_1}(H_A - H_B)}{\frac{K_4}{L_4}} + H_E \tag{4.23}$$

$$Q_1 = Q_3 \tag{4.24}$$

$$K_1 * \left(\frac{(H_A - H_B)}{L_1} \right) * A = K_3 * \left(\frac{(H_C - H_D)}{L_3} \right) * A \tag{4.25}$$

Solving for H_C ,

$$H_C = \frac{\frac{K_1}{L_1}(H_A - H_B)}{\frac{K_3}{L_3}} + H_D \tag{4.26}$$

$$Q_1 = Q_2 \tag{4.27}$$

$$K_1 * \left(\frac{(H_A - H_B)}{L_1} \right) * A = K_2 * \left(\frac{(H_B - H_C)}{L_2} \right) * A \tag{4.28}$$

Solving for H_C ,

$$H_C = -\frac{\frac{K_1}{L_1}(H_A - H_B)}{\frac{K_2}{L_2}} + H_B \tag{4.29}$$

Equating equation (4.26) and equation (4.29), we have the following relation:

$$\frac{\frac{K_1}{L_1}(H_A - H_B)}{\frac{K_3}{L_3}} + H_D = -\frac{\frac{K_1}{L_1}(H_A - H_B)}{\frac{K_2}{L_2}} + H_B \tag{4.30}$$

Substituting the value of H_D from equation (4.23) in equation (4.30) yield:

$$\frac{\frac{K_1}{L_1}(H_A - H_B)}{\frac{K_3}{L_3}} - \frac{\frac{K_1}{L_1}(H_A - H_B)}{\frac{K_4}{L_4}} + H_E = -\frac{\frac{K_1}{L_1}(H_A - H_B)}{\frac{K_2}{L_2}} + H_E \qquad (4.31)$$

In equation (4.31), H_B is the only unknown, therefore rearranging this equation gives:

$$\frac{K_1}{L_1} H_A\left(\frac{L_2}{K_2} + \frac{L_3}{K_3} + \frac{L_4}{K_4}\right) + H_E = \left[\frac{K_1}{L_1}\left(\frac{L_2}{K_2} + \frac{L_3}{K_3} + \frac{L_4}{K_4}\right) + 1\right] H_E \qquad (4.32)$$

Given:

$K_1/L_1 = 0.0029/1 = 0.0029$

$L_2/K_2 = 29/0.00117 = 2478.63$

$L_3/K_3 = 130/ 0.0402 = 3233.83$

$L_4/K_4 = 81.8/ 0.0189 = 4328.04$

H_A = elevation head at point A - pressure head at A

= 170.4 - 21.3

= 191.7 cm of H_2O

Similarly

H_E = elevation head at point E - pressure head at E

=10.4 - 130

= 140.4 cm of H_2O

Substituting these values in equation 4.32 gives:

$$0.0029\,(10040.5)191.7 - 140.4 = (0.0029(10040.5)-1)H_B$$

solving for H_B we get:

$$H_B = 190.0 \text{ cm}$$

Substituting the value of H_B in equation (4.29) we get:

$$H_C = -0.0029(191.7-190.0) - 190.0$$
$$= 177.8 \text{ cm}$$

similarly

$$H_D = 0.0029\,(191.7-190.0) - 140.4$$
$$= 161.7 \text{ cm}$$

The results of the pressure distribution in the J-tube are summarized in Table 4.7. Figure 4.8 shows the total head distribution along the tube using both Darcy's law and the finite element (FEM) program FLUID.

Table 4.7 Pressure distribution at the top and bottom of each layer in the J-tube.

Point	Pressure head (cm)	Elevation head (cm)	Total head (cm)
A	21.3	170.4	191.7
B	48.6	141.4	190.0
C	37.4	140.4	177.8
D	151.3	10.4	161.7
E	130.0	10.4	140.4

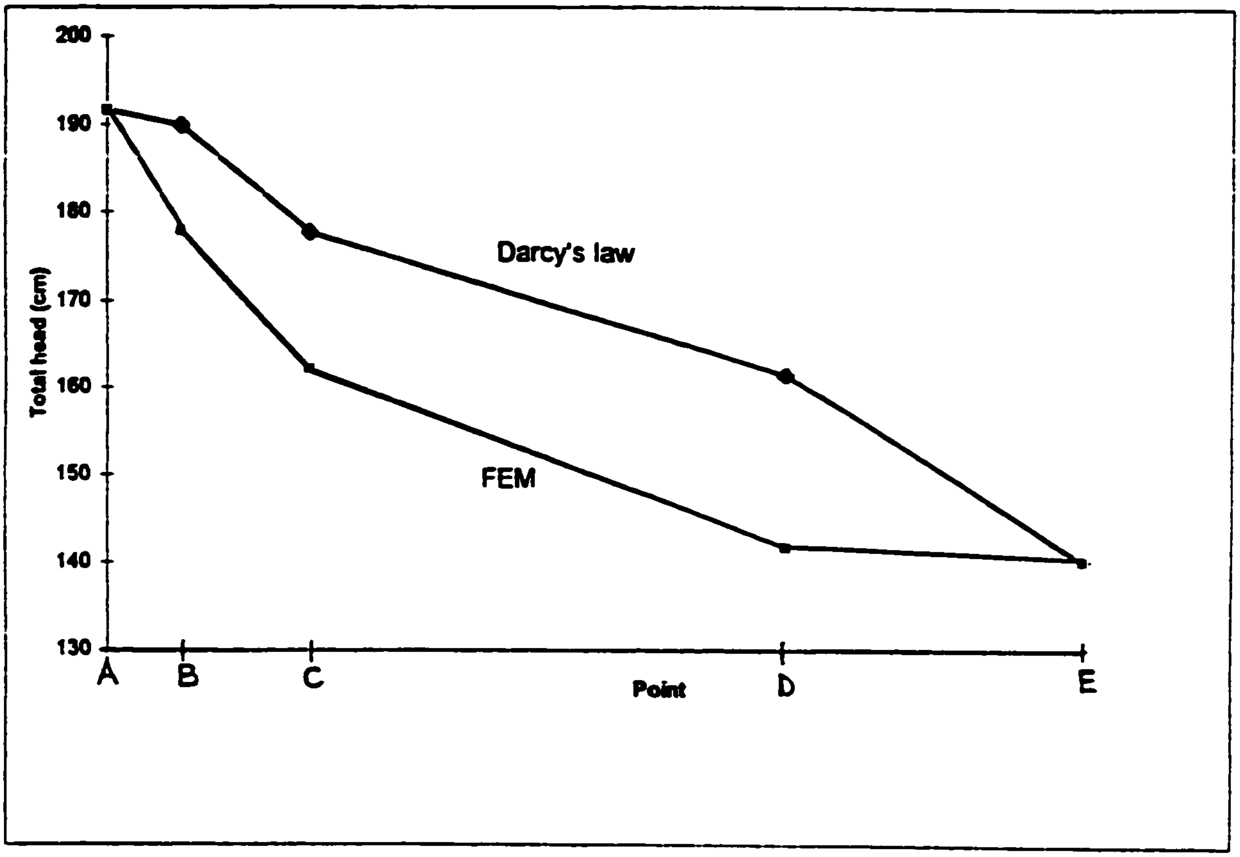

Figure 4.8 Variation of the total head distribution along the J-Tube.

4.7.1 Comparison of the total head obtained using both methods.

The results of the variation of the total head distribution using Darcy's law and the finite element program FLUID shows that the total head distribution obtained with the finite element method (FEM) were underestimated, since the program assumed that the soil was isotropic. This was not the case. In fact the layers composing the soil

4.7.2 Determination of the hydraulic conductivities of oil contaminated soil.

At this juncture of the dissertation, the hydraulic conductivities are determined for the oil contaminated layers composing the soil system, including the partially saturated sand. the fully saturated sand in the left vertical column, and the highly saturated packed fully saturated sand contained in the horizontal tube.

It took respectively 5, 62, and 100 days for the contaminant to reach the partially saturated sand layer, the fully saturated in the left vertical column, and the highly packed fully saturated in the horizontal tube. Figures 4.9, 4.10, and 4.12 show the location of the oil's front in the J-tube after 5, 62, and 100 days. Darcy's law was once again used to determine the hydraulic conductivity of the oil contaminated soil layers.

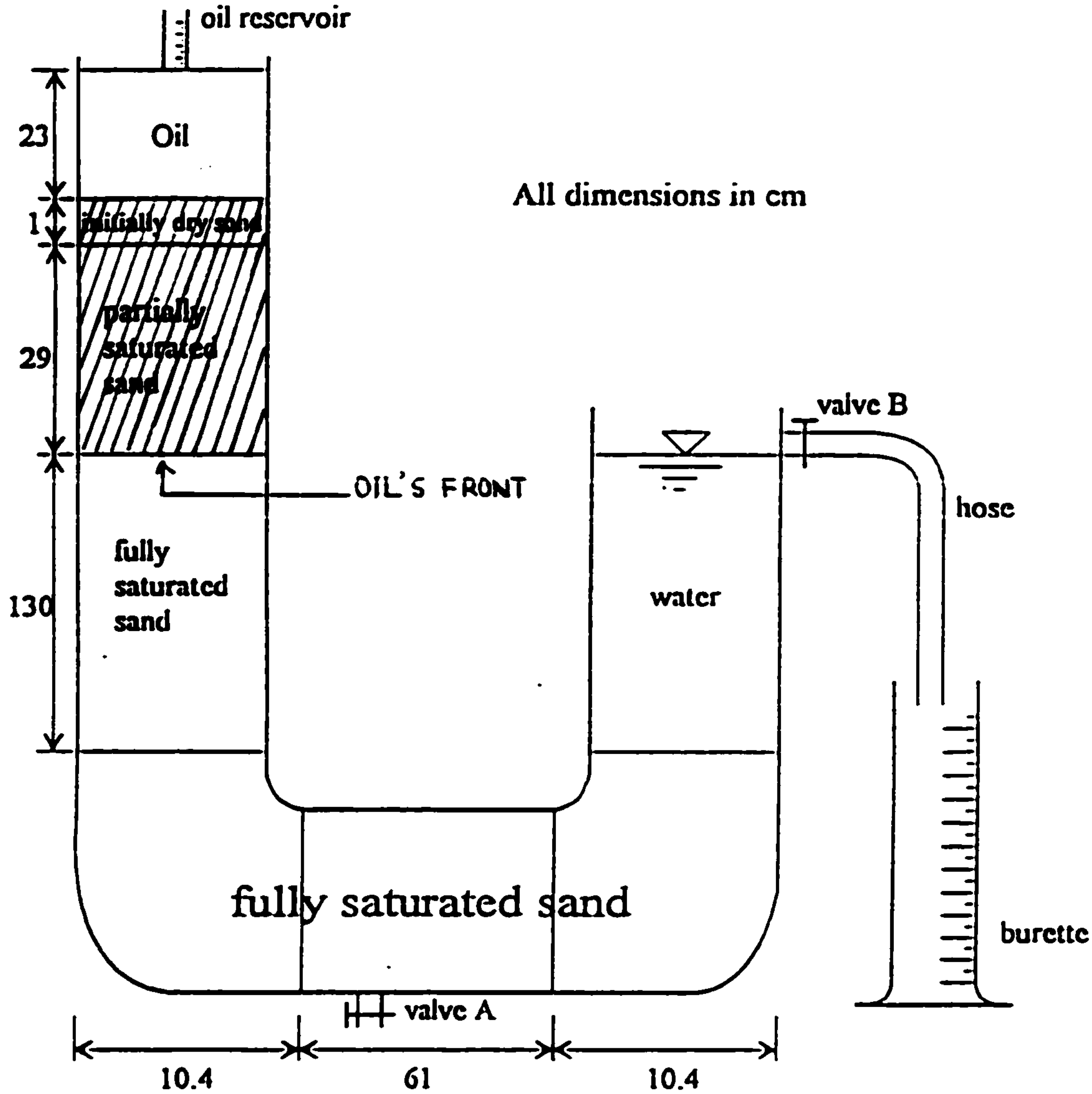

Figure 4.9 Location of the oil's front in the J-tube after 5 days.

The flow rate at the oil's front after 5 days is given by:

$$Q_1 = K^*_5 \frac{H_A - H^*_5}{L^*_5} A * \Delta t \tag{4.33}$$

Where:

Q_1 = volume of water displaced by oil after 5 days,

K^*_5 = hydraulic conductivity of the contaminated soil after 5 days.

H^*_5 = total head at the location of the oil's front after days.

H_A = total head at the top of the initially dry sand layer,

A = cross sectional area of the J-tube,

Δt = time corresponding to the location of the contaminant in the soil,

L^*_5 = location of the contaminant in the soil after 5 days.

Solving for K^*_5, gives:

$$K^*_5 = \frac{Q_1 * L^*_5}{\left(H_A - H^*_5\right) * A * \Delta t} \tag{4.34}$$

Similarly,

$$Q_2 = K_3 \frac{H^*_5 - H_D}{L_3} A * \Delta t \tag{4.35}$$

Where:

Q_2 = volume of water displaced by oil after 5 days.

K_3 = hydraulic the fully saturated clean sand in the left vertical column.

H_D = total head at the top of the saturated clean sand layer in the left vertical column.

L_3 = length of the fully saturated sand in the left vertical column.

H^*_5, A, and Δt are defined above.

Solving for H^*_5, we get:

$$H^*_5 = \frac{Q_2 * L_3}{K_3 * A * \Delta t} + H_D \qquad (4.36)$$

Similarly:

$$Q_3 = K_4 \frac{H_D - H_E}{L_4} A * \Delta t$$

Q_3 = volume of water displaced by oil after 5 days.

K_4 = hydraulic conductivity of the highly packed saturated clean sand in the horizontal tube.

H_E = total head at the end of the highly packed saturated clean sand in the horizontal tube.

L_4 = length of the highly packed saturated clean sand in the horizontal tube.

H_D, A, and Δt are defined above.

Solving for H_D:

$$H_D = \frac{Q_3 * L_4}{K_4 * A * \Delta t} + H_E \qquad (4.37)$$

For continuity, the flow going in and out in the soil system must be same, hence:

$Q_1 = Q_2 = Q_3$

Given:

$Q_3 = 5\ cm^3$

$L_4 = 81.8\ cm$

$K_4 = 0.0189\ cm/s$

$A = 19.81\ cm^2$

$\Delta t = 432000\ sec$

$H_A = 191.7\ cm$

$H_E = 140.4\ cm$

Solving for H_D gives:

$$H_D = \frac{5 * 81.8}{0.0189 * 19.81 * 432000} + 140.4$$

$$= 2.53 * 10^{-4} - 140.4$$

$$= 140.403\ cm$$

Therefore,

$$H^*_5 = \frac{5 * 130}{0.0402 * 19.81 * 432000} + 140.403$$

$$= 140.405\ cm/s$$

Hence,

$$K^*_5 = \frac{5 * 30}{(191.7 - 140.405) * 19.81 * 432000} = 3.42 * 10^{-7}\ cm/s$$

Table 4.8 Total head distribution at selected points in the J-tube after 5 days.

Point	Pressure head (cm)	Elevation head (cm)	Total head (cm)
A	21.3	170.4	191.7
location of oil front	0.05	140.4	140.405
D	130.03	10.4	140.403
E	130.0	10.4	140.400

After 62 days, the previous procedure was repeated:

$$Q_1 = K^{\bullet}_{62} \frac{H_A - H^{\bullet}_{62}}{L^{\bullet}_{62}} A * \Delta t \qquad (4.38)$$

Solving for $K^{\bullet}_{62}$, gives:

$$K^{\bullet}_{62} = \frac{Q_1 * L^{\bullet}_{62}}{\left(H_A - H^{\bullet}_{62}\right) * A * \Delta t} \qquad (4.39)$$

$$Q_2 = \frac{H^{\bullet}_{62} - H_E}{L_4} A * \Delta t \qquad (4.40)$$

Solving for $H^{\bullet}_{62}$, we get:

$$H^{\bullet}_{62} = \frac{Q_2 * L_4}{K_4 * A * \Delta t} + H_E \qquad (4.41)$$

Given:

$Q_2 = 635\ cm^3$

$L_4 = 81.8$

$K_4 = 0.0189$

$A = 19.81\ cm^2$

$\Delta t = 5356800\ sec$

$L^*_{62} = 160\ cm$

$H_A = 191.7\ cm$

$H_E = 140.4\ cm$

Substituting these values gives:

$$H^*_{62} = \frac{635 * 81.8}{0.0189 * 19.81 * 5356800} + 140.4 \quad = 140.4003$$

Therefore,

$$K^*_{62} = \frac{635 * 160}{(191.7 - 140.4003) * 19.81 * 5356800} = 18.66*10\text{-}6\ cm/s$$

Table 4.9 Total head distribution at selected points in the J-tube after 62 days.

Point	Pressure head (cm)	Elevation head (cm)	Total head (cm)
A	21.3	170.4	191.7
location of oil front	$3*10^{-3}$	140.4	140.4003
E	130.0	10.4	140.400

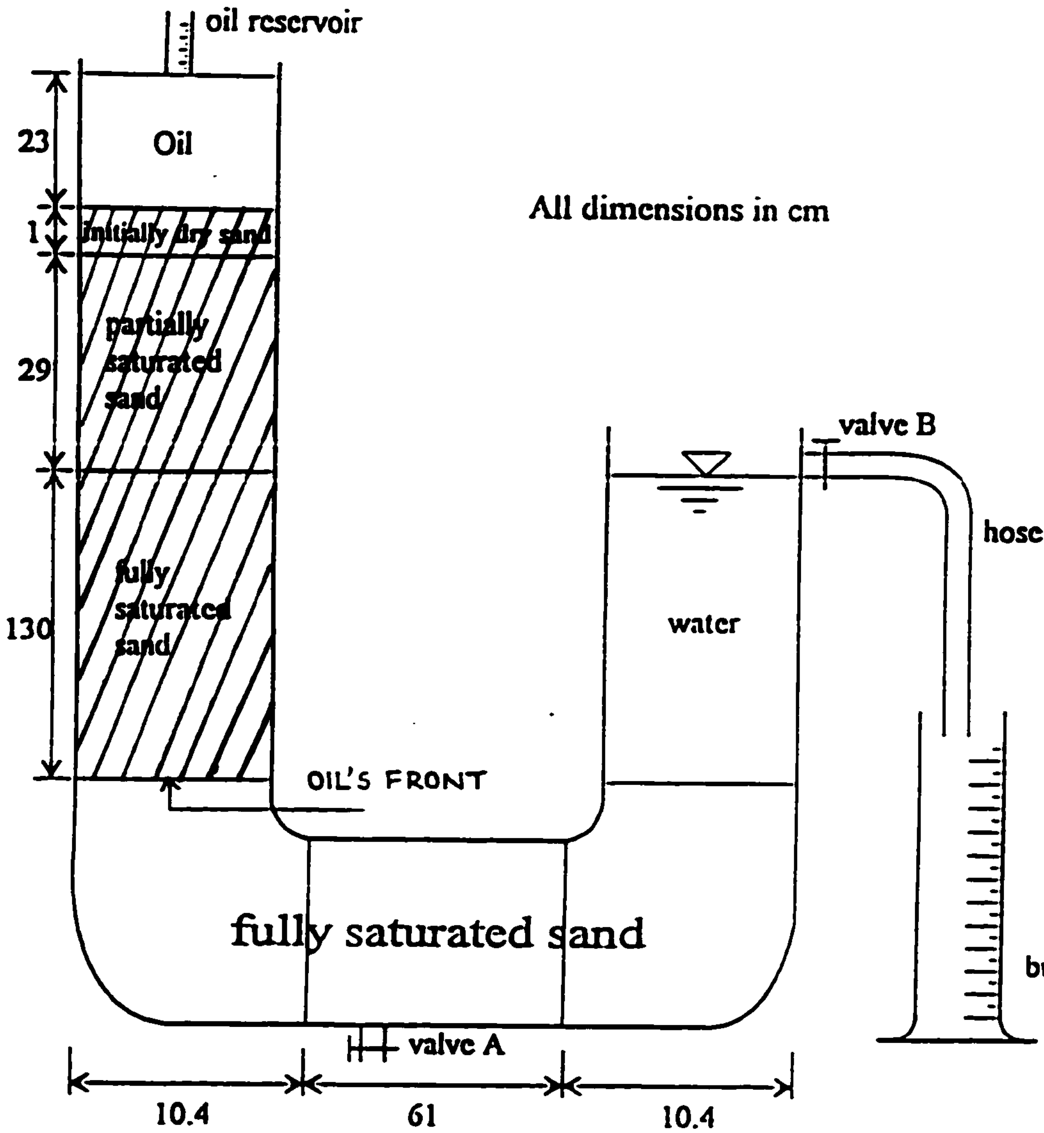

Figure 4.10 Location of the oil's front in the J-tube after 62 days.

Similarly after a 100 days, the entire soil was contaminated and:

$$K^{*}_{100} = \frac{Q * L^{*}_{100}}{(H_A - H_E) * A * \Delta t} \tag{4.42}$$

Given:

$Q = 3250\ cm^3$

$L^{*}_{100} = 241.8\ cm$

$H_A = 191.7\ cm$

$H_E = 140.4\ cm$

$A = 19.81\ cm^2$

$\Delta t = 8640000\ sec$

Solving for K^{*}_{100}, gives:

$K^{*}_{100} = 8.95 * 10^{-5}\ cm/s$

Table 4.10 Total head distribution at selected points in the J-tube after 100 days.

Point	Pressure head (cm)	Elevation head (cm)	Total head (cm)
A	21.3	170.4	191.7
location of oil front	130	10.4	140.4

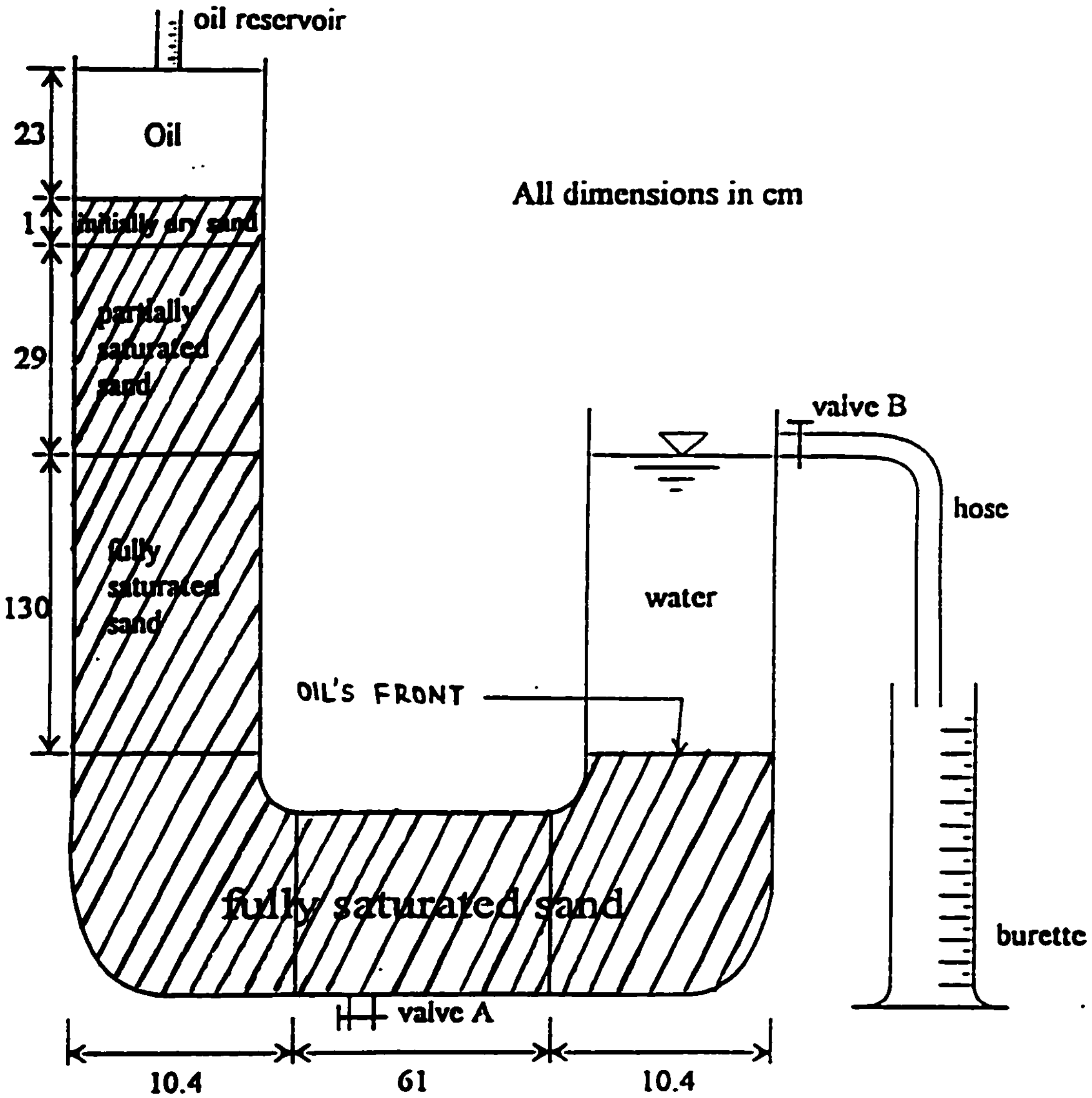

Figure 4.11 Location of the oil's front in the J-tube after 100 days.

Table 4.11 Hydraulic conductivity in the oil contaminated soil with time.

Time (days)	Location of oil in the soil	Hydraulic conductivity of oil contaminated soil (cm/s)
0	top of the initially dry sand layer	$2.0*10^{-2}$
5	bottom of partially saturated sand layer in the left vertical column	$3.42*10^{-7}$
62	bottom of the saturated sand layer in the vertical column	$18.66*10^{-6}$
100	entire soil system	$8.95*10^{-5}$

Note: At the beginning of the oil migration process, the hydraulic conductivity considered is that of the equivalent soil system.

The ratio of change of the hydraulic conductivity due to the oil contamination of the soil is given by:

$$R = \frac{K^{*}_{0}}{K^{*}_{100}} = \frac{2.0*10^{-2}}{8.95*10^{-5}} = 223.5$$

Figure 4.12 shows the total head distribution in the J-tube at 5, 62, and 100 days.

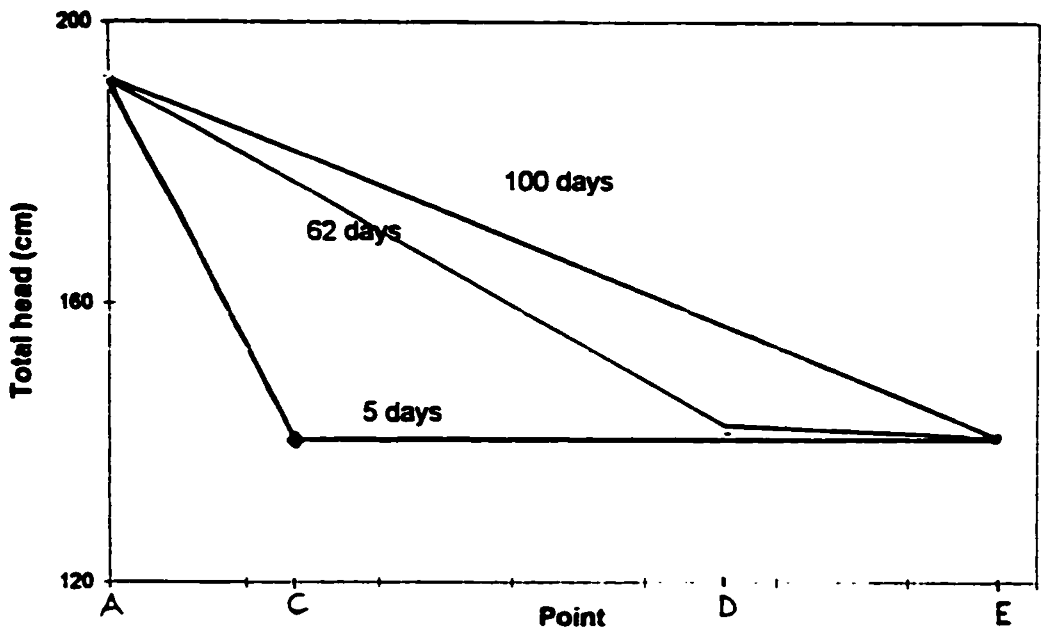

Fig. 4.11 Total head distribution in the J-tube as a function of time

4.7.3 Flow nets

It is aknowledged that oil migration in the artificial islands immediately following a blowout is a transient problem. However, in the following calculations steady-state conditions are assumed. The migration of oil in soils can be determined using a seepage analysis. Possible methods of solution of this problem include, the finite difference method, the finite element method, the use of physical hydraulic models, and construction of flow nets. In this problem trial and error sketching of flow nets were used to determine the time required by oil to travel in the caisson retained structure under steady-state conditions. Flow nets which are two-dimensional construction of a family of flow lines and a family of equipotential lines (lines of equal total head) were considered here because they are less complex than the other methods.

Problem

A caisson retained structure filled with a layer of 21 m of sand built on top of a 23.5 m thick layer of sand berm overlying an impermeable bed rock. The depth of water surrounding the caisson structure is 21 m.

Assumptions:

1. The head of oil on top of the sand filled core is 2 m.

2. The hydraulic conductivity of the sand is that of the equivalent soil consisting of the layers of sand in the laboratory scaled J-tube.

3. The caisson retained structure is symmetrical from its center line, thus the flow net of half of the structure is constructed with a scale of 1 mm = 0.5m. Figure 4.13 shows the construction of flow nets.

Given:

$$k = 2.0*10^{-2} \text{ cm/s} = 2.0*10^{-4} \text{ m/s}$$

$$h_1 = 2 \text{ m of oil} = 2\left(\frac{0.927}{1}\right) = 1.854 \text{ m of } H_2O$$

$$h_2 = 21 \text{ m}$$

The datum is 52.5 m below the deck of the caisson structure.

$$elv_1 = 44.5 \text{ m}$$

$$elv_2 = 23.5 \text{ m}$$

$$H_1 = h_1 + elv_1 = 1.854 + 44.5 = 46.354 \text{ m}$$

$$H_2 = h_2 + elv_2 = 21 + 23.5 = 44.5 \text{ m}$$

where:

H_1 and H_2 are the total heads at points 1 and 2, respectively.

h_1 and h_2 are the pressure heads at point 1 and 2, respectively.

elv_1 and elv_2 are the elevation heads at point 1 and 2, respectively.

Required:

The time required by Motormaster grade 50 oil to travel in the caisson retained structure if the structure is filled with Carp Airport sand.

Solution

From Darcy's law, the velocity in each flowline is given by:

$$v = ki \tag{4.43}$$

where:

v = the oil velocity from one equipotential to the other.

k = the hydraulic conductivity of the soil.

i = hydraulic gradient between two adjacent equipotential lines..

$$i = \frac{h_l}{l} = \frac{\left(\frac{\Delta H}{N_d}\right)}{l} = \frac{\Delta H}{N_d l} \tag{4.44}$$

l = distance travelled by oil between two adjacent equipotential lines.

ΔH = the head loss between the first and last equipotential lines.

N_d = the total number of potential drops.

$h_l = \frac{\Delta H}{N_d}$ = equipotential drop between two flow lines.

The time required by oil to travel between two adjacent equipotential lines is given by:

$$t_i = \frac{l_i}{v_i} = \frac{N_d (l_i)^2}{k\Delta H} \tag{4.45}$$

The total time required to travel is then:

$$t = \sum t_i = \sum_{1}^{7} t_i = \left(\frac{N_d}{k\Delta H}\right)\sum_{1}^{7} (l_i)^2 \tag{4.46}$$

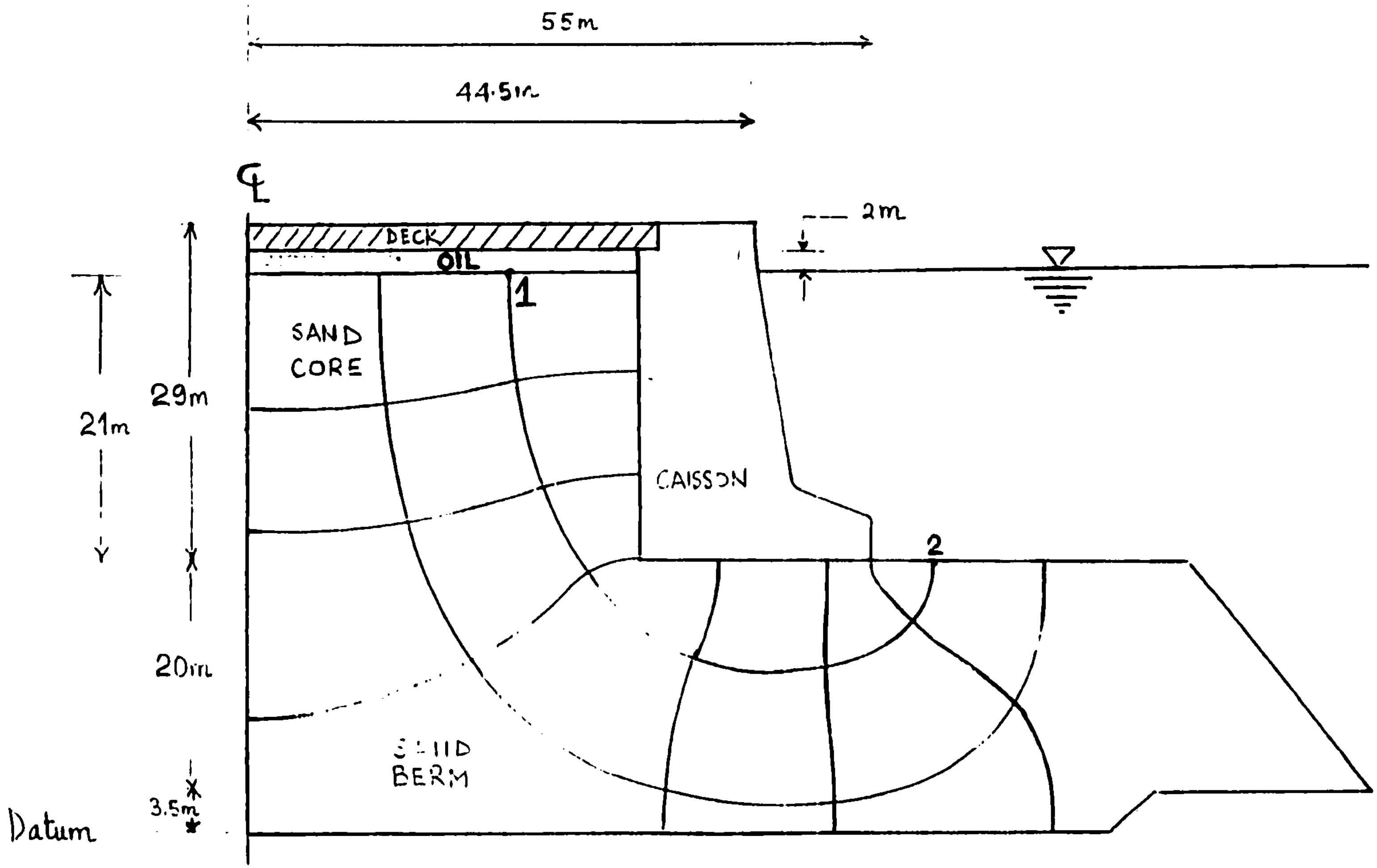

Figure 4.13 Flow net for oil migration.

From the flow nets construction, the following parameters were obtained:

$N_f = 3$ (number of flow channels)

$N_d = 7$

$l_1 = 9.50$ m

$l_2 = 9.50$ m

$l_3 = 9.00$ m

$l_4 = 12.0$ m

$l_5 = 11.5$ m

$l_6 = 9.00$ m

$l_7 = 4.50$ m

From equation (4.46) we get:

$$t = \left(\frac{7}{2 * 10^{-4} * 1.85}\right) \sum \left(9.5^2 + 9.5^2 + 9^2 + 12^2 + 11.5^2 + 9^2 + 4.5^2\right) = 120.9 * 10^5 \, seconds$$

t = 139.9 days or about 5 months.

4.8 Experimental Results

The displacement of one fluid by another within a porous medium can frequently be represented by a moving boundary problem. In this study, the duration of the migration of oil from the sand-filled core to the sea water level was monitored over a period of 8 months. At the end of the migration process, a large portion of the oil appeared to be immobilized in the soil. The results of oil migration through the soil in the J-tube are listed in appendix C.

Figure 4.14 shows the variation of the average velocity of oil in the soil. It appears from this graph that the displacement of oil through the soil was significant on the first week than the following weeks. The migration process was faster at that stage of the experiment since the first two layers composing the soil system were partly unsaturated and partly saturated under capillary effects, hence the oil found its way easily between the voids. On the fifth day, the velocity of oil migration reached a peak value of 5.6 cm /day, then gradually decreased to a local minimum of 3.82 cm /day on the tenth day. The velocity decreased considerably when the contaminant reached the initially water saturated layer.

The readings taken from the reservoir, includes the amount of oil added and the volume of water displaced. No water was displaced in the first 5 days, but 5 ml of water was collected in the burette on the 6th day of the experiment. Once the contaminant reached the right hand side of the J-tube, the displacement of water stopped.

The first appearance of oil on the right hand side of the tube occurred 100 days after it was released from the reservoir. Nevertheless only 20 ml of oil was recovered from the first 4000 ml initial applied oil from the reservoir. But oil was not the only fluid recovered. A mixture of oil-water-soil with a brownish color was also sampled. At first a greater percentage of this mixture was recorded, but at the end of the experiment only 250 ml of the mixture was collected, amounting only to 5 % of the total 5000 ml of oil used throughout the entire experiment. Meanwhile the total amount of oil recovered was about 350 ml which represents only 7 % of the total oil used. Since there was no leakage in the tube, it is fair to say that the remaining 88 % of the contaminant was trapped.

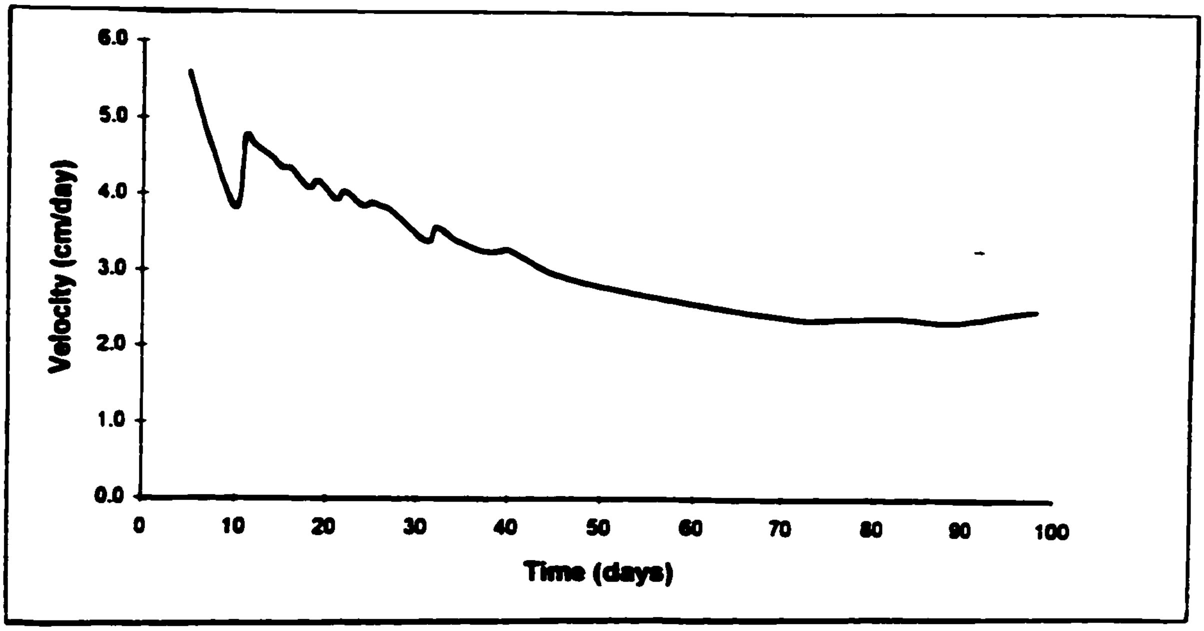

Figure 4.14 Variation of the average velocity of oil in the soil

4.8 Discussion of the Results

Laboratory experiments conducted in a scale Plexiglas J-tube to evaluate the mobility of a Motormaster grade 50 oil through a partially saturated Carp Airport sand (Ottawa), showed that oil tends to migrate through the unsaturated soil zone, replacing the air and some water. The migration's rate is governed by various factors including the viscosity of oil (a low-viscosity gasoline moving rapidly, a high-viscosity fuel moving slowly) and the permeability of soil.

In general, all oils are less dense than water, except bitumen and chlorinated solvents. Thus oil tend to float at the interface between the water saturated and unsaturated zones and spread horizontally. Oil usually moves as small droplets. Droplets smaller than soil pore dimensions, tend to move rapidly with the water. In order to generate such droplets, a considerable amount of energy is required, because of the large surface area in the J-tube cross section in comparison to the oil droplet surface. This energy requirement can be reduced if surfactants are present, since the presence of surfactant facilitates the formation of small mobile oil drops.

The observations of laboratory experiments of the current study concluded that the extent of residual oil saturation depends on the volume of oil applied. However other factors are responsible for the immobilised fraction of initially applied oil in the columns. Ajit et al. (1994) conducted a similar experiment. In their study, the concentration of oil residuals in the columns varied from 5% to 30% on a mass basis. They stated that the trapped oil in the soil during the migration process was due to the fact that the soil has a capacity to sorb hydrocarbons as they migrate with water in the subsurface. If for instance the amount sorbed is 10 times the dissolved amount, this will result to an immobilisation of 90% of the hydrocarbons, consequently the average velocity of oil migration will be reduced by a retardation factor of 10. This is why the migration velocity of hydrocarbons may depend on the sorption phenomenon.

Hydrocarbon sorption is governed by the presence of organic matter (detritus) in the soil. Sorption will prevail if only 1% or more of organic matter is present in the soil. Methods of estimating organic sorption are available. Lyman et al. (1982) reviewed schemes of estimating organic sorption. Extensive data and methods have also been provided by Hansch and Leo (1979), Mackay et al. (1985.b), Verschueren (1983), Zwolinski and Wilhoit (1971).

The immobilisation of oil in the soil is governed by other phenomena taking place in the subsurface environment during the migration process. In a porous medium containing more than one fluid, if one the fluid is nonwetting (oil) is in contact with a wetting phase (water), the wetting phase displaces some of the nonwetting phase in a process known as "free imbibition". After the oil has been displaced and mobilised by the infiltrating wetting fluid, oil will move as a result of viscous, gravitational and capillary forces. Through this migration process, oil is gradually spread in the soil and the capillary forces begin to immobilise the oil. At low oil saturation, the induced capillary forces creates discontinuities of the oil phase, eventually producing loss of continuity and as a result oil blobs are formed. According to Wilkinson et al. (1983), the high capillary forces are caused by the highly curved menisci between the oil and water phases in the soil pores. Studies conducted by Chatzis et al. (1984) concluded that residual oil can occupy up to 90% of the pore space. The present study is in agreement with them, since the residual oil concentration in our experiment amounted 88%.

It should also be noted that some fluids are soluble in water, thus they dissolve and migrate as a solution. Petroleum products, to a first approximation are insoluble in water. Nevertheless only a negligible portion dissolves. But this small amount (i.e., a few percent) is not negligible from the point of view of groundwater contamination. It only takes 1g of oil to contaminate a cubic meter of water to a level of 1 PPM. The solubility of oil in water depend on its composition and temperature but also the amount of water to which the oil has been exposed. According to Mackay (1983), a fuel oil may contaminate water to the extent of $10 g/m^3$ initially (ignoring oil droplets emulsions in the water), but as oil is washed with more water, this concentration may drop steadily. The rate at which the oil concentration will drop is uncertain. It is not clear if $1 g/m^3$ will be reached in 1 day or 1 month or 1 year.

In the present study, it was observed that a significant portion (88 %) of oil initially applied remained trapped in the soil. The mobilization or the trapping of the oily phase is usually governed by the capillary forces, but these forces can be overcome by the gravity forces or pressure gradient.

In order to understand the mechanisms taking place during the trapping of a nonwetting phase (oil) in saturated porous media, a quantitative analysis was carried out by Morrow and Songkran (1981). They introduced the ratio of the viscous to capillary forces expressed as a dimensionless number, commonly known as the capillary number (N_{CA}) and the ratio of gravity to capillary forces called the Bond number (N_B), which is also a dimensionless number. From their nonwetting phase mobilization experiments, they observed that for a Bond number less than 0.005 and a capillary number less than 10^{-6}, the trapping mechanism is dominated by capillary forces, and the residual oil saturation is constant.

Experiments conducted by Foster (1973) reported that the critical capillary number required to complete oil recovery from sandstone samples is of the order of 10^{-2} to 10^{-1}. Melrose and Brandner (1974) concluded that the parameters governing the critical capillary numbers are the pore structure and pore size distribution, consequently these parameters considerably affect the mobilization/immobilization process of the oil phase.

In Chapter 3, the Bond number and capillary number for Carp Airport soil were computed to be $0.7386.10^{-5}$ and $0.364.10^{-5}$, respectively. These numbers were below the critical values required to enhance any oil movement after immobilization. With the aid of these dimensionless numbers the explanation of why a high percentage (88 %) of oil trapped in the soil was clarified.

CHAPTER 5

SAND-STEEL INTERFACE BEHAVIOUR

5.1 Introduction

Oil contamination of soils may occur for various reasons including offshore accidents, accidental spills during transportation on land, leakage from the underground storage tanks and pipelines. In this study an experimental work is carried out to determine the changes that might be caused by oil contamination in the stress-strain behaviour of soils and the load transfer characteristics of interfaces between soils and structural materials. A series of monotonic two-dimensional interface tests with both clean and oil contaminated sands are investigated using the newly developed C3DSSI apparatus (Evgin and Fakharian,1995) and (Fakharian and Evgin,1993, 1995, 1996).

5.2 C3DSSI Apparatus

All the experiments were conducted with a constant surcharge pressure (accuracy: 5 KN) applied on the sand surface using the new C3DSSI (Cyclic 3-Dimensional Simple Shear testing of Interfaces) developed by (Fakharian and Evgin 1993, 1996). Figures 5.1 and 5.2 show the C3DSSI apparatus used herein. The C3DSSI is equipped with a computer control system consisting of a personal computer (PC) and two electric-pneumatic (E/P) transducers.

The PC connected to the computer system must have sufficient memory (at least 4 Meg of Ram and 100 Meg of hard drive) in order to run the test. The primary task of the PC is to collect and process raw experimental data during each test at a frequency controlled by a variable included in the source code of the program. The algorithm of this program written in basics computes the engineering quantities such as stiffness, shear stress, volume change in the sand mass and tangential displacement. These quantities are displayed on the PC monitor and stored on the hard drive. The output results transferred from the electric pneumatic transducers to the PC are easily retrieved if the latter is equipped with Windows and its applications including Microsoft Excel.

The E/P transducers regulate the aforementioned engineering quantities including the normal load while the experiment is in progress. These quantities are measured in terms of voltage transmitted from appropriate electric signals to the E/P transducers. The E/P transducers then transfer these informations to the PC for processing through an analogue/digital (A/D) converter. During two-dimensional testing only one of the E/P transducers is in operation.

One of the virtues of the C3DSSI apparatus lies on its flexibility to allow the use of either a simple shear box or a direct shear box container. For the purposes of these monotonic tests a direct shear box was used.

The container of the sand mass was a square aluminium box with a 100 x 100 mm internal area and a height of 28 mm. The thickness of the sand mass in the box was about 24 mm. The bottom of the aluminium container was attached to a foam. The requirement to use the layer of foam were to minimise the leakage of sand and oil during shearing. In addition, to minimise the friction between the steel surface and the aluminium box a 1 mm thick sheet of Teflon was coated to the bottom of the foam layer.

The C3DSSI apparatus was equipped with two transducers (stepper motors) measuring the tangential loads (in the x and y directions) and five linear variable differential transformers (LVDTs) monitoring the displacements (tangential and normal). During 2D monotonic tests only two of the five LVDTs and one stepper motor were in operation. One of the LVDTs was used to measure the tangential displacement in the x direction (accuracy: 0.002 mm) and the other measured the change of sand height (accuracy: 0.004 mm). The tangential load in the x direction was applied with the aid of the stepper motor in operation.

The structural steel material used throughout these experiments had a space of 315 mm in length and 315 mm in breadth. The sand-blasted sand-steel interface was 160 mm in length and 160 mm in breadth. The roughness of the steel surface was evaluated in R_{max} with a gage length L= 2.5 mm (Uesugi and Kishida, 1986).

5.3 Type of materials

a) Sand

The soil used in these experiments is a crushed quartz sand, Silica-24, with a specific gravity of 2.65. Figure 5.3 shows the grain size distribution of the sand (sand = 2). From the grain size distribution it appears that the sand is a fine to medium sand. Using the

ASTM standards, the minimum and maximum void ratio where obtained: $e_{min} = 0.42$ and $e_{max} = 1.13$.

b) Oil

The oil used throughout these experiments is a Motomaster grade 50 heavy duty oil. At 24° C the density of this oil is about 0.927 g/cm^3 and its viscosity is 455 mPa.s.

c) Structural Material

Sand-blasted structural steel specimen with a roughness of R_{max} (L= 2.5 mm) were used throughout the experiments.

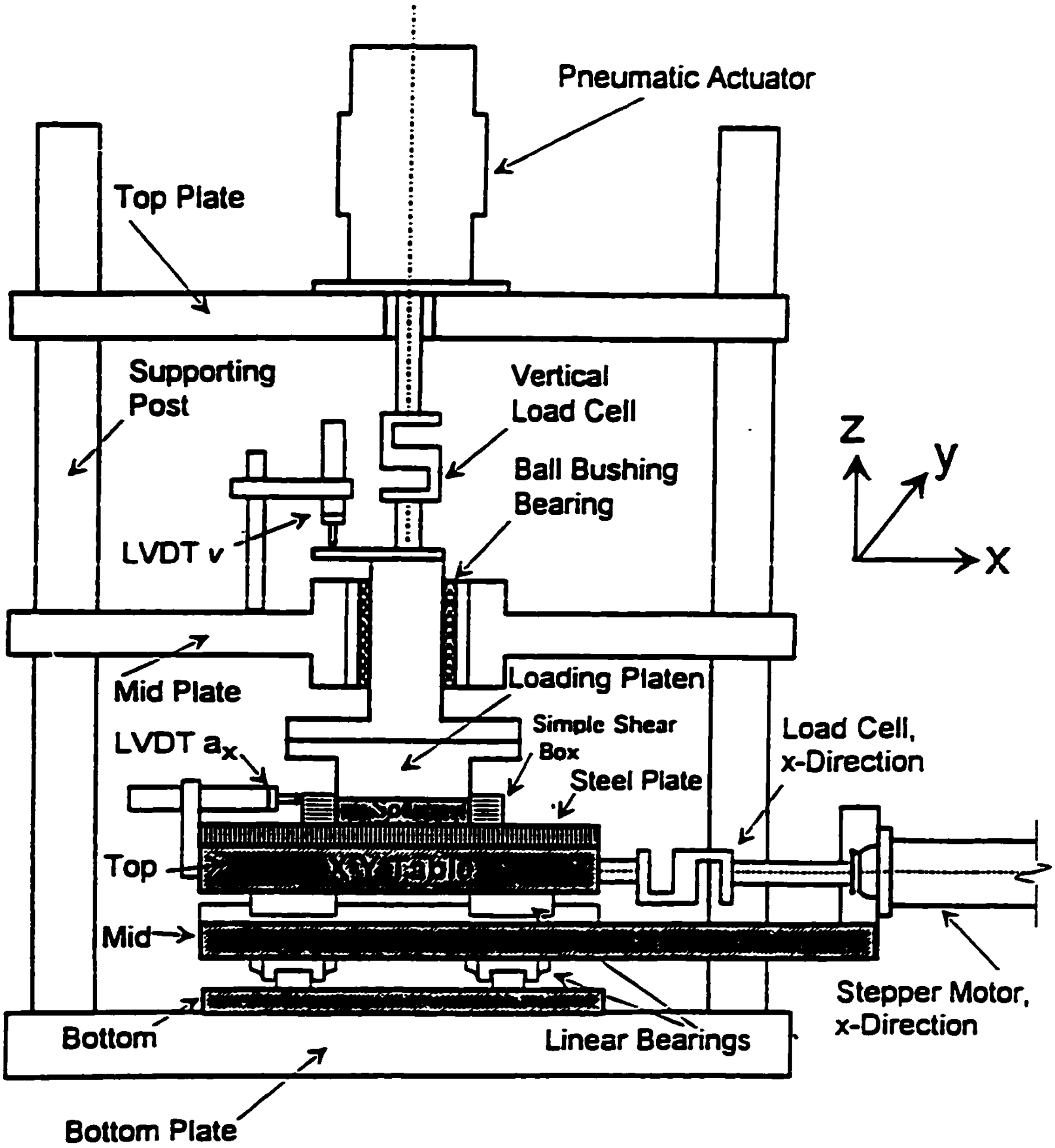

Figure 5.1 Schematic view of C3DSSI. (After Fakharian, 1996)

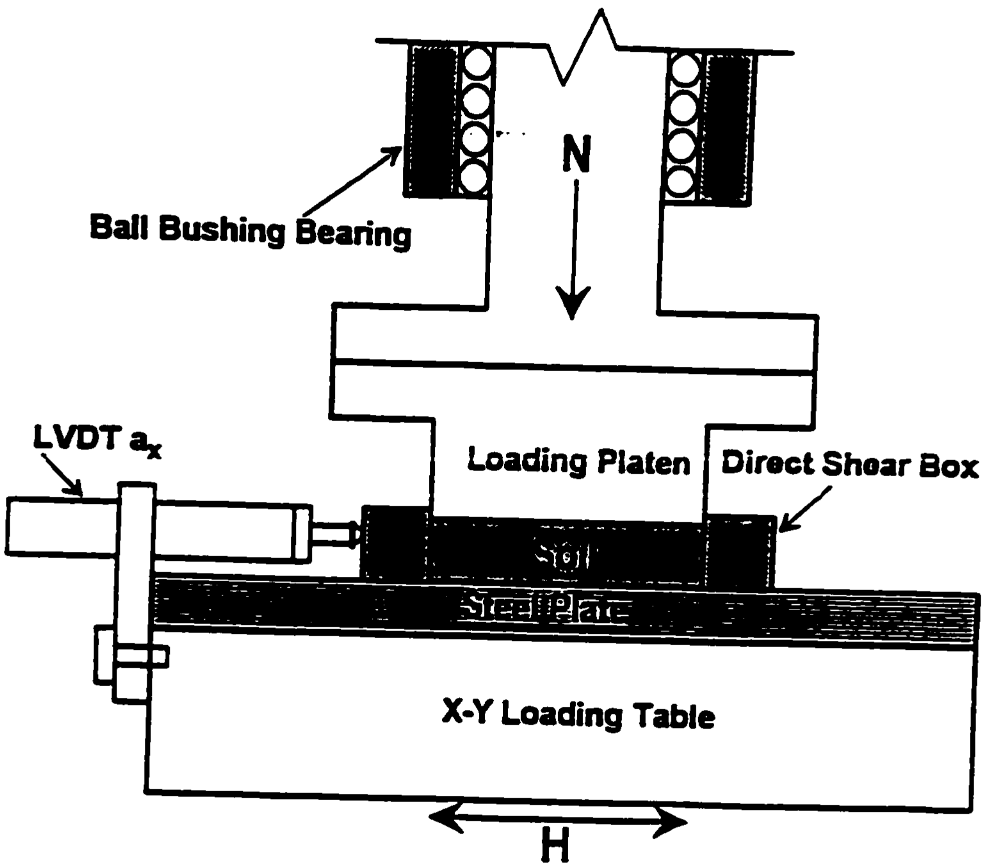

Figure 5.2 Schematic of the direct shear box assembly. (After Fakharian, 1996)

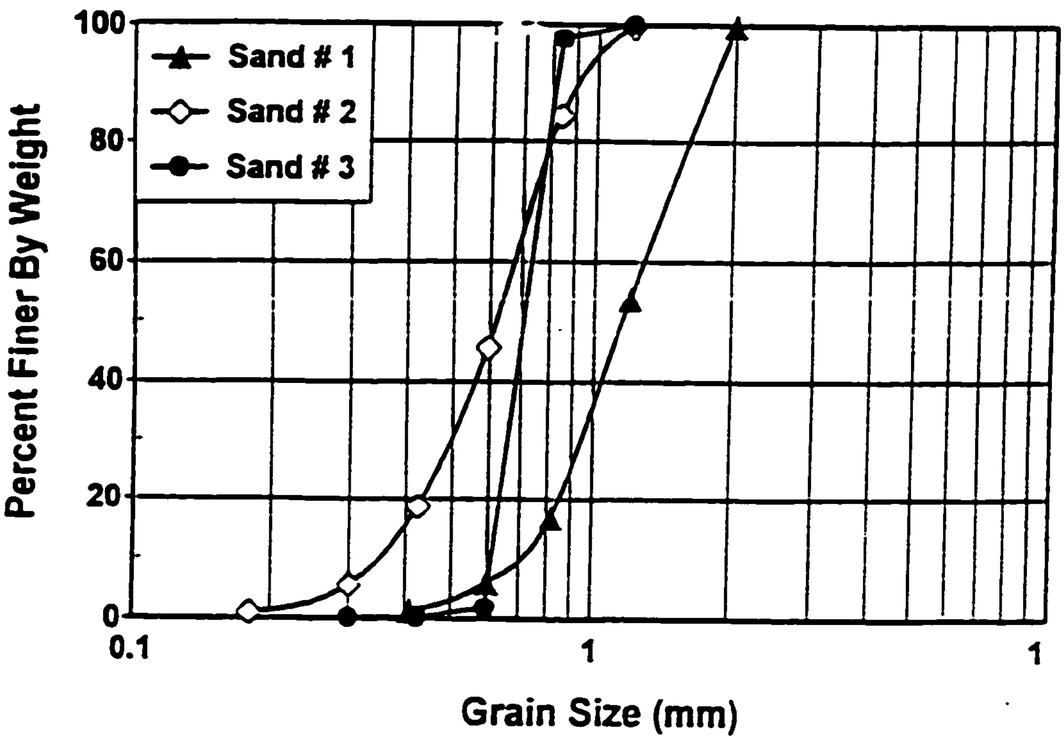

Sand # 1: Coarse Crushed Quartz (local # 16)

Sand # 2: Medium Crushed Quartz (local #24)

Sand # 3: Ottawa Sand, 20-30, ASTM C-190

Figure 5.3 Grain size distribution of crushed quartz sand.

5.4 Sample Preparation

5.4.1 Preparation of Clean Sand Specimen

The sand was placed in the rigid aluminium container and it was in contact with the sand-blasted steel surface. Two methods were used to prepare the sand samples, namely the multiple sieving pluviation (MSP) method for dense sand specimens and the scooping method for loose sand specimens.

5.4.1.a Multiple Sieving Pluviation Method

Studies on the mechanical properties of cohesionless soils have shown that non-uniformity may be introduced during the sample preparation. The multiple sieve pluviation (MSP) method has been proven to be free from human error. For material having a relatively small uniformity coefficient, Miura and Tori (1982) found that the high density can be achieved by the MSP without vibration or impact. The reasons for using the MSP stems from the fact that static and dynamic deformation-strength characteristics at various densities are affected by the manner in which the soils are prepared.

A preparation method of sand specimen using a multiple sieving pluviation apparatus was used. With this method the desired specimen density can be achieved by controlling the rate of sand discharge and by adjusting the height of fall. The apparatus used herein consists of a funnel to store sand, a stopper to release the sand in the cylinder, a cylinder equipped with four layers of sieves each with a square opening of 4.76 mm and a fixing device to set up both the funnel and cylinder vertically. The requirements for using square opening sieves of 4.76 mm diameter were to account for the maximum soil particle size and thus insure a uniform deposition of sand, so as to produce a homogeneous sample. The rate of discharge was controlled by changing the diameter of the nozzle attached at the bottom of the funnel. To achieve a desired density the height of fall and the nozzle diameter were adjusted accordingly. Experimental results presented in the Japanese Society of Soil Mechanics and Foundation Engineering of 1979 have shown that the relative density slightly decreases with an increase in the height of fall for larger nozzles diameters. It therefore appears that the governing factors of the MSP method are: (1) the size of nozzle opening and (2) the height of fall.

Following the description of the MSP method a dense sand with a relative density of 84% was prepared. To achieve that density a 13 mm diameter nozzle and a height of 550 mm were used. A necessary weight of sand was then filled in the funnel, with the stopper in position. As soon as the stopper was removed, the sand was pluviated into the container (braced to the steel plate) through the four sieves until it was filled to its capacity. Then the stopper was placed in position again to stop the sand from flowing in the container. Excess sand from the box was sucked through a tube connected to a vacuum source in such a way that the height of the sand in the box was brought to 24 mm.

5.4.1.b The Scooping Method

This method was used to achieve loose sand densities. To avoid disturbance of the sample the sand was carefully scooped with a spoon in the sand container and filled to its capacity. The excess sand in the container was sucked using a vacuum to obtain the desired 24 mm sand height in the box.

5.4.2 Preparation of Oil Contaminated Sand Specimen

Before raining or scooping the sand using the aforementioned methods in sections 5.2.1 and 5.2.2, a volume of 25 ml of Motormaster oil grade 50 was poured at the bottom of the sand container. There was no need to fill up the aluminium container with oil since the present study is only interested in the activities taking place at the sand-steel interface.

Observations of clean sand particles near the interface using a macroscopic photography was made by Uesugi et al. (1989) to determine the shear zone formation along the sand-steel interface. These observations indicated that the tangential displacement of sand particles were distributed linearly in the shear zone at about 65% for a the total tangential displacement of 4.0 mm. Large shear deformations occurred between 65 and 90% of the total displacement. These observations showed that the shear zone formation was about 5 mm or 21% of the sand mass above the steel plate. Assuming that some capillary rise of oil will take place in the shear box, therefore the 25 ml (or 2.5 mm in height) of oil used in the box is reasonable.

5.5 Type of Loading

The applied normal load at the top of sand mass was kept constant at a specified value during each test. The tangential displacement was increased at a constant rate of 1.0 mm/min while a load cell measured the tangential load.

5.6 Experimental Results

Characteristics of sand-steel interfaces have been presented by Kishida and Uesugi (1987). Their test results concluded that direct shear tests could be used only to obtain the coefficient of interface friction. Their conclusions were based on the fact that the total tangential displacement in the direct shear tests includes the displacement due to deformation of the sand within the box as well as the sliding displacement of the interface. Thus the values of the displacements are influenced by the height of the sand mass. But depending on the type of engineering applications, the results of sand-steel interface behaviour using the direct shear box may be of interest. A parameter such as the angle of friction between soil and structural material, δ is very useful for instability investigation in problems involving the design of structures such as piles. retaining walls. and foundations. For these aforementioned problems the results of interface testing using a direct shear device could be reliable.

A series of direct shear tests conducted by Acar et al. (1982) showed that the relative density and normal stress were indeed the governing parameters influencing the angle of friction between sand and various structural materials such as steel, wood, and concrete. Other factors such as the roughness of the surface, composition of soil, grain size distribution, moisture content, and rate of shearing also influence the shear strength of the interface under conditions of normal stress and monotonic shearing. These studies concluded that a combination of low normal stress and high relative density will yield a high angle of friction. Their results are presented in Figure 5.4.

The experimental results of the current study (two-dimensional monotonic tests for interface between sand and sand-blasted surface on a steel plate) are plotted in the form of shear stress (kPa) versus tangential displacement (mm), and normal displacement (mm) versus tangential displacement (mm) curves presented in Figures 5.5 through 5.26. The ratio of the normal and the shear stress were also computed. The maximum shear resistance versus normal stress gave frition angle δ between sand and the steel surface at the interface. The frition angle δ was calculated using the following equation:

$$\tau = c + \sigma \tan \delta \qquad (5\text{-}1)$$

Where τ is the peak shear strength of the soil, σ is the applied normal stress, c is the cohesion of the soil, for sand $c = 0$, and δ is the friction angle between the soil and the structural material. The variations of the peak strength versus the applied normal load strength were plotted for all the cases (clean dense, oil contaminated dense, clean loose, and oil contaminated loose sand) in Figures 5.12, 5.13, 5.14, and 5.15 respecitvely. The strength parameter δ for each scenario is given in Table 5.1.

Table 5.1 Values of δ for various soil conditions.

Soil condition	Value of δ (degrees)
Clean dense sand	37 3
Oil contaminated dense sand	27 7
Clean loose sand	30 4
Oil contaminated loose sand	25 1

A comparison of the results between clean and contaminated sand showed that there was a significant difference in the interface friction angle δ. For instance at a normal load of 300 kPa under clean dense conditions, the value of the interface friction angle was about 36.1°. For the same normal load under contaminated dense sand conditions this value was about 27.0°.

A similar comparison was made between loose samples for a normal load of 300 kPa. Experimental results showed that under clean conditions the interface friction angle was 29.7 °, while a value of 25.2° was recorded under contaminated conditions.

For both medium and loose sand the fiction angle changed significantly as a result of oil contamination. The effects of oil contamination on the stress-displacement relations were also evaluated.

Uesugi et al. (1989) evaluated the amount of particle crushed during testing by sieving the sand before and after the friction tests. They concluded that the influence of the sand type and normal stress in the increase of the coefficient of friction was overwhelming. Obviously it would be difficult to evaluate the amount of particles crushed for contaminated samples for the simple reason that a sieve analysis of contaminated specimen after testing is beyond our control for the time being. Therefore following their conclusions, it is fair to speculate that the amount of particles crushed at the interface layer under contaminated conditions is smaller than under clean conditions.

For a given normal stress, a more pronounced peak value was observed for the shear stress under clean conditions than for contaminated conditions. At relatively higher normal stresses (50, 100, 300, and 500 kPa) dense clean samples experienced strain softening after the peak until the shear stress leveled off at the residual shear value. This was not the case for contaminated dense specimen where no strain softening was observed. Under these normal stresses, volume change results of clean dense samples indicated some initial compression followed by an important dilation, whereas contaminated samples only exhibited a substantial compression.

At lower stresses (30, and 40 kPa) for all cases (dense- or loose-clean and dense- or loose-contaminated), the specimen reached a peak value and leveled off at that value with no record of strain softening. The results of the volume change indicated a compression of the sand mass for all cases. Nevertheless the magnitude of the mass compression was more pronounced in loose-contaminated samples than in other cases.

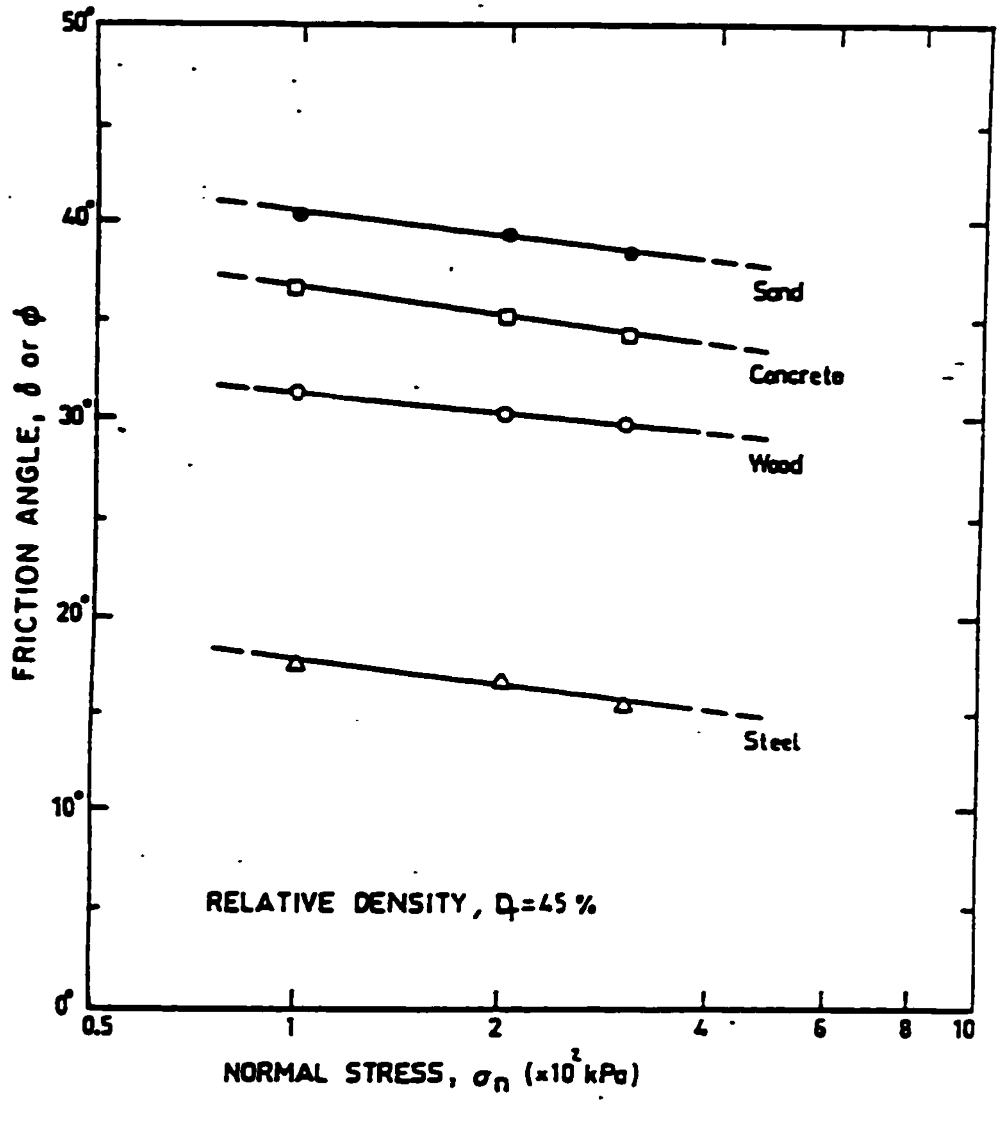

Figure 5.4 Variation of friction angle with normal stress. (After Acar et al., 1982)

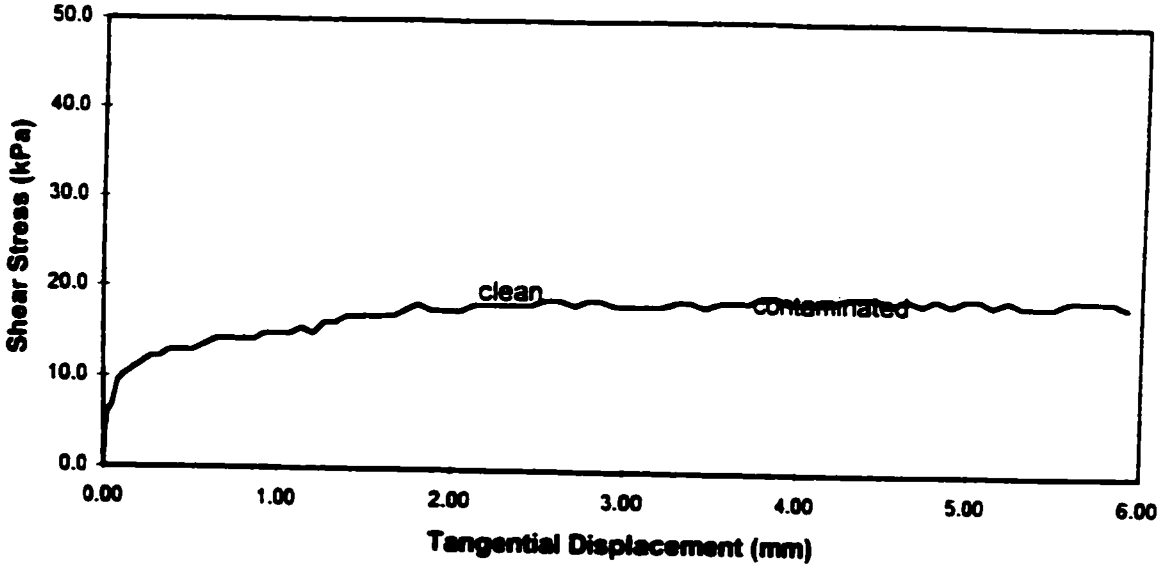

Fig. 5.5 2D monotonic test with constant normal stress of 30 kPa for dense sand.

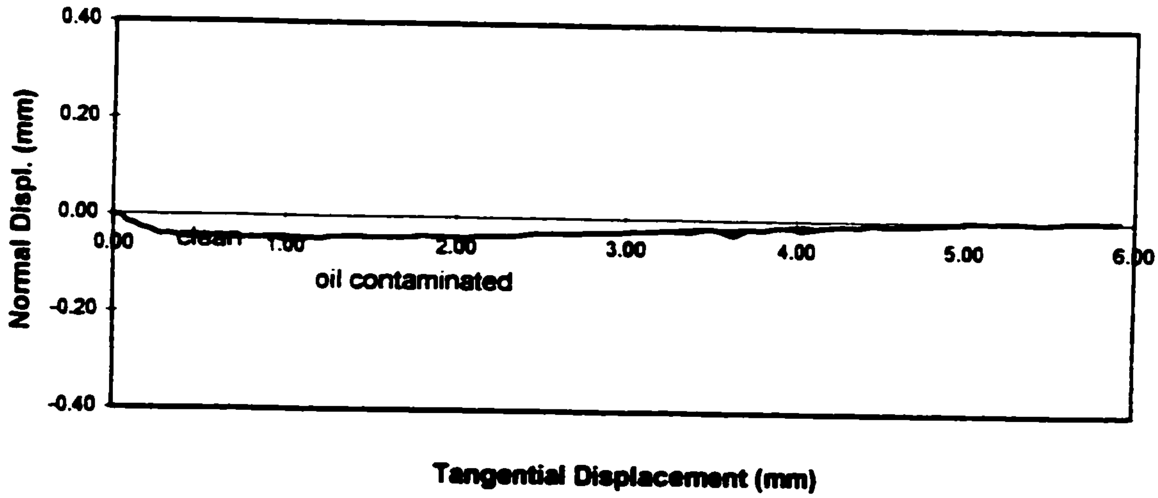

Fig. 5.6 2D monotonic test with constant normal stress of 30 kPa for dense sand

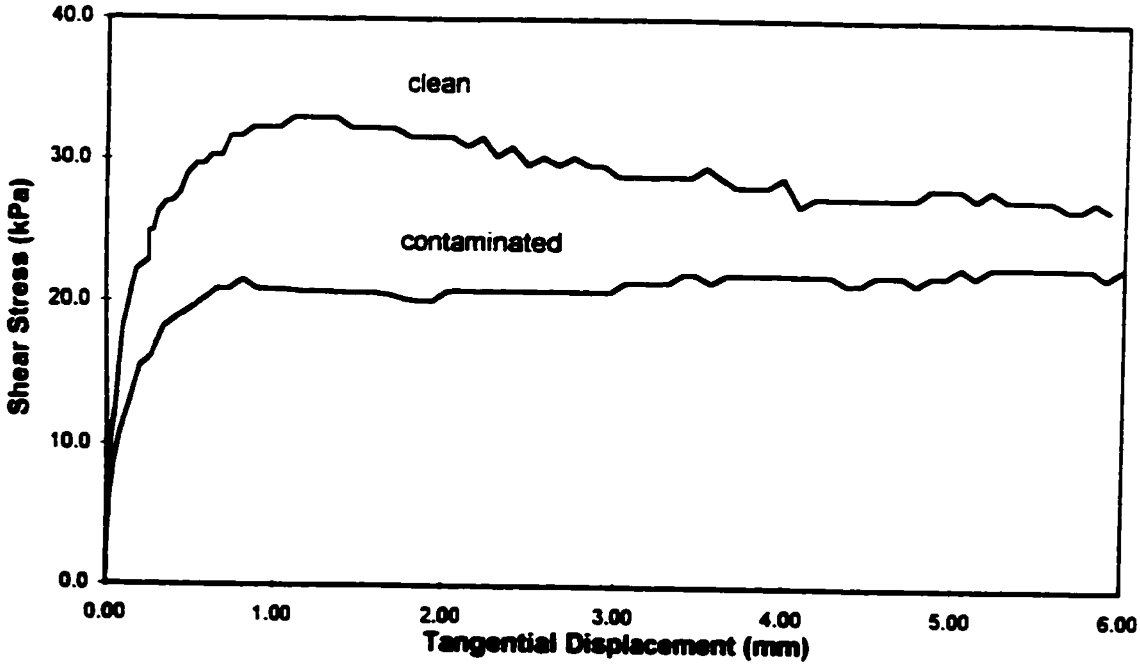

Fig. 5.7 2D monotonic test with constant normal stress of 40 kPa for dense sand.

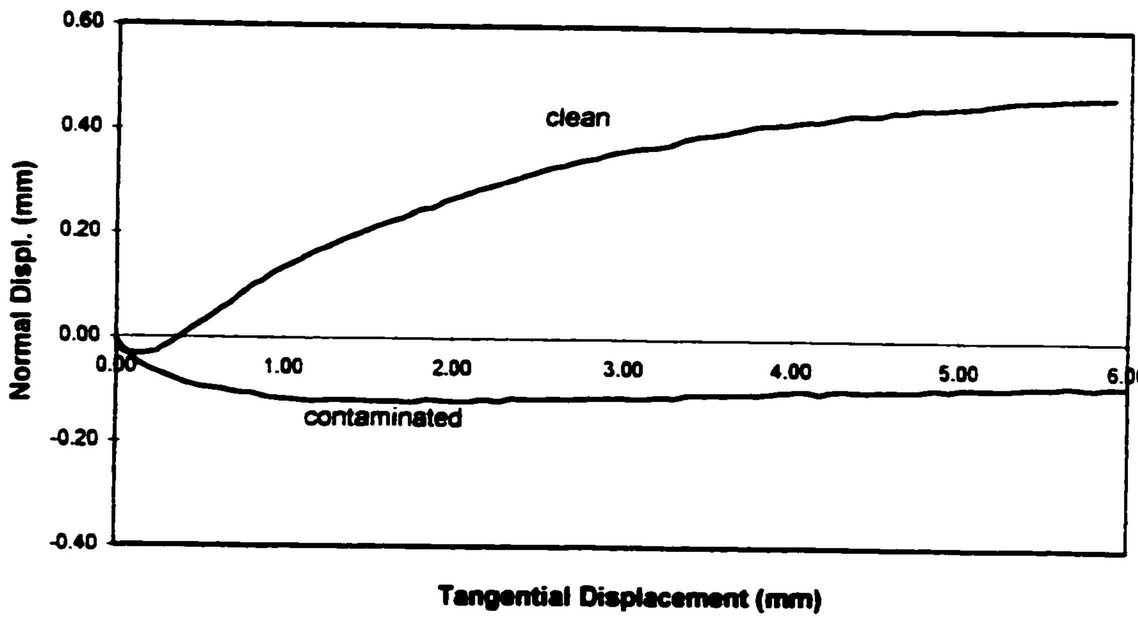

Fig. 5.8 2D monotonic test with constant normal stress of 40 kPa for dense sand

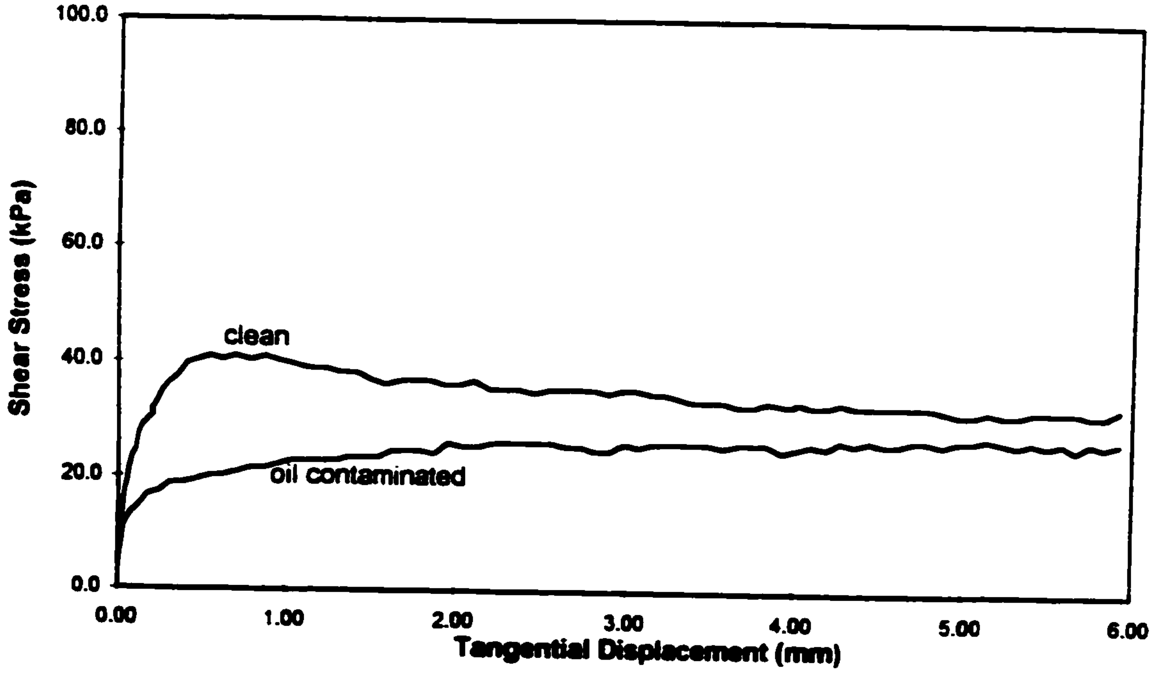

Fig. 5.9 2D monotonic test with constant normal stress of 50 kPa for dense sand.

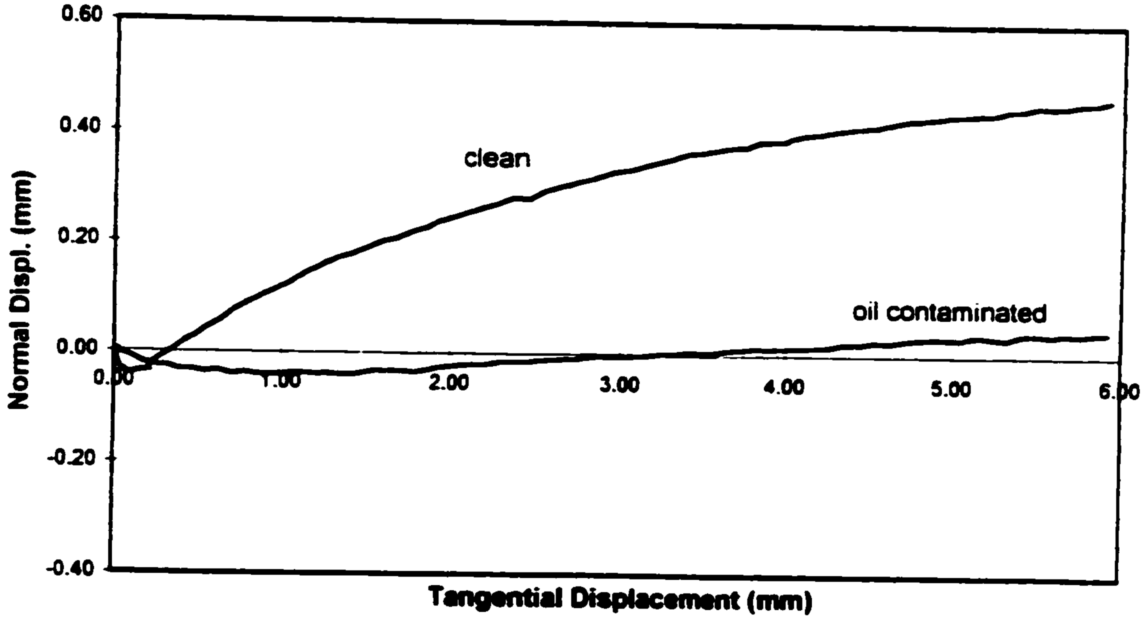

Fig. 5.10 2D monotonic test with constant normal stress of 50 kPa for dense sand

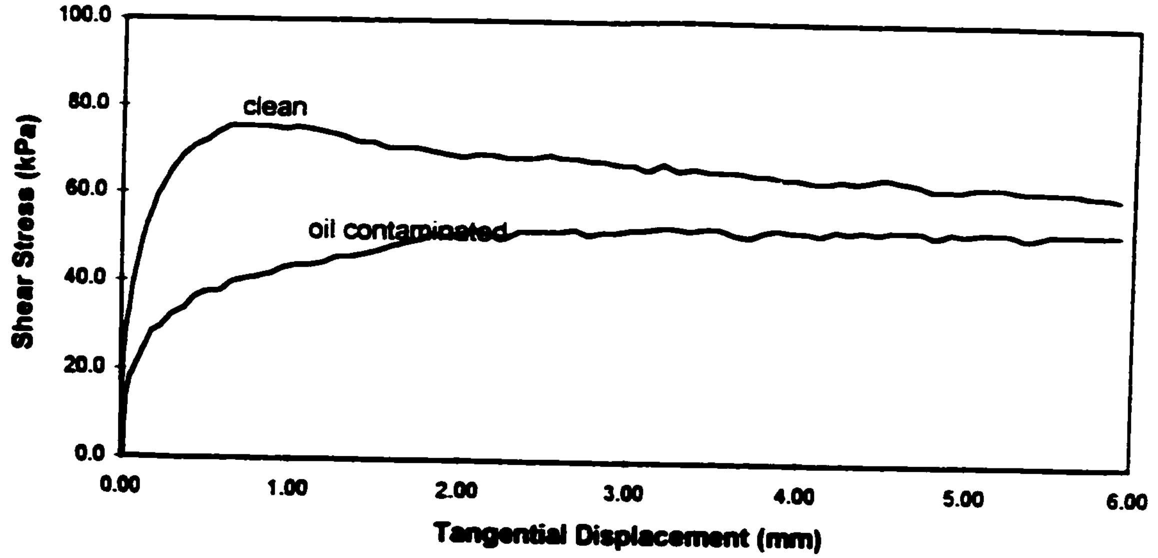

Fig. 5.11 2D monotonic test with constant normal stress of 100 kPa for dense sand.

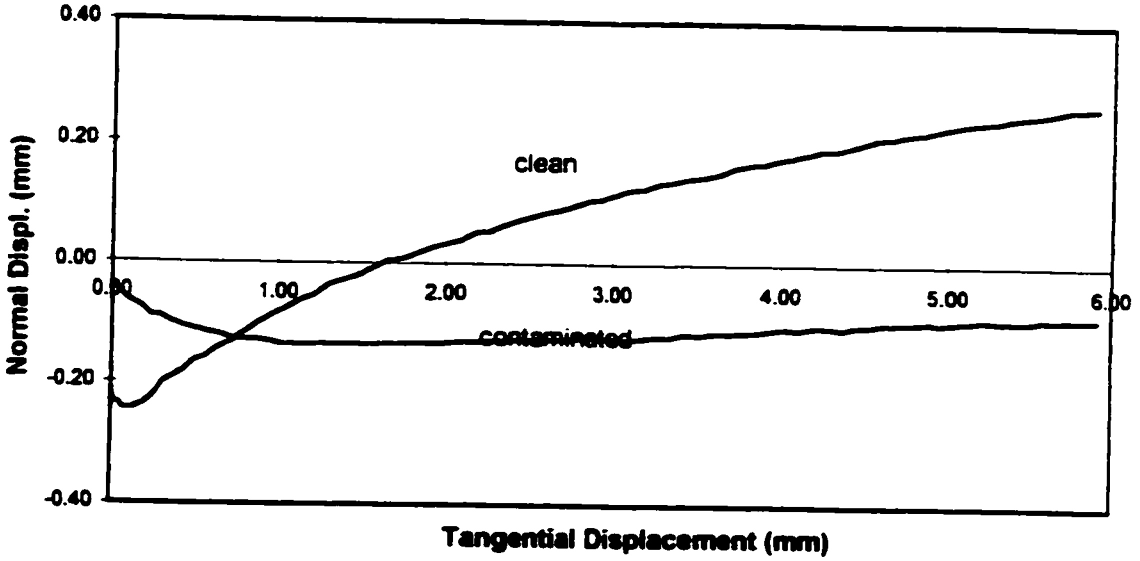

Fig. 5.12 2D monotonic test with constant normal stress of 100 kPa for dense sand

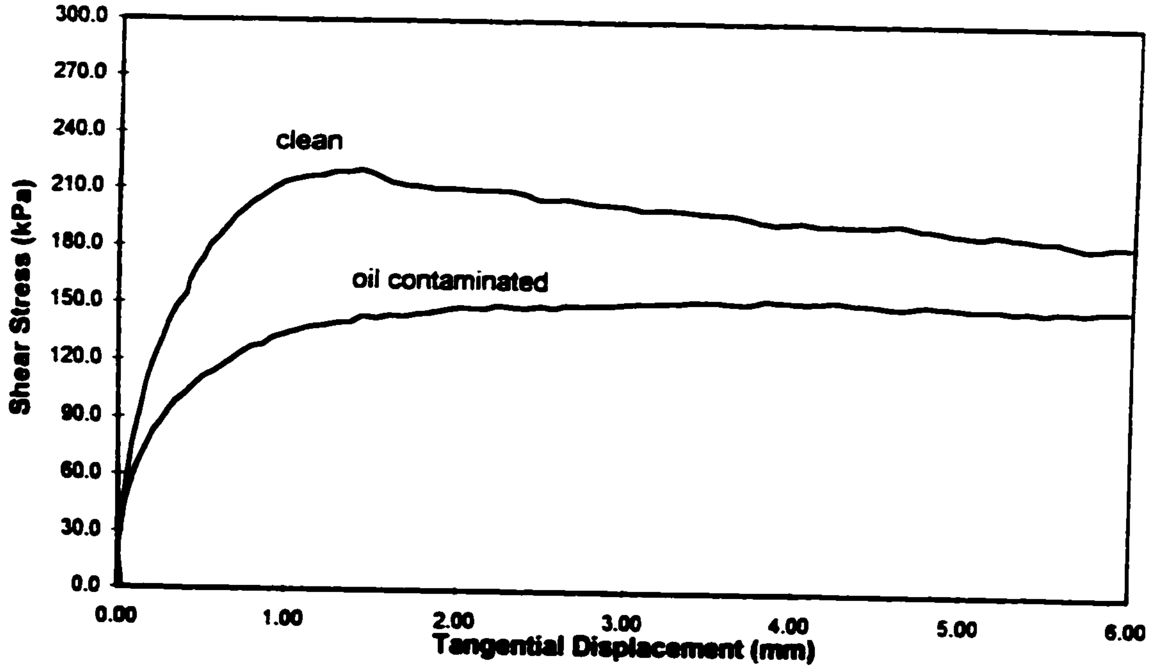

Fig. 5.13 2D monotonic test with constant normal stress of 300 kPa for dense sand.

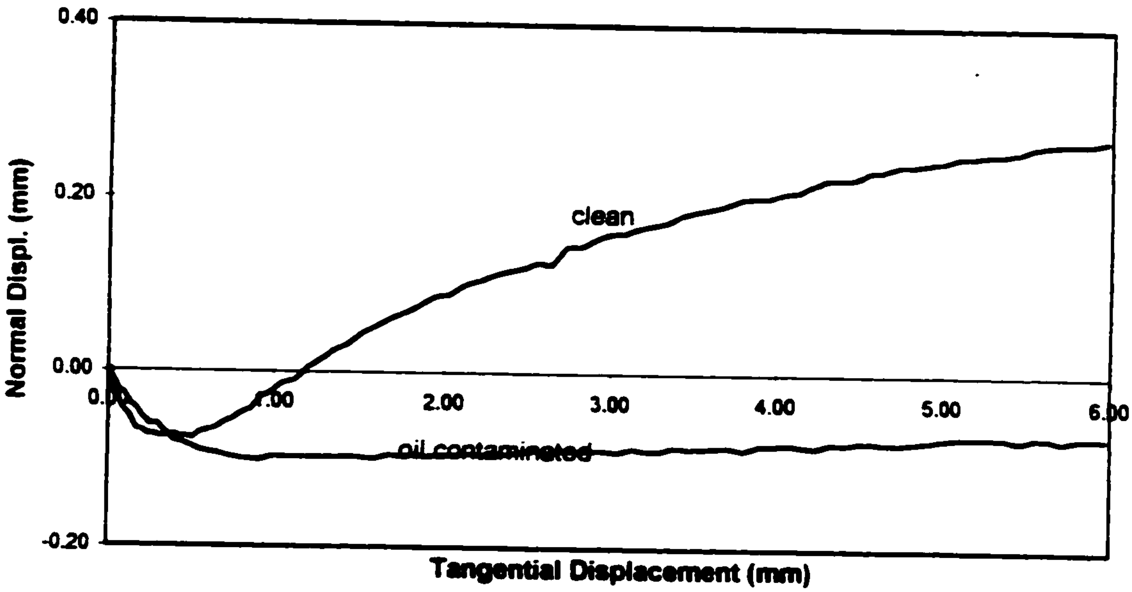

Fig. 5.14 2D monotonic test with constant normal stress of 300 kPa for dense sand

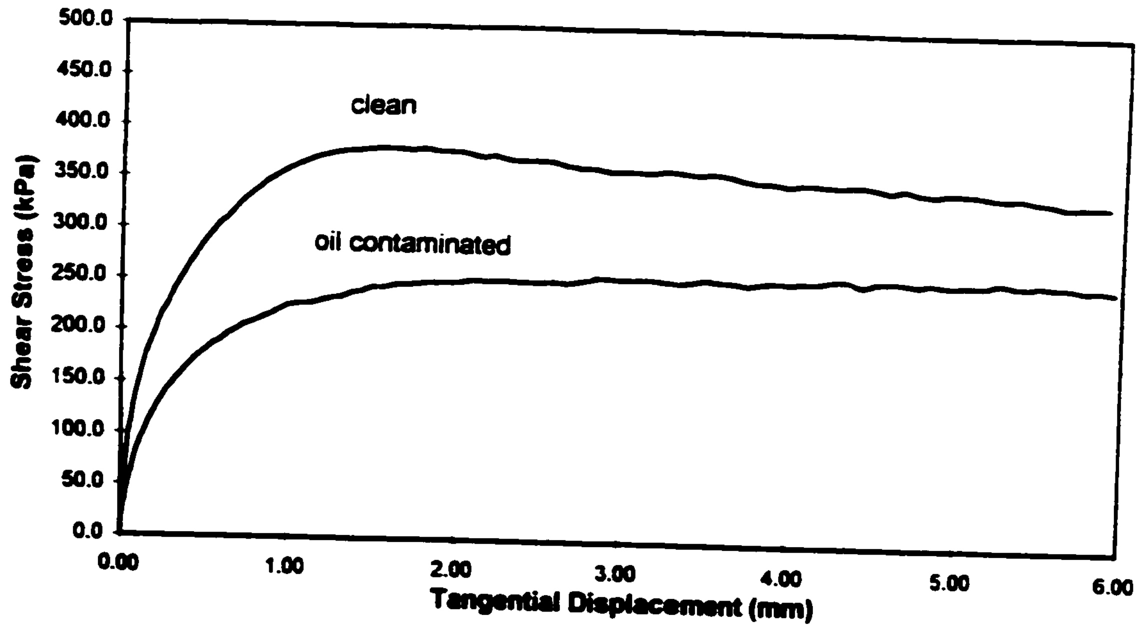

Fig. 15 2D monotonic test with constant normal stress of 500 kPa for dense sand.

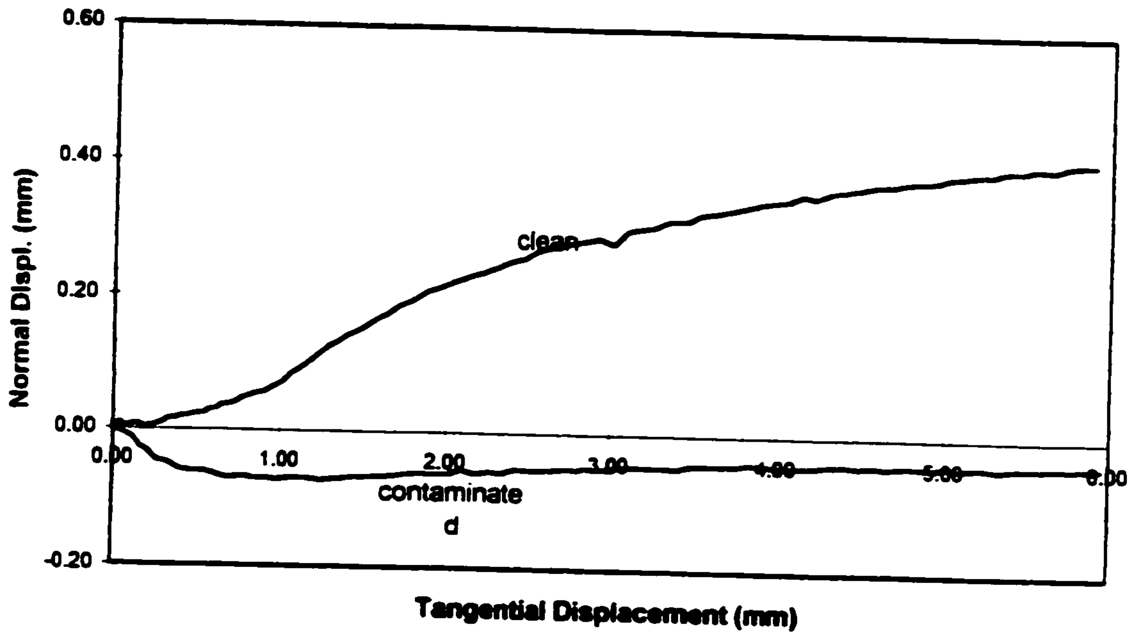

Fig. 5.16 2D monotonic test with constant normal stress of 500 kPa for dense sand

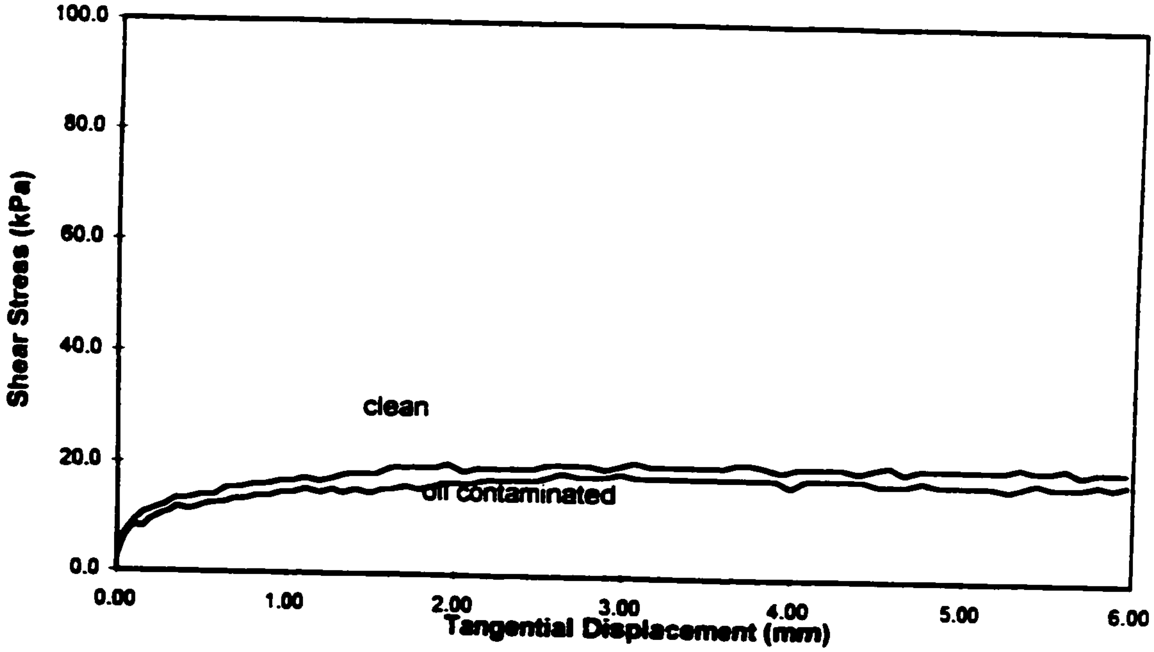

Fig. 5.17 2D monotonic test with constant normal stress of 40 kPa for loose sand.

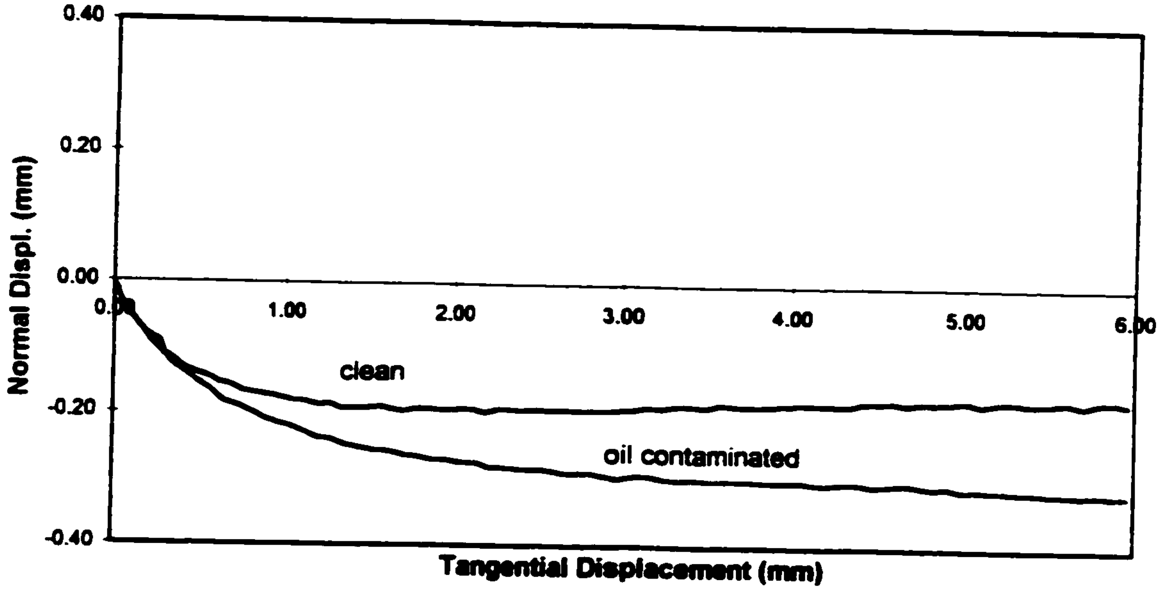

Fig. 5.18 2D monotonic test with constant normal stress of 40 kPa for loose sand

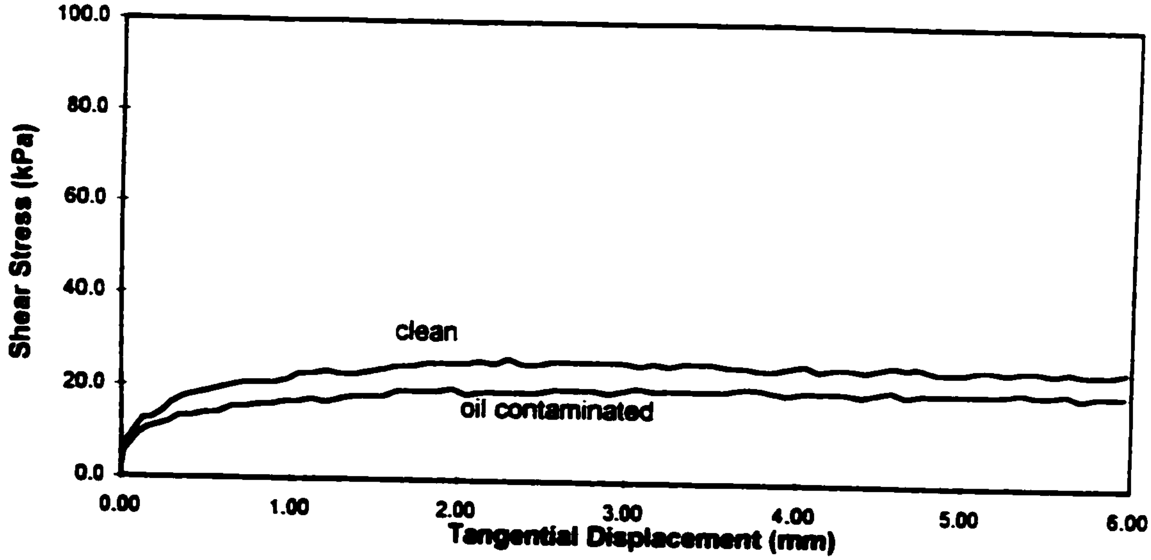

Fig. 5.19 2D monotonic test with constant normal stress of 40 kPa for oil contaminated loose sand.

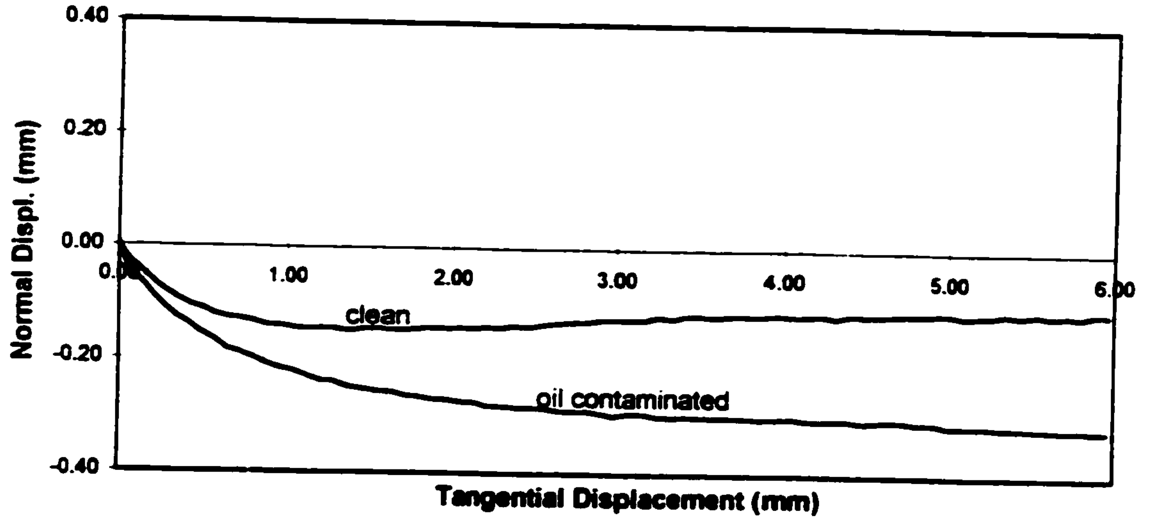

Fig. 5.20 2D monotonic test with constant normal stress of 40 kPa for oil contaminated loose sand

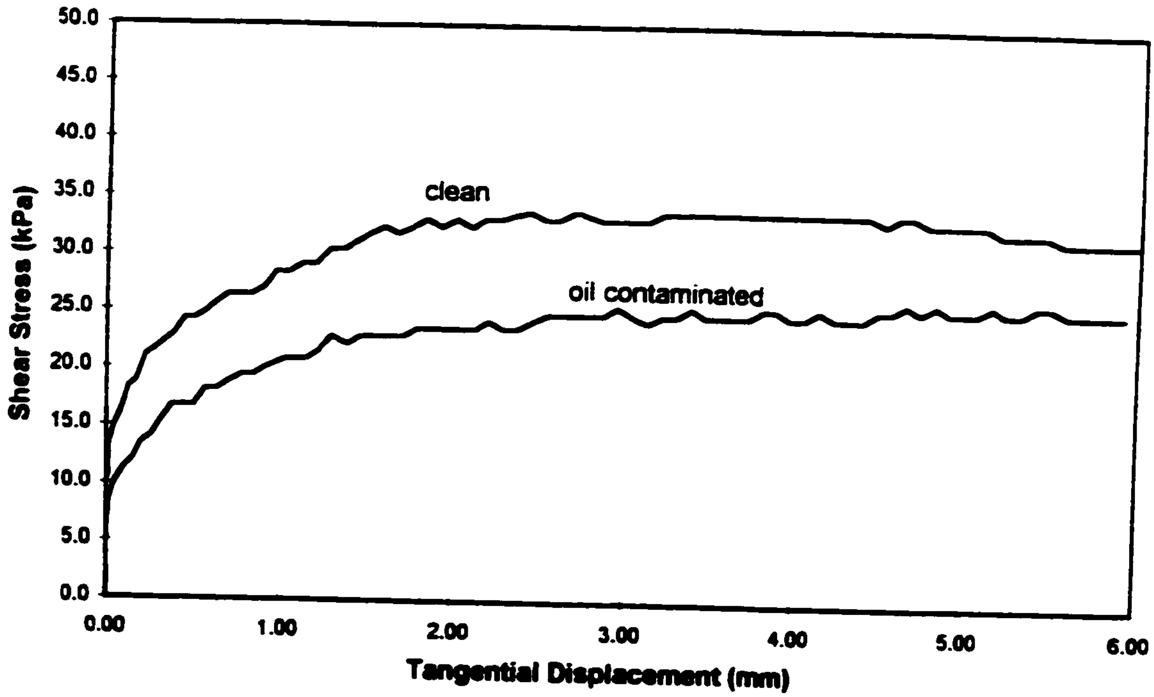

· **Fig. 5.21 2D monotonic test with constant normal stress of 50 kPa for loose sand.**

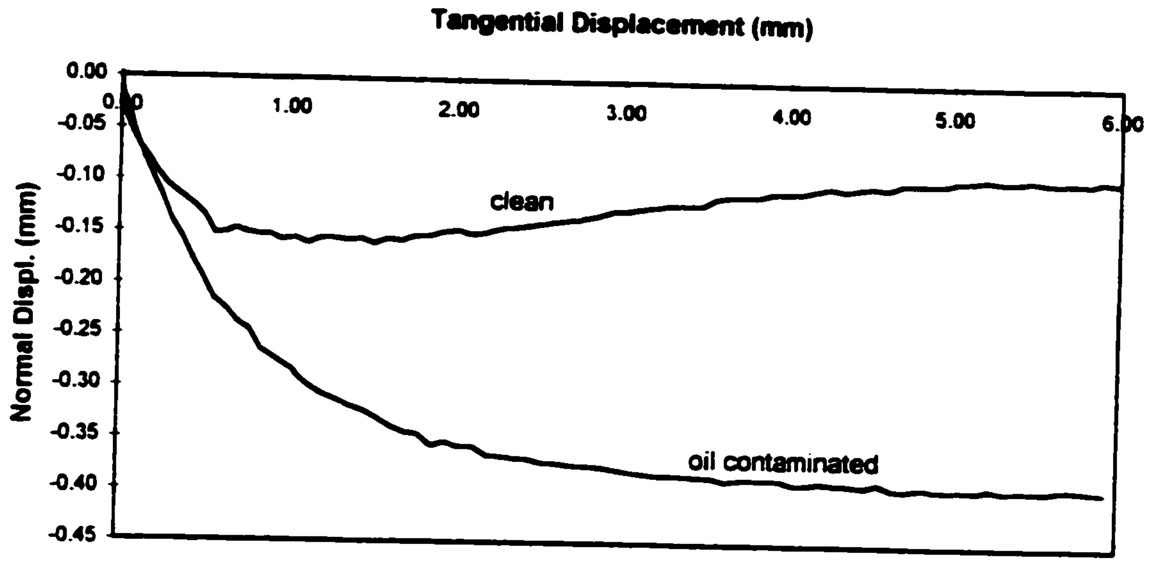

Fig. 5.22 2D monotonic test with constant normal stress of 50 kPa for loose sand

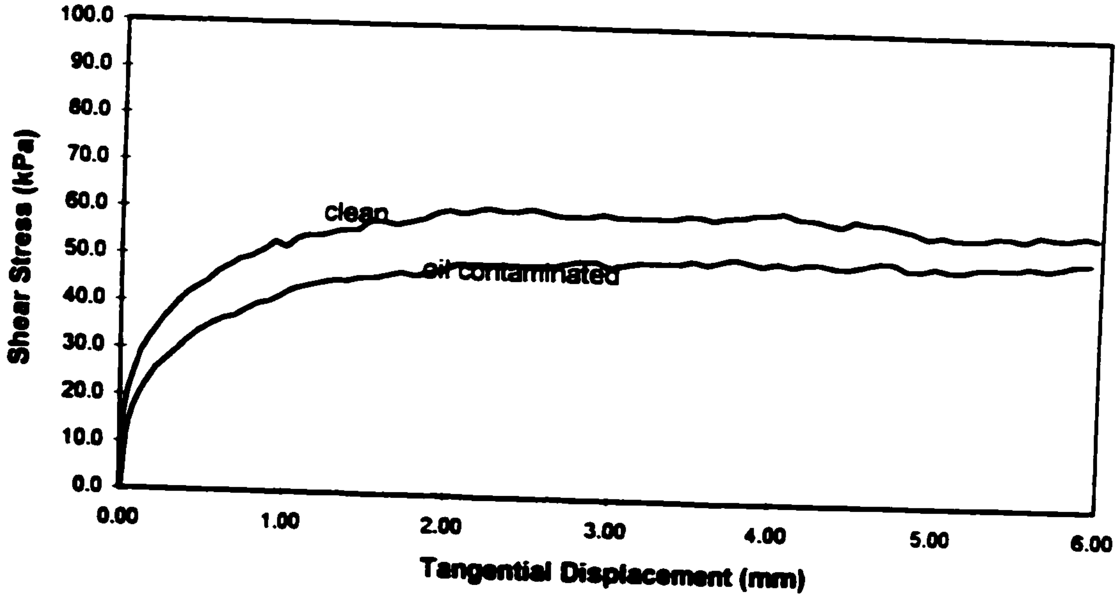

Fig. 5.23 2D monotonic test with constant normal stress of 100 kPa for loose sand.

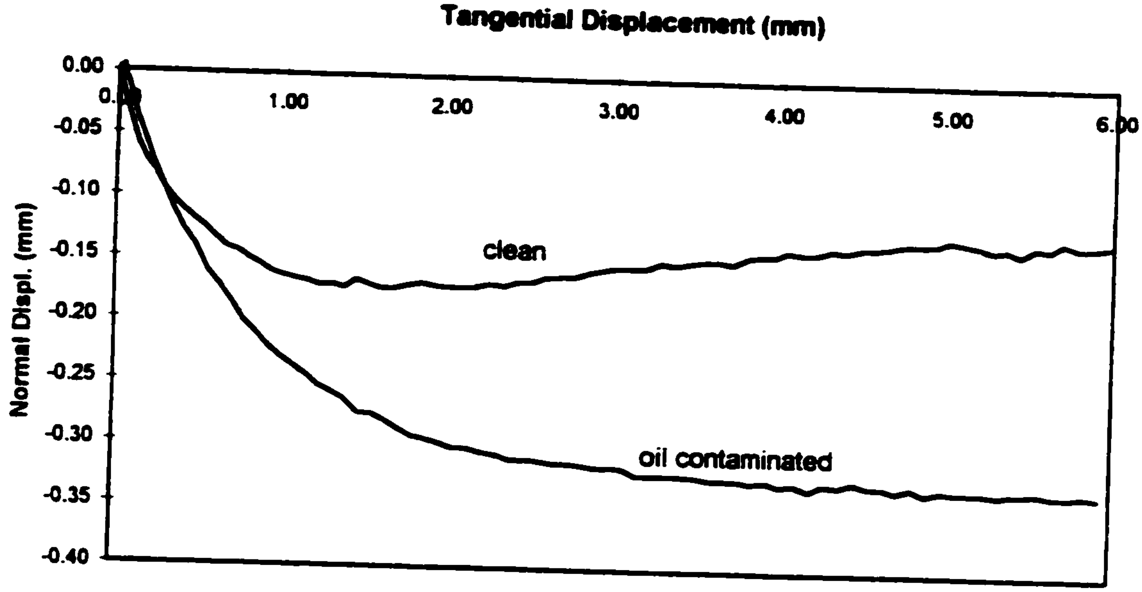

Fig. 5.24 2D monotonic test with constant normal stress of 100 kPa for loose sand

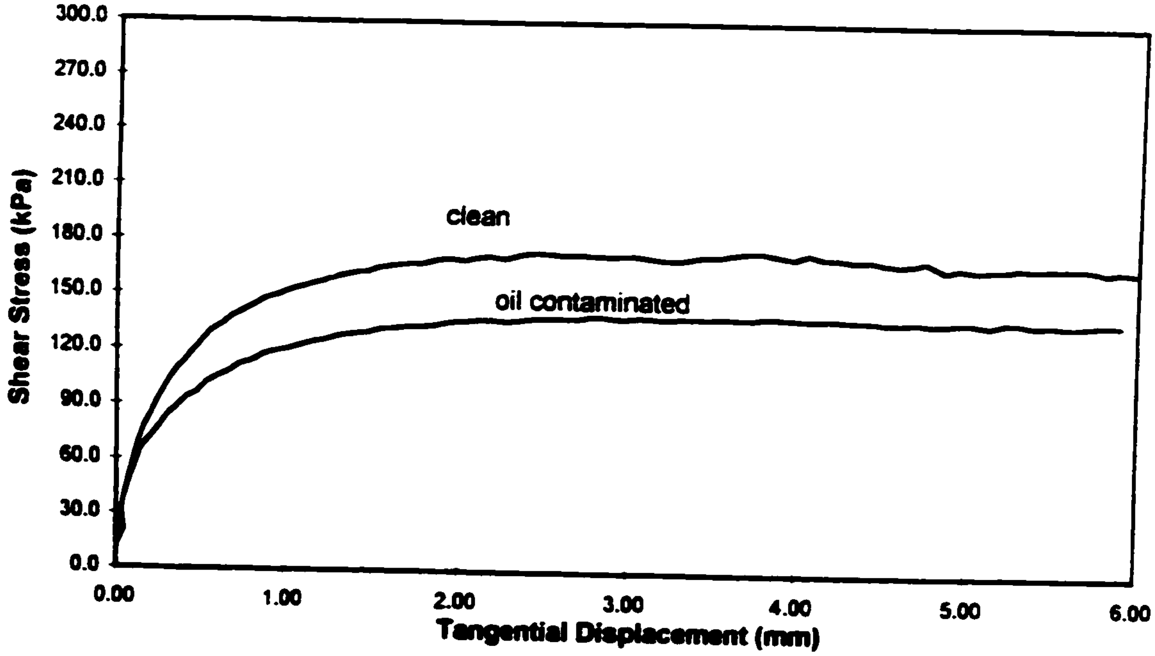

Fig. 5.25 2D monotonic test with constant normal stress of 300 kPa for loose sand.

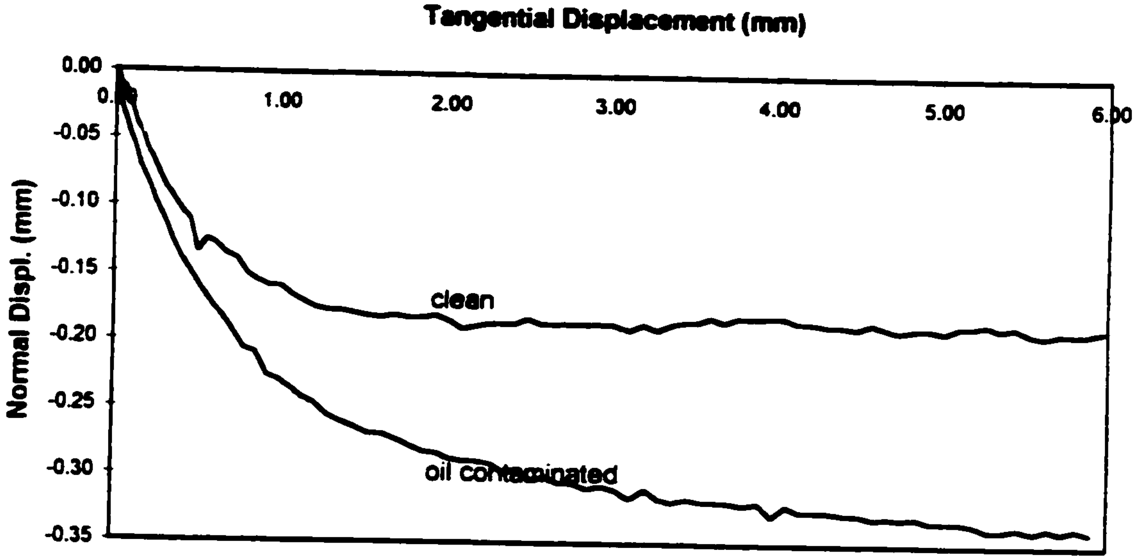

Fig. 5.26 2D monotonic test with constant normal stress of 300 kPa for loose sand

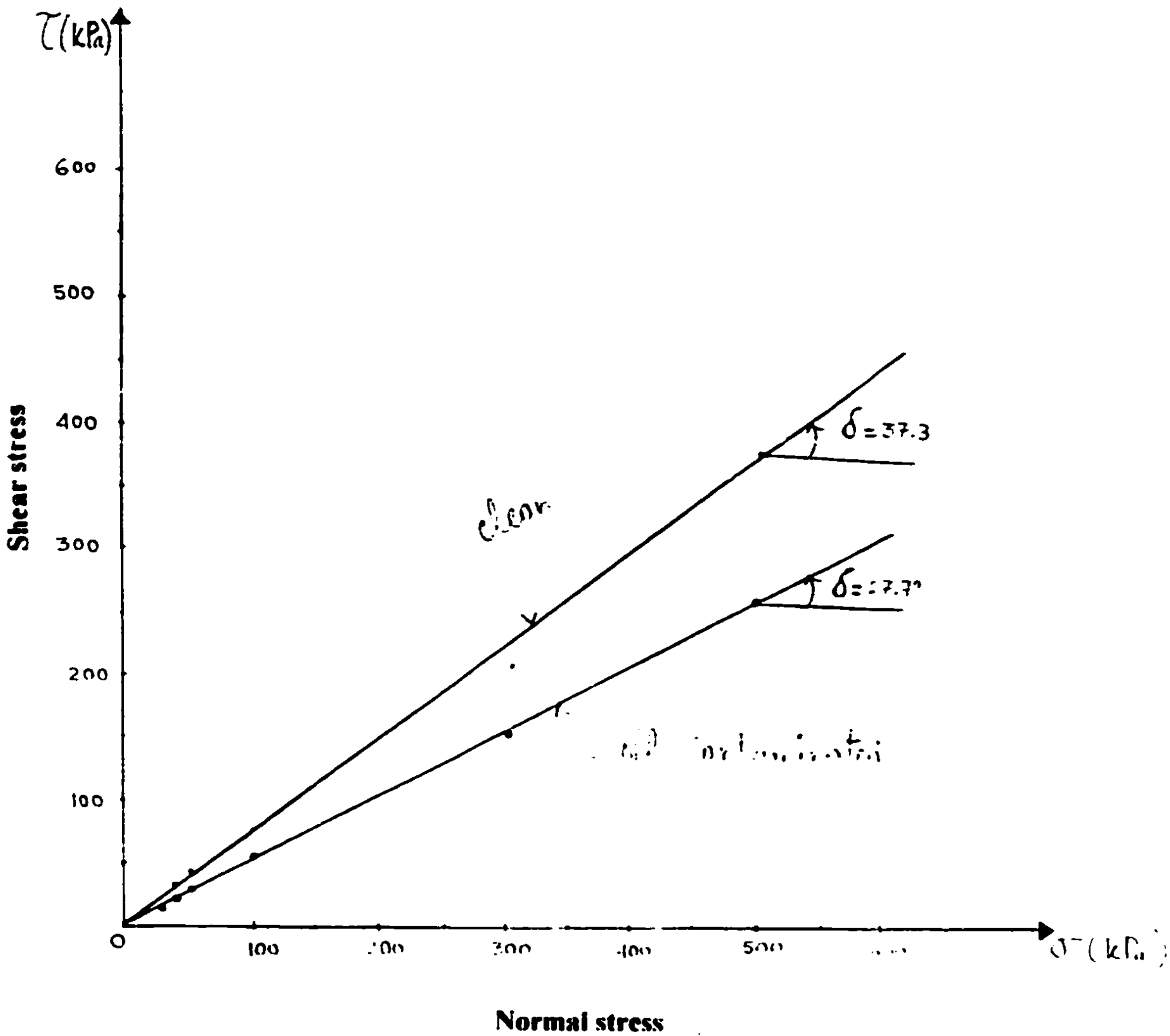

Fig 5.27 Internal frictional angle between dense sand and the steel plate.

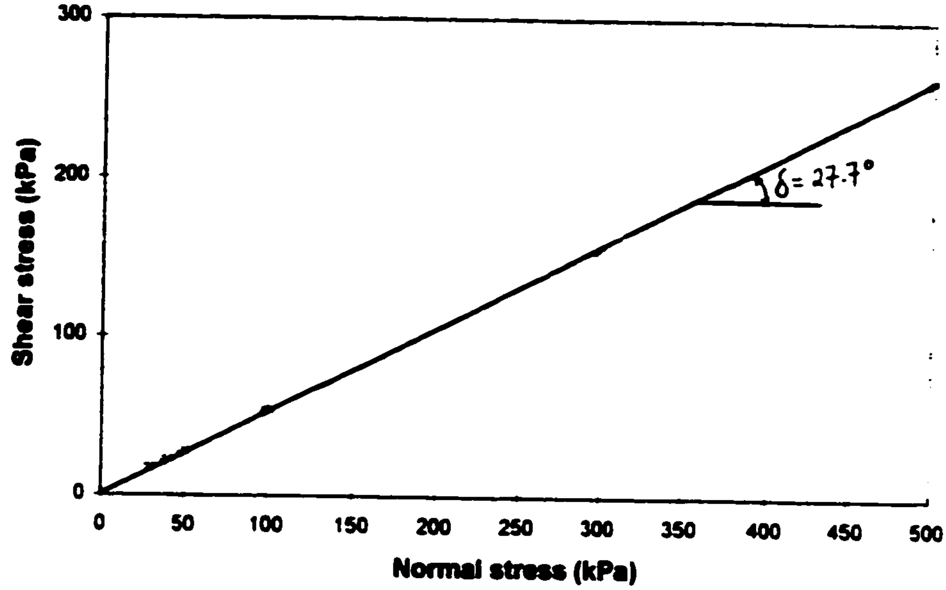

Fig. 5.28 Interface frictional angle for oil contaminated dense sand.

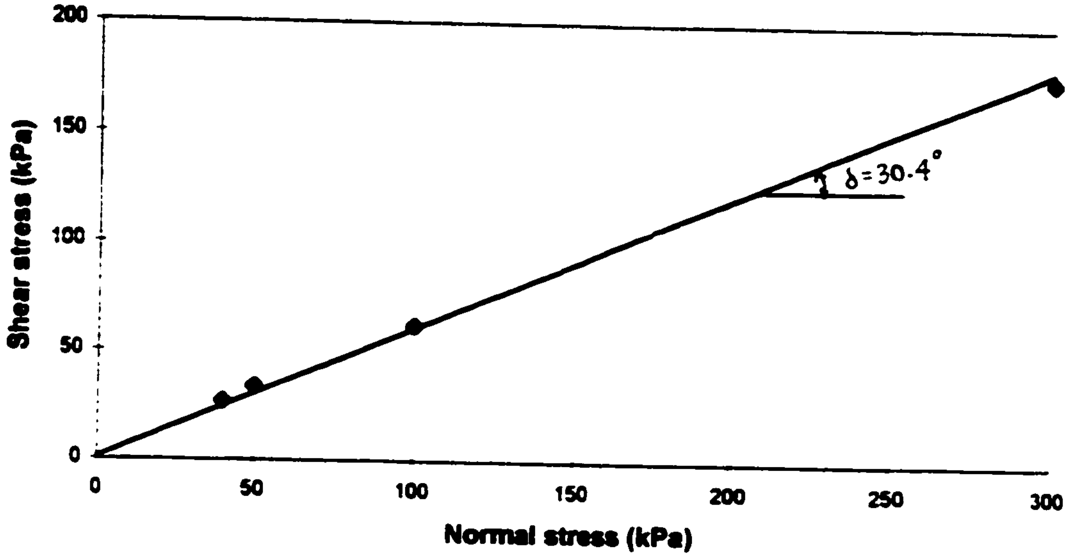

Fig. 5.29 Interface frictional angle for clean loose sand.

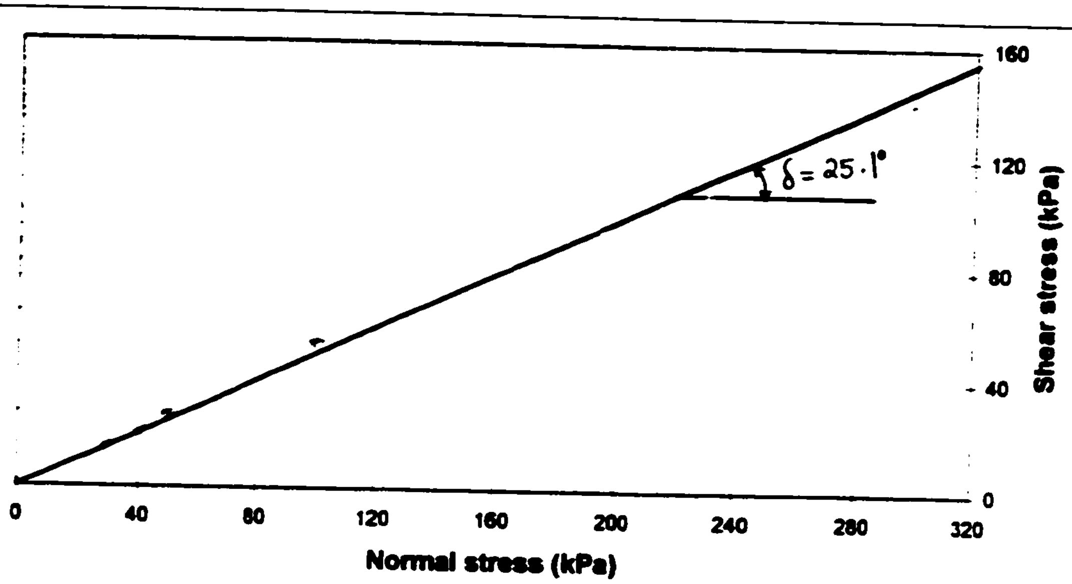

Fig. 5.30 Interface frictional angle for oil contaminated loose sand.

CHAPTER 6

CONCLUSIONS AND RECOMMENDATIONS

6.1 Conclusions

The objectives of this experimental work were (1) to investigate the fate of oil in artificial islands in the event of a blowout and (2) to determine the influence of oil contamination on the deformation-strength properties of an interface.

This investigation showed that, during a blowout, oil migration in an artificial island depends on various parameters. The parameters governing the oil migration process were identified and their effects were analyzed. From the experimental results obtained, an attempt is made to correlate these results with what would happen in real life if a significant volume of oil is spilled on sand during exploration.

The boundary conditions of this experimental investigation did not match exactly the conditions of the artificial island in the sea where the boundary conditions are more complex. But nevertheless some parameters that govern the movement of oil in soils have nothing to do with the scale of the structure containing the soil. When oil percolates through the soil from the surface toward the water table some of this oil can be held by surface tension around the points of contact between particles.

A good indication of how much fluid is trapped in soils is often obtained by computing the Bond and Capillary numbers. These numbers depend strongly on the properties of the fluids involved (in this case oil and water) including: the surface tension between the fluids of interests (oil and water), the average size of the soil particle, the density difference between the fluids (water and oil), the viscosity of oil, and the rate of oil movement in the soil (velocity). The grain size distribution of Ukalerk (Beaufort sea) and Carp Airport sands proved that the material properties of these two soils were similar, therefore the difference between the Bond and Capillary numbers of Ukalerk and Carp Airport sand depend strongly on the surface tension between the type of water and oil studied. In this experiment, tap water and Motormaster grade 50 oil (which is a lubricating oil) were used. In the sea, the water is salty and cold and crude oil is the contaminant. Values of surface tensions are listed for crude oil and they range from 0.023-0.038 σ /N while lubricating oil values (e.g. Motormaster grade 50 oil) range from 0.035-0.038 σ /N. (Streeter and Wiley, 1985). The laboratory experiment was conducted at room temperature, which is not the case at the sea where the water is much colder. If one assumes that the conditions in the field are identical to the laboratory test conditions, about 88 % of the spilled oil will be contained in the sand and 12 % will seep out to the sea.

The analysis of the database of oil migration experimental results showed that for the scaled J-shape tube used, it took approximately 3 months for oil to travel through the entire soil system. Obviously for a bigger structure, such as the artificial island, the time of contamination will be much longer. Under steady-state conditions the estimated time is about 5 months.

The location of the water table also plays an important role on how fast the oil would migrate in the soil. Above the water table the oil migrates in unsaturated soil and the

Bond and Capillary numbers are relevant parameters. Below the water table, the hydraulic gradient is the driving force.

With regard to the interface experiments, an attempt was made to observe the patterns of oil contaminated sand-steel interface behaviour.

The results of load tests showed that, for a given normal stress, a more pronounced peak value of the shear stress was observed for clean samples than oil contaminated ones. In general, dense clean samples experienced strain softening. After the peak, the shear stress leveled off at a residual value equal to about 60% of the maximum shear stress. This was not the case for contaminated dense specimen where no strain softening was observed. Volume change results of clean dense samples indicated some initial compression followed by an important amount of dilation, whereas contaminated samples exhibited a substantial compression and no dilation.

In particular, the response of the interface to the applied low stresses (30, and 40 kPa), in all cases (dense- or loose-clean and dense- or loose-contaminated) was characterized by no strain softening. The results of the volume change indicated compression of the sand mass for all cases. Nevertheless, the magnitude of the sand mass compression was more pronounced in loose oil-contaminated samples than in other cases. The ramifications of the scenarios mentioned above were overwhelming on some engineering parameters.

This study found that for a parameter such as the angle of friction between a medium crushed quartz sand and a sand-blasted steel surface, the relative density and normal stress were indeed the governing parameters influencing the angle of friction. Other factors such as the roughness of the surface, composition of soil, grain size distribution, moisture content, and rate of shearing were not investigated.

The effect of oil contamination on the strength behaviour of sand-steel (sand-blasted surface) was large. For dense sand specimens the interface friction angle was reduced about 9 ° after oil-contamination. However oil contamination on loose samples, the friction angle was reduced about 5°. Since the interface behaviour as well as the behaviour of sand mass change significantly as a result of oil contamination, the resistance of the caisson structure to the applied load will also change.

6.2 Recommendations

This research sets forth future recommendations as follows:

1- More tests are needed on oil migration in soils by changing the parameters involved in the experimental analysis namely the type of soil, oil, viscosity, and temperature in order to develop a better understanding of the process of oil migration as well as to develop mathematical models.

2- If laboratory glass columns (i.e., the J-tube) are to be used in the future, it would necessary to incorporate various devices capable of measuring the air and liquid pressure distributions in the soil system during the migration of oil. Incorporating these devices would give more insights on the displacement of trapped air and fluid flow during the oil migration process.

Further research on contaminated soil-construction material interfaces may be conducted with extensive tests including:

3- Two- and three-dimensional monotonic tests using the simple shear box, since in reality, structures are three-dimensional, and the simple shear box gives separately the tangential displacement of the sand mass and the sliding displacement at the interface.

4- Two- and three-dimensional cyclic loading tests. The need to study the effects of repeated loading stems from the fact that ice loading is generally cyclic in nature in the winter and during the summer waves generates load cycles.

5- Correlating the experimental work with models capable of predicting the strength-displacements characteristics of interfaces for clean and oil contaminated cases.

REFERENCES

[1] ACAR, Y. B., DURGUNOGLU, H. T. and TUMAY, M.T., 1982. Interface properties of sand. Journal of Geotechnical Engineering, ASCE, 108 (GT4), pp. 648-658.

[2] AJIT, T. J., WILLIAM, J. G., and STEVENS, D. K., 1994. Oil migration through unsaturated soils and its effect on the vadose zone interactive processes (VIP) model output. Wat. Sci. Tech., 30(3), pp. 39-51.

[3] AMERICAN PETROLEUM INSTITUTE, 1985. Oil spill conference, American Petroleum Institute, Washington, DC.

[4] BEAR, J., 1972. " Dynamics of fluids in Porous Medium." American Elsevier, New York.

[5] BEN AMOR, F. 1990. Effects of Oil contamination on the Properties of Sand. M. A. Sc. thesis, University of Ottawa, Canada.

[6] CALABRESE, E. J. and KOSTECKI, P. T., 1988. Soils Contaminated by Petroleum. Environmental and Public Health Effects. pp. 10. John Willey and sons. New York.

[7] CALVO, A., PATERSON, I., CHERTCOFF, R., ROSEN, M., and HULIN, J. P., 1990. In proceedings " Fundamentals of Fluid Transport in Porous Media, " May 14-18, Arles, France.

[8] CARY, J. W., SIMMONS, C. S., and McBRIDE, J. F., 1989. Predicting oil infiltration and redistribution in unsaturated soils. Soil Science Society of America Journal, Vol. 53, pp. 335-342.

[9] CHAN, S. F. and HANNA, T. H., 1980. Repeated loading on single piles in sand. Journal of Geotechnical Engineering, ASCE, 106(2), pp. 171-188.

[10] CLARK, J. I. and JORDAAN, I. J., 1987. Geotechnical predictions in ice affected marine environments. Proceedings, International Symposium on Prediction and Performance in Geotechnical Engineering. Calgary, Alta., pp. 15-26.

[11] CHATZIS, I. and DULLIEN, F. A. L., J. ICE Vol. 25, pp. 47.

[12] CHATZIS, I., and MORROW, N. R., SPE 10114, presented at the 56 th SPE conference, October, San Antonio, Texas.

[13] CRAIG, F. F. Jr., 1971. " The reservoir Engineering aspects of Waterflooding". Society of Petroleum Engineers of AIME, New York.

[14] COLLINS, R. E., 1961. " Flow of Fluids through Porous Materials." Van Nostrand-Reinhold, Princeton, New Jersey.

[15] DULLIEN, F. A. L., 1979. Porous Media. Fluid Transport and pore structure. p 118. Second edition. Academic Press, Inc. Toronto.

[16] EL-SAYED, M. S. and DULLIEN, F. A. L., 1977. Investigation of transport phenomena and pore structure of sandstone samples. Preprint for the ann. Technique. Meeting Petrol. Soc. CIM, 28 th, Edmonton, May 10-June 3.

[17] ENVIRONMENT CANADA, 1979. Oil spill scenario for the Labrador Sea. Report EPS 3-EC-79-4, pp. 300-350.

[18] EVGIN, E. and FAKHARIAN, K., 1996. Three-dimensional cyclic behavior of interfaces. Proc. 3rd Int. Conf. on Recent Advances in Geot. Earth. Eng. & Soil Dyn., April 2-7, 1995, Vol. 1, pp. 9-12, St. Louis, Missouri, USA.

[19] EVGIN, E., BOULON, M., and ARMAND, G., 1995. Effect of oil contamination on the behavior of an interface. 49 th Canadian Geotechnical Conference of the Canadian Geotechnical Society, September 23-25, 1996, pp. 377-384. St. John's, Newfoundland.

[20] FATT, I., 1961. Science Vol. 134, pp. 1750.

[21] FATT, I., 1966. J. Inst. Pet. Vol. 52, pp. 231.

[22] FAKHARIAN, K. and EVGIN, E., 1993. A three dimensional apparatus for cyclic testing of interfaces. Proceedings, 46 th Annual Canadian Geotechnical Conference, Saskatoon, Canada, pp. 485-493.

[23] FAKHARIAN, K. and EVGIN, E., 1995. Simple shear versus direct shear tests on interfaces during cyclic loading. Proc., 3 rd Int., Conf., on Recent Advances in Geot. Earth. Eng. & Soil Dyn., April 2-7, 1995, Vol. 1, pp. 13-16, St. Louis, Missouri, USA.

[24] FAKHARIAN, K. and EVGIN, E., 1996. An automated apparatus for three-dimensional monotonic and cyclic testing of interfaces. Geotechnical Testing Journal. GTJODJ, 19(1). pp. 22-31.

[25] FAKHARIAN, K., 1996. Three-Dimensional Monotonic and Cyclic Behaviour of Sand-Steel Interfaces: Testing and Modelling. Ph. D. Dissertation. Department of Civil Engineering, University of Ottawa, Canada.

[26] FARAH. W. G. G. 1992. Mechanical behavior of Oil contaminated Sand and Cleanup methods. M. Eng. thesis. University of Ottawa, Ottawa, Canada.

[27] FREEZE, R. A., and CHERRY. J. A. 1979. Groundwater. Prentice-Hall. Inc. New Jersey.

[28] GREENKORN, R. A., 1983. " Flow phenomena in Porous Media." Marcel Dekker Inc.

[29] GREFFEN, T. M., OWENS, W. W., PARRISH, D. R., AND MORSE, R. A., 1951. Trans. Am. Inst. Min. Eng. Vol. 192, pp. 99.

[30] HANSCH, C. and LEO. A., 1979. Substituent Constants for correlation analysis in Chemistry and Biology, Wiley, New York.

[31] HORTON, A. K., 1969. From " Groundwater in Civil Engineering, Developments in Geotechnical Engineering, 35. pp. 57-59. By RETHATI D. L. 1983. Elsevier Scientific Publishing Company.

[32] KISHIDA, H. and UESUGI. M., 1987. Tests of interface between sand and steel in the simple shear apparatus. Geotechnique, 37 (1), pp. 45-52.

[33] LEVERETT, M. C., 1941. Trans. AIME Vol. 142, pp. 152.

[34] LOGAN, D. L., 1992. A finite course in the finite element method. PWS-KENT Publishing Company. Boston. USA.

[35] LYMAN, W. J., REEHT, W. F., and ROSENBLATT, D. H., 1982. Handbook of Chemical Property Estimation methods, McGraw-Hill. New York.

[36] MACKAY, D., 1988. The chemistry and modeling of soil contamination with petroleum. Conference on soils contaminated by petroleum. University of Massachusetts, pp. 5-18. John Willey and sons, N. Y. USA.

[37] MACKAY, D., SHUI, W. Y., CHAU, A., SOUTHWOOD. J. and JOHNSON. C. I., 1985. Environmental fate of diesel fuel spills on land. Report (in press) of

Department of Chemical Engineering and Applied Chemistry of University of Toronto for Association of American Railroads. Washington, D. C.

[38] MARLE, C. M., 1981. Multiphase flow in porous media. Paris: Editions Technip.

[39] MIURA, S. and TORI, S., 1982. A sample preparation method and its effect on static and cyclic deformation-strength properties of sands. Soils and Foundations. 22 (2), pp. 61-77.

[40] MORROW, N. R. and SONGKRAN, B., 1981. Effect of viscous and buoyancy forces on nonwetting phase trapping in porous media. Surface phenomena in enhanced oil recovery, pp. 387-412.

[41] NAAL, J. K., 1976. From " Groundwater in Civil Engineering, Developments in Geotechnical Engineering 35, pp. 57-59. By RETHATI D, L. 1983. Elsevier Scientific Publishing Company.

[42] PHILIP, J. R., 1963. Aust. J. Phys. Vol. 16, 287.

[43] PHILIP, J. R., 1983. Infiltration in one, two , and three dimensions. Advances in infiltration, proceedings of the National Conference on Advances in Infiltration December 12-13, 1983, Chicago, Illinois, pp. 1-13.

[44] RUBIN, M. A., and SHERMAN, M. C. 1973. From " Groundwater in Civil Engineering, Developments in Geotechnical Engineering 35, pp. 57-59. By RETHATI, D. L. 1983. Elsevier Scientific Publishing Company.

[45] SANDERSON, T. J. O., 1988. Ice mechanics, risks to offshore structures. Graham & Trotman, London, U. K., p. 253.

[46] SCHEIDEGGER, A. E., 1974. The physics of flow through Porous Media. University of Toronto Press, Toronto, Canada.

[47] SHERMAN, M. C., HORTON, K. and MUSGRAVE, F., 1967. From " Groundwater in Civil Engineering, Developments in Geotechnical Engineering 35, pp. 57-58. By RETHATI, D. L. 1983. Elsevier Scientific Publishing Company.

[48] STREETER, V. L. and WYLIE, E. B., 1985. pp. 557. Fluids mechanics. Eight edition. McGraw-Hill book company. New York.

[49] SLADEN, J. A., and HEWITT, K. J., 1989. Influence of placement method on the in situ density of hydraulic sand fills. Canadian Geotechnical Journal. Vol. 26, pp. 453-466.

[50] TABER, J. J., 1981. From " Surface Phenomena in Enhanced Oil Recovery." Plenum Press, New York.

[51] UESUGI, M. and KISHIDA, H., 1986a. Influential factors between steel and dry sand. Soils and Foundations, 26(2), pp. 33-46.

[52] UESUGI, M. and KISHIDA, H., 1986b. Frictional resistance at yield between dry sand and mild steel. Soils and Foundations, 26(4), pp. 139-149.
A
[53] UESUGI, M., KISHIDA, H., and, TSUBAKIHARA, Y., 1989. Friction between sand and steel under repeated loading. Soils and Foundations, 29(3), pp. 127-137.

[54] VERSCHUEREN, K., 1985. Handbook of Environmental Data on Organic Chemicals, 2nd ed. Van Nostrand Reinhold, New York.

[55] YOSHIMI, Y. and KISHIDA, T., 1981. Friction between sand and metal surface. Proceedings, 10th International Conference on Soils Mechanics and Foundation Engineering, Vol. 1, pp. 831-834.

[56] ZWOLINSKI, B. J. and WILHOIT, R. C., 1971. Handbook of vapor pressures and Heats of vaporization of hydrocarbons and related compounds. API-44, TRC Publ. No. 101, Texas, A&M University, College Station.

APPENDIX B

SAND-STEEL INTERFACE RESULTS

Table B1: 2-D Monotonic test on dense sand σ_n = 100 kPa

Date of testing: 23/04/1996
Tested by: Alain Mabia
Type of sample: Dense clean sand
Plate: sand-blasted steel plate
Density: 1.89 g/cm^3

TIME Sec.	Ux (mm)	Ux2 (mm)	Ux1 (mm)	V (mm)	Tau-x (kPa)	Sig-n (kPa)	T/S
0	0.01	0.00	0.00	0.21	0.0	98.5	0.00
5.0	0.01	0.00	0.00	0.21	0.6	98.5	0.01
10.0	0.00	0.00	0.00	0.21	4.7	99.5	0.05
15.0	0.00	0.00	0.00	0.21	7.4	98.5	0.08
20.0	0.00	0.00	0.00	0.21	10.1	98.5	0.10
25.0	0.01	0.00	0.00	0.21	16.8	98.5	0.17
30.0	0.01	0.00	0.01	0.21	22.9	98.5	0.23
35.0	0.03	0.00	0.03	0.21	29.0	99.5	0.29
40.0	0.05	0.00	0.05	0.21	34.4	99.5	0.35
45.0	0.06	0.00	0.06	0.21	38.4	98.5	0.39
50.0	0.09	0.00	0.09	0.21	42.5	99.5	0.43
55.0	0.11	0.00	0.10	0.21	46.5	99.5	0.47
60.0	0.13	0.00	0.13	0.21	49.9	100.5	0.50
65.0	0.15	0.00	0.14	0.21	52.6	100.5	0.52
70.0	0.17	0.00	0.16	0.21	54.6	100.5	0.54
75.0	0.19	0.00	0.19	0.21	57.3	100.5	0.57
80.0	0.21	0.00	0.21	0.21	59.3	101.5	0.58
85.0	0.23	0.00	0.23	0.21	60.7	101.5	0.60
90.0	0.26	0.00	0.26	0.21	62.7	100.5	0.62
95.0	0.29	0.00	0.29	0.21	64.7	101.5	0.64
100.0	0.31	0.00	0.31	0.21	66.1	101.5	0.65
105.0	0.36	0.00	0.36	0.21	68.8	101.5	0.68
110.0	0.43	0.00	0.43	0.21	70.8	101.5	0.70
115.0	0.50	0.00	0.49	0.21	72.2	100.5	0.72
120.0	0.57	0.00	0.57	0.21	74.2	101.5	0.73
125.0	0.64	0.00	0.64	0.21	75.5	101.5	0.74
130.0	0.72	0.00	0.71	0.21	75.5	100.5	0.75
135	0.79	0.00	0.79	0.21	75.5	100.5	0.75
140	0.88	0.00	0.87	0.21	75.5	101.5	0.74
145	0.96	0.00	0.96	0.21	74.9	100.5	0.75

150	1.04	0.00	1.04	0.21	75.5	100.5	0.75
155	1.13	0.00	1.13	0.21	74.9	100.5	0.75
160	1.21	0.00	1.21	0.21	74.2	100.5	0.74
165	1.30	0.00	1.30	0.21	73.5	101.5	0.72
170	1.39	0.00	1.39	0.21	72.2	101.5	0.71
175	1.48	0.00	1.48	0.21	72.2	100.5	0.72
180	1.57	0.00	1.56	0.21	70.8	100.5	0.70
185	1.65	0.00	1.65	0.21	70.8	100.5	0.70
190	1.74	0.00	1.74	0.21	70.8	100.5	0.70
195	1.83	0.00	1.82	0.21	70.1	100.5	0.70
200	1.91	0.00	1.91	0.21	69.5	100.5	0.69
205	2.00	0.00	2.00	0.21	68.8	100.5	0.68
210	2.08	0.00	2.08	0.21	69.5	100.5	0.69
215	2.17	0.00	2.17	0.21	69.5	100.5	0.69
220	2.25	0.00	2.25	0.21	68.8	100.5	0.68
225	2.34	0.00	2.34	0.21	68.8	100.5	0.68
230	2.42	0.00	2.42	0.21	68.8	100.5	0.68
235	2.51	0.00	2.51	0.21	69.5	100.5	0.69
240	2.59	0.00	2.59	0.21	68.8	99.5	0.69
245	2.68	0.00	2.68	0.21	68.8	99.5	0.69
250	2.76	0.00	2.75	0.21	68.1	99.5	0.68
255	2.85	0.00	2.85	0.21	68.1	99.5	0.68
260	2.93	0.00	2.93	0.21	67.4	99.5	0.68
265	3.02	0.00	3.02	0.21	67.4	98.5	0.68
270	3.10	0.00	3.10	0.21	66.1	99.5	0.66
275	3.19	0.00	3.19	0.21	67.9	99.5	0.68
280	3.28	0.00	3.27	0.21	66.1	99.5	0.66
285	3.36	0.00	3.36	0.21	66.8	99.5	0.67
290	3.46	0.00	3.46	0.21	66.1	99.5	0.66
295	3.54	0.00	3.54	0.21	66.1	99.5	0.66
300	3.63	0.00	3.63	0.21	66.1	99.5	0.66
305	3.72	0.00	3.72	0.21	65.4	99.5	0.66
310	3.80	0.00	3.80	0.21	65.4	99.5	0.66
315	3.89	0.00	3.89	0.21	64.7	99.5	0.65
320	3.98	0.00	3.98	0.21	64.7	99.5	0.65
325	4.07	0.00	4.07	0.21	64.1	99.5	0.64
330	4.15	0.00	4.15	0.21	64.1	99.5	0.64
335	4.24	0.00	4.24	0.21	64.7	99.5	0.65
340	4.33	0.00	4.33	0.21	64.1	99.5	0.64
345	4.41	0.00	4.41	0.21	64.7	99.5	0.65
350	4.50	0.00	4.50	0.21	65.4	99.5	0.66
355	4.59	0.00	4.59	0.21	64.7	99.5	0.65
360	4.68	0.00	4.68	0.21	64.1	99.5	0.64
365	4.77	0.00	4.77	0.21	62.7	99.5	0.63
370	4.86	0.00	4.85	0.21	62.7	99.5	0.63
375	4.94	0.00	4.94	0.21	62.7	99.5	0.63
380	5.02	0.00	5.02	0.21	63.4	99.5	0.64
385	5.11	0.00	5.11	0.21	63.4	99.5	0.64
390	5.19	0.00	5.19	0.21	63.4	99.5	0.64
395	5.29	0.00	5.29	0.21	62.7	98.5	0.64

400	5.38	0.00	5.38	0.21	62.7	99.5	0.63
405	5.47	0.00	5.47	0.21	62.7	98.5	0.64
410	5.56	0.00	5.55	0.21	62.7	99.5	0.63
415	5.64	0.00	5.64	0.21	62.7	99.5	0.63
420	5.73	0.00	5.73	0.21	62.0	99.5	0.62
425	5.82	0.00	5.82	0.21	62.0	98.51	0.63
430	5.91	0.00	5.91	0.21	61.4	99.5	0.62

Table B2: 2-D Monotonic test on dense sand σ_n = 300 kPa

Date of testing: 23/04/1996
Tested by: Alain Mabia
Type of sample: Dense clean sand
Plate: sand-blasted steel plate
Density: 1.89 g/cm^3

TIME Sec.	Ux (mm)	Ux2 (mm)	Ux1 (mm)	V (mm)	Tau-x (kPa)	Sig-n (kPa)	T/S
0	0.00	0.01	-0.01	0.00	0.0	300.3	0.00
5	0.02	0.01	0.01	0.00	0.6	300.3	0.00
10	0.00	0.00	0.00	0.00	4.7	300.3	0.02
15	0.00	0.01	0.00	0.00	8.7	300.3	0.03
20	0.00	0.01	-0.01	0.00	12.8	299.3	0.04
25	0.00	0.01	0.00	-0.01	17.5	299.3	0.06
30	0.01	0.01	0.00	-0.01	24.9	299.3	0.08
35	0.02	0.01	0.01	-0.02	35.7	300.3	0.12
40	0.03	0.01	0.03	-0.02	46.5	300.3	0.15
45	0.05	0.01	0.04	-0.02	56.6	300.3	0.19
50	0.06	0.00	0.06	-0.03	66.8	299.3	0.22
55	0.08	0.01	0.07	-0.04	76.2	299.3	0.25
60	0.10	0.01	0.10	-0.05	85.7	299.3	0.29
65	0.13	0.00	0.12	-0.05	93.8	299.3	0.31
70	0.15	0.01	0.14	-0.06	102.5	299.3	0.34
75	0.17	0.01	0.16	-0.07	110.6	300.3	0.37
80	0.20	0.01	0.19	-0.07	118.0	299.3	0.39
85	0.23	0.01	0.22	-0.07	124.8	299.3	0.42
90	0.26	0.00	0.26	-0.07	132.2	299.3	0.44
95	0.30	0.01	0.29	-0.07	140.3	299.3	0.47
100	0.34	0.00	0.34	-0.07	148.4	300.3	0.49
105	0.41	0.01	0.40	-0.07	155.2	300.3	0.52
110	0.42	0.01	0.41	-0.08	161.9	300.3	0.54
115	0.46	0.01	0.45	-0.07	168.6	301.3	0.56
120	0.50	0.00	0.50	-0.08	174.0	300.3	0.58
125	0.54	0.00	0.54	-0.07	180.8	300.3	0.60
130	0.59	0.00	0.59	-0.07	184.8	300.3	0.62
135	0.64	0.00	0.64	-0.07	190.2	300.3	0.63
140	0.69	0.00	0.69	-0.06	195.6	301.3	0.65
145	0.75	0.00	0.74	-0.05	199.7	301.3	0.66

150	0.80	0.00	0.80	-0.05	203.7	301.3	0.68
155	0.86	0.00	0.86	-0.04	207.1	301.3	0.69
160	0.92	0.00	0.92	-0.03	210.5	302.3	0.70
165	0.98	0.00	0.98	-0.02	213.9	302.3	0.71
170	1.05	0.01	1.04	-0.01	215.9	301.3	0.72
175	1.13	0.00	1.12	-0.01	217.2	302.3	0.72
180	1.20	0.00	1.19	0.01	217.9	303.3	0.72
185	1.27	0.00	1.26	0.01	219.9	302.3	0.73
190	1.34	0.00	1.34	0.03	219.9	302.3	0.73
195	1.42	0.00	1.42	0.03	221.3	302.3	0.73
200	1.51	0.00	1.50	0.05	218.6	302.3	0.72
205	1.60	0.00	1.59	0.05	214.5	302.3	0.71
210	1.68	0.00	1.68	0.06	213.2	302.3	0.71
215	1.77	0.00	1.77	0.07	212.5	302.3	0.70
220	1.86	0.00	1.85	0.08	211.2	302.3	0.70
225	1.94	0.00	1.94	0.09	211.8	302.3	0.70
230	2.03	0.00	2.02	0.09	211.2	301.3	0.70
235	2.11	0.00	2.11	0.10	210.5	302.3	0.70
240	2.20	0.01	2.20	0.11	210.5	302.3	0.70
245	2.29	0.01	2.28	0.11	210.5	302.3	0.70
250	2.37	0.01	2.37	0.12	209.1	302.3	0.69
255	2.47	0.01	2.46	0.12	205.8	302.3	0.68
260	2.56	0.00	2.55	0.13	205.8	302.3	0.68
265	2.64	0.00	2.63	0.13	206.4	303.3	0.68
270	2.73	0.01	2.72	0.15	205.1	302.3	0.68
275	2.82	0.01	2.81	0.15	203.7	303.3	0.67
280	2.90	0.01	2.90	0.16	203.7	302.3	0.67
285	2.99	0.01	2.99	0.16	203.1	302.3	0.67
290	3.08	0.01	3.08	0.16	201.0	301.3	0.67
295	3.16	0.01	3.16	0.17	201.7	302.3	0.67
300	3.25	0.00	3.25	0.17	201.7	302.3	0.67
305	3.34	0.01	3.33	0.18	201.0	302.3	0.66
310	3.42	0.01	3.42	0.18	200.4	303.3	0.66
315	3.51	0.01	3.50	0.19	199.7	302.3	0.66
320	3.59	0.01	3.58	0.19	199.7	302.3	0.66
325	3.68	0.01	3.67	0.20	198.3	302.3	0.66
330	3.78	0.00	3.77	0.20	196.3	303.3	0.65
335	3.87	0.01	3.86	0.20	195.0	302.3	0.65
340	3.95	0.01	3.94	0.20	195.6	301.3	0.65
345	4.03	0.01	4.02	0.21	196.3	302.3	0.65
350	4.13	0.01	4.12	0.21	194.3	302.3	0.64
355	4.20	0.00	4.20	0.22	195.0	302.3	0.65
360	4.30	0.00	4.29	0.23	194.3	303.3	0.64
365	4.38	0.00	4.38	0.23	195.0	302.3	0.65
370	4.46	0.00	4.46	0.23	194.3	302.3	0.64
375	4.55	0.00	4.54	0.24	195.6	302.3	0.65
380	4.63	0.00	4.63	0.24	195.6	302.3	0.65
385	4.72	0.00	4.72	0.24	193.6	302.3	0.64
390	4.82	0.00	4.81	0.24	192.9	303.3	0.64
395	4.91	0.00	4.90	0.25	191.6	302.3	0.63

400	5.00	0.00	5.00	0.25	190.9	302.3	0.63
405	5.09	0.00	5.09	0.25	189.6	302.3	0.63
410	5.17	0.00	5.17	0.25	191.6	302.3	0.63
415	5.26	0.00	5.26	0.26	190.2	302.3	0.63
420	5.35	0.00	5.35	0.26	189.6	303.3	0.63
425	5.44	0.00	5.44	0.26	188.2	302.3	0.62
430	5.53	0.00	5.52	0.26	188.9	303.3	0.62
435	5.62	0.00	5.61	0.27	186.9	302.3	0.62
440	5.71	0.00	5.71	0.27	184.8	302.3	0.61
445	5.80	0.00	5.80	0.27	185.5	302.3	0.61
450	5.88	0.00	5.88	0.27	186.9	302.3	0.62
455	5.98	0.00	5.97	0.27	186.2	302.3	0.62

Table B3: 2-D Monotonic test on dense sand σ_n = 500 kPa

Date of testing: 23/04/1996
Tested by: Alain Mabia
Type of sample: Dense clean sand
Plate: sand-blasted steel plate
Density: 1.89 g/cm^3

TIME Sec.	Ux (mm)	Ux2 (mm)	Ux1 (mm)	V (mm)	Tau-x (kPa)	Sig-n (kPa)	T/S
0	0.00	0.01	-0.01	0.00	0.0	500.1	0.00
5	0.00	0.01	-0.01	0.00	2.7	500.1	0.01
10	0.01	0.01	-0.01	0.00	8.8	499.2	0.02
15	0.01	0.01	0.00	0.00	12.2	499.2	0.02
20	0.01	0.01	0.00	0.00	16.2	499.2	0.03
25	0.01	0.01	0.00	0.00	23.0	499.2	0.05
30	0.01	0.01	0.00	0.00	32.4	499.2	0.06
35	0.01	0.01	0.00	0.00	42.5	500.1	0.08
40	0.02	0.01	0.01	0.00	54.7	499.2	0.11
45	0.03	0.01	0.01	0.01	66.8	499.2	0.13
50	0.03	0.01	0.02	0.01	77.6	498.2	0.16
55	0.04	0.01	0.03	0.01	89.8	498.2	0.18
60	0.05	0.01	0.03	0.01	101.3	498.2	0.20
65	0.06	0.01	0.05	0.01	112.7	498.2	0.23
70	0.07	0.01	0.06	0.00	124.2	498.2	0.25
75	0.08	0.01	0.07	0.01	135.7	497.2	0.27
80	0.10	0.01	0.09	0.01	147.1	497.2	0.30
85	0.11	0.01	0.10	0.01	157.9	498.2	0.32
90	0.13	0.01	0.12	0.01	168.0	498.2	0.34
95	0.15	0.01	0.14	0.01	179.5	497.2	0.36
100	0.17	0.01	0.16	0.00	189.0	498.2	0.38
105	0.20	0.01	0.19	0.00	199.1	498.2	0.40
110	0.22	0.01	0.21	0.01	207.9	498.2	0.42
115	0.24	0.01	0.23	0.01	217.3	498.2	0.44
120	0.27	0.00	0.27	0.01	226.1	497.2	0.45
125	0.30	0.00	0.29	0.01	234.8	497.2	0.47
130	0.32	0.00	0.32	0.02	243.6	498.2	0.49
135	0.35	0.01	0.34	0.02	251.0	498.2	0.50
140	0.38	0.00	0.37	0.02	259.1	499.2	0.52
145	0.41	0.00	0.41	0.02	267.9	500.1	0.54
150	0.44	0.00	0.44	0.02	275.3	501.1	0.55

155	0.47	0.01	0.46	0.02	283.4	501.1	0.57
160	0.51	0.00	0.51	0.03	290.9	502.1	0.58
165	0.54	0.00	0.54	0.03	297.6	502.1	0.59
170	0.57	0.00	0.57	0.03	304.3	502.1	0.61
175	0.62	0.00	0.61	0.03	310.4	503.1	0.62
180	0.65	0.00	0.65	0.04	317.2	504.1	0.63
185	0.69	0.00	0.69	0.04	323.9	503.1	0.64
190	0.73	0.00	0.72	0.04	329.3	505.1	0.65
195	0.77	0.00	0.77	0.05	336.1	505.1	0.67
200	0.82	0.00	0.81	0.05	340.8	505.1	0.67
205	0.85	0.00	0.85	0.06	346.9	506.0	0.69
210	0.90	0.00	0.90	0.06	351.6	506.0	0.69
215	0.95	0.00	0.95	0.07	356.3	507.0	0.70
220	1.00	0.00	1.00	0.07	361.0	508.0	0.71
225	1.06	0.00	1.06	0.09	364.4	507.0	0.72
230	1.11	0.00	1.11	0.09	368.4	508.0	0.73
235	1.16	0.00	1.16	0.10	371.1	508.0	0.73
240	1.23	0.00	1.23	0.11	373.8	507.0	0.74
245	1.29	0.00	1.29	0.13	376.5	508.0	0.74
250	1.36	0.00	1.35	0.13	377.9	508.0	0.74
255	1.42	0.00	1.42	0.14	378.6	508.0	0.75
260	1.50	0.00	1.49	0.15	379.9	508.0	0.75
265	1.57	0.00	1.56	0.16	381.3	508.0	0.75
270	1.64	0.00	1.64	0.18	380.6	508.0	0.75
275	1.72	0.00	1.72	0.19	379.2	509.0	0.74
280	1.79	0.00	1.79	0.20	381.3	509.0	0.75
285	1.88	0.00	1.88	0.21	378.6	509.0	0.74
290	1.96	0.00	1.95	0.22	378.6	509.0	0.74
295	2.04	0.00	2.04	0.22	377.2	509.0	0.74
300	2.14	0.00	2.14	0.23	373.2	507.0	0.74
305	2.21	0.00	2.21	0.24	375.2	508.0	0.74
310	2.31	0.00	2.30	0.25	371.1	509.0	0.73
315	2.38	0.00	2.38	0.26	370.5	508.0	0.73
320	2.47	0.01	2.46	0.26	371.1	509.0	0.73
325	2.56	0.00	2.55	0.27	370.5	508.0	0.73
330	2.66	0.00	2.65	0.28	366.4	509.0	0.72
335	2.74	0.00	2.73	0.28	365.1	509.0	0.72
340	2.83	0.00	2.83	0.29	364.4	508.0	0.72
345	2.93	0.00	2.93	0.29	361.0	507.0	0.71
350	3.01	0.00	3.00	0.28	361.7	508.0	0.71
355	3.09	0.00	3.09	0.30	361.7	508.0	0.71
360	3.17	0.00	3.17	0.31	361.0	509.0	0.71
365	3.25	0.00	3.24	0.31	363.7	510.0	0.71
370	3.34	0.01	3.33	0.32	361.7	509.0	0.71
375	3.43	0.00	3.42	0.32	359.7	509.0	0.71
380	3.50	0.00	3.50	0.33	361.7	510.0	0.71
385	3.60	0.00	3.60	0.33	360.4	509.0	0.71
390	3.69	0.00	3.69	0.34	357.0	509.0	0.70
395	3.79	0.00	3.79	0.34	353.6	509.0	0.69
400	3.88	0.00	3.87	0.35	354.3	509.0	0.70

405	3.97	0.00	3.97	0.35	350.9	509.0	0.69
410	4.05	0.01	4.04	0.35	352.9	509.0	0.69
415	4.14	0.00	4.13	0.36	352.9	509.0	0.69
420	4.21	0.00	4.21	0.36	352.3	509.0	0.69
425	4.31	0.00	4.30	0.37	351.6	510.0	0.69
430	4.38	0.00	4.38	0.37	352.9	509.0	0.69
435	4.48	0.00	4.48	0.37	350.9	509.0	0.69
440	4.58	0.00	4.57	0.38	347.5	509.0	0.68
445	4.66	0.00	4.66	0.38	350.9	510.0	0.69
450	4.75	0.00	4.74	0.38	347.5	509.0	0.68
455	4.84	0.00	4.84	0.38	345.5	508.0	0.68
460	4.92	0.00	4.92	0.38	348.2	509.0	0.68
465	5.01	0.00	5.00	0.39	348.2	510.0	0.68
470	5.10	0.00	5.10	0.39	346.9	510.0	0.68
475	5.19	0.00	5.19	0.40	344.8	509.0	0.68
480	5.28	0.00	5.27	0.40	343.5	510.0	0.67
485	5.36	0.01	5.36	0.40	344.8	509.0	0.68
490	5.46	0.00	5.46	0.40	342.1	510.0	0.67
495	5.55	0.00	5.55	0.41	340.8	510.0	0.67
500	5.66	0.00	5.65	0.40	336.7	509.0	0.66
505	5.73	0.00	5.73	0.41	338.1	509.0	0.66
510	5.82	0.01	5.81	0.41	338.1	509.0	0.66
515	5.90	0.00	5.90	0.41	338.1	508.0	0.67

Table B4: 2-D Monotonic test on dense sand σ_n = 100 kPa

Date of testing: 23/04/1996
Tested by: Alain Mabia
Type of sample: Oil contaminated dense sand
Plate: sand-blasted steel plate
Density: 1.89 g/cm^3

TIME Sec.	Ux (mm)	Ux2 (mm)	Ux1 (mm)	V (mm)	Tau-x (kPa)	Sig-n (kPa)	T/S
	0.01	0.01	0.01	0.04	0.0	97.5	0.00
5	0.03	0.01	0.02	0.04	13.5	98.5	0.14
10	0.05	0.01	0.04	0.04	18.3	99.5	0.18
15	0.09	0.01	0.08	0.04	21.0	98.5	0.21
20	0.13	0.00	0.12	0.04	24.3	100.5	0.24
25	0.18	0.01	0.17	0.04	28.4	99.5	0.29
30	0.24	0.01	0.23	0.04	29.7	100.5	0.30
35	0.30	0.01	0.29	0.04	32.4	99.5	0.33
40	0.37	0.01	0.36	0.04	33.8	100.5	0.34
45	0.43	0.01	0.43	0.04	36.5	99.5	0.37
50	0.51	0.01	0.50	0.04	37.8	99.5	0.38
55	0.58	0.01	0.57	0.04	37.8	99.5	0.38
60	0.65	0.01	0.64	0.04	39.8	100.5	0.40
65	0.72	0.01	0.71	0.04	40.5	99.5	0.41
70	0.80	0.01	0.79	0.04	41.2	98.5	0.42
75	0.88	0.01	0.87	0.04	41.9	99.5	0.42
80	0.95	0.00	0.95	0.04	43.2	99.5	0.43
85	1.03	0.01	1.02	0.04	43.9	99.5	0.44
90	1.11	0.01	1.11	0.04	43.9	100.5	0.44
95	1.20	0.01	1.19	0.04	44.6	99.5	0.45
100	1.27	0.01	1.27	0.04	45.9	99.5	0.46
105	1.35	0.01	1.35	0.04	45.9	99.5	0.46
110	1.43	0.01	1.43	0.04	46.6	100.5	0.46
115	1.51	0.01	1.51	0.04	47.3	100.5	0.47
120	1.60	0.00	1.60	0.04	48.6	100.5	0.48
125	1.68	0.00	1.67	0.04	49.3	99.5	0.50
130	1.76	0.00	1.76	0.04	50.0	100.5	0.50
135	1.84	0.00	1.83	0.04	51.3	100.5	0.51
140	1.92	0.00	1.91	0.04	50.6	101.5	0.50
145	2.00	0.00	1.99	0.04	51.3	100.5	0.51
150	2.08	0.00	2.07	0.04	52.0	100.5	0.52
155	2.16	0.00	2.16	0.04	51.3	100.5	0.51
160	2.25	0.00	2.25	0.04	50.6	100.5	0.50
165	2.34	0.00	2.33	0.04	52.0	100.5	0.52
170	2.42	0.00	2.41	0.04	52.0	100.5	0.52

175	2.51	0.00	2.50	0.04	52.0	100.5	0.52
180	2.58	0.01	2.58	0.04	52.0	101.5	0.51
185	2.67	0.00	2.66	0.04	52.7	99.5	0.53
190	2.75	0.00	2.75	0.04	51.3	100.5	0.51
195	2.84	0.00	2.83	0.04	52.0	100.5	0.52
200	2.92	0.01	2.92	0.04	52.0	101.5	0.51
205	3.00	0.00	3.00	0.04	52.7	101.5	0.52
210	3.09	0.00	3.09	0.04	52.7	101.5	0.52
215	3.17	0.00	3.17	0.04	53.3	101.5	0.53
220	3.26	0.00	3.25	0.04	53.3	100.5	0.53
225	3.35	0.00	3.35	0.04	52.7	101.5	0.52
230	3.43	0.00	3.43	0.04	53.3	101.5	0.53
235	3.52	0.00	3.52	0.04	53.3	100.5	0.53
240	3.61	0.01	3.60	0.04	52.0	101.5	0.51
245	3.69	0.00	3.69	0.04	51.3	100.5	0.51
250	3.78	0.00	3.77	0.04	52.7	101.5	0.52
255	3.85	0.00	3.85	0.04	53.3	100.5	0.53
260	3.95	0.00	3.94	0.04	52.7	100.5	0.52
265	4.03	0.00	4.03	0.04	52.7	100.5	0.52
270	4.12	0.00	4.12	0.04	52.0	100.5	0.52
275	4.20	0.00	4.20	0.04	53.3	100.5	0.53
280	4.29	0.00	4.28	0.04	52.7	100.5	0.52
285	4.37	0.00	4.37	0.04	53.3	100.5	0.53
290	4.46	0.00	4.45	0.04	52.7	100.5	0.52
295	4.54	0.00	4.54	0.04	53.3	100.5	0.53
300	4.63	0.00	4.63	0.04	53.3	100.5	0.53
305	4.72	0.00	4.72	0.04	53.3	100.5	0.53
310	4.80	0.00	4.79	0.04	52.0	100.5	0.52
315	4.88	0.00	4.88	0.04	53.3	101.5	0.53
320	4.96	0.00	4.96	0.04	52.7	100.5	0.52
325	5.05	0.00	5.05	0.04	53.3	100.5	0.53
330	5.14	0.00	5.14	0.04	53.3	101.5	0.53
335	5.23	0.00	5.22	0.04	53.3	99.5	0.54
340	5.32	0.00	5.31	0.04	52.0	100.5	0.52
345	5.37	0.00	5.36	0.04	52.0	100.5	0.52
350	5.48	0.00	5.48	0.04	53.3	100.5	0.53
355	5.57	0.01	5.56	0.04	53.3	99.5	0.54
360	5.65	0.00	5.65	0.04	53.3	99.5	0.54
365	5.74	0.00	5.73	0.04	53.3	100.5	0.53
370	5.82	0.00	5.82	0.04	53.3	99.5	0.54
375	5.92	0.00	5.91	0.04	53.3	99.5	0.54

Table B5: 2-D Monotonic test on dense sand σ_n =300 kPa

Date of testing: 7/05/1996
Tested by: Alain Mabia
Type of sample: Oil contaminated dense sand
Plate: sand-blasted steel plate
Density: 1.89 g/cm^3

TIME Sec.	Ux (mm)	Ux2 (mm)	Ux1 (mm)	V (mm)	Tau-x (kPa)	Sig-n (kPa)	T/S
	0.02	0.00	0.01	0.00	0.0	299.3	0.00
5	0.02	0.00	0.01	0.00	4.1	299.3	0.01
10	0.01	0.00	0.01	0.00	10.2	298.3	0.03
15	0.01	0.00	0.01	0.00	13.5	299.3	0.05
20	0.01	0.00	0.01	0.00	17.6	299.3	0.06
25	0.00	0.00	0.00	0.00	24.3	298.3	0.08
30	0.01	0.00	0.00	0.00	31.8	298.3	0.11
35	0.03	0.00	0.02	-0.01	39.8	298.3	0.13
40	0.04	0.00	0.04	-0.01	47.9	298.3	0.16
45	0.07	0.00	0.07	-0.02	56.0	298.3	0.19
50	0.10	0.00	0.09	-0.03	63.5	298.3	0.21
55	0.13	0.00	0.13	-0.04	70.2	298.3	0.24
60	0.17	0.00	0.16	-0.04	76.3	298.3	0.26
65	0.20	0.00	0.20	-0.05	83.0	297.4	0.28
70	0.25	0.00	0.25	-0.06	87.8	298.3	0.29
75	0.29	0.00	0.29	-0.06	93.8	297.4	0.32
80	0.34	0.00	0.33	-0.07	98.6	298.3	0.33
85	0.39	0.00	0.39	-0.08	102.6	297.4	0.35
90	0.44	0.00	0.44	-0.08	106.6	297.4	0.36
95	0.50	0.00	0.49	-0.09	111.4	297.4	0.37
100	0.55	0.00	0.55	-0.09	114.1	298.3	0.38
105	0.62	0.00	0.61	-0.09	117.4	298.3	0.39
110	0.67	0.00	0.67	-0.09	120.8	297.4	0.41
115	0.73	0.00	0.73	-0.10	124.2	298.3	0.42
120	0.79	0.00	0.79	-0.10	127.6	297.4	0.43
125	0.86	0.00	0.86	-0.10	128.9	298.3	0.43
130	0.92	0.00	0.92	-0.10	132.3	297.4	0.44
135	0.99	0.00	0.98	-0.10	134.3	298.3	0.45
140	1.06	0.00	1.06	-0.10	136.3	297.4	0.46
145	1.13	0.00	1.13	-0.10	138.4	298.3	0.46

150	1.21	0.00	1.21	-0.10	139.0	299.3	0.46
155	1.29	0.00	1.28	-0.10	140.4	298.3	0.47
160	1.37	0.00	1.36	-0.10	141.1	298.3	0.47
165	1.43	0.00	1.43	-0.10	144.4	300.3	0.48
170	1.52	0.00	1.51	-0.10	143.1	299.3	0.48
175	1.59	0.00	1.59	-0.10	145.1	299.3	0.48
180	1.67	0.00	1.67	-0.09	144.4	300.3	0.48
185	1.75	0.00	1.75	-0.10	145.8	300.3	0.49
190	1.82	0.00	1.82	-0.09	146.5	300.3	0.49
195	1.90	0.00	1.90	-0.10	147.8	300.3	0.49
200	1.98	0.00	1.98	-0.09	149.2	300.3	0.50
205	2.06	0.00	2.06	-0.09	149.2	300.3	0.50
210	2.15	0.00	2.14	-0.09	148.5	300.3	0.49
215	2.23	0.00	2.22	-0.09	150.5	299.3	0.50
220	2.31	0.00	2.31	-0.09	149.8	300.3	0.50
225	2.40	0.00	2.39	-0.09	149.2	301.3	0.50
230	2.48	0.00	2.47	-0.09	150.5	301.3	0.50
235	2.56	0.00	2.56	-0.09	149.2	301.3	0.50
240	2.64	0.00	2.63	-0.09	151.2	300.3	0.50
245	2.72	0.00	2.72	-0.09	150.5	300.3	0.50
250	2.80	0.00	2.80	-0.09	151.2	301.3	0.50
255	2.89	0.00	2.89	-0.09	151.2	300.3	0.50
260	2.97	0.00	2.97	-0.09	151.9	300.3	0.51
265	3.05	0.00	3.05	-0.09	152.5	300.3	0.51
270	3.14	0.00	3.13	-0.09	152.5	300.3	0.51
275	3.22	0.00	3.22	-0.09	153.2	301.3	0.51
280	3.31	0.00	3.31	-0.09	153.2	300.3	0.51
285	3.38	0.00	3.38	-0.08	153.9	301.3	0.51
290	3.47	0.01	3.46	-0.09	153.9	301.3	0.51
295	3.56	0.00	3.55	-0.09	153.9	301.3	0.51
300	3.64	0.00	3.64	-0.08	153.2	300.3	0.51
305	3.73	0.00	3.73	-0.08	153.2	300.3	0.51
310	3.81	0.00	3.81	-0.09	155.2	300.3	0.52
315	3.90	0.00	3.89	-0.08	154.6	301.3	0.51
320	3.98	0.00	3.98	-0.08	154.6	301.3	0.51
325	4.07	0.00	4.06	-0.08	153.9	300.3	0.51
330	4.16	0.00	4.15	-0.08	154.6	300.3	0.51
335	4.24	0.00	4.24	-0.08	155.2	300.3	0.52
340	4.33	0.00	4.33	-0.08	153.9	301.3	0.51
345	4.41	0.00	4.41	-0.08	153.9	301.3	0.51
350	4.51	0.00	4.50	-0.08	153.2	301.3	0.51
355	4.59	0.00	4.59	-0.08	151.9	300.3	0.51
360	4.67	0.00	4.67	-0.08	152.5	301.3	0.51
365	4.76	0.00	4.75	-0.08	153.9	301.3	0.51
370	4.84	0.01	4.84	-0.08	153.2	301.3	0.51
375	4.93	0.00	4.93	-0.07	153.2	301.3	0.51
380	5.03	0.01	5.02	-0.07	151.9	300.3	0.51
385	5.11	0.00	5.10	-0.07	151.9	300.3	0.51
390	5.20	0.00	5.19	-0.07	152.5	300.3	0.51
395	5.29	0.00	5.28	-0.07	151.2	300.3	0.50

400	5.37	0.00	5.37	-0.07	151.9	301.3	0.50
405	5.46	0.00	5.46	-0.07	150.5	300.3	0.50
410	5.55	0.00	5.54	-0.07	151.9	301.3	0.50
415	5.63	0.00	5.63	-0.07	151.9	301.3	0.50
420	5.72	0.00	5.72	-0.074	151.2	301.3	0.50
425	5.80	0.01	5.79	-0.07	152.5	300.3	0.51
430	5.89	0.00	5.88	-0.07	152.5	301.3	0.51
435	5.98	0.00	5.97	-0.07	152.5	300.3	0.51

Table B6: 2-D Monotonic test on dense sand σ_n =500 kPa

Date of testing: 7/05/1996
Tested by: Alain Mabia
Type of sample: Oil contaminated dense sand
Plate: sand-blasted steel plate
Density: 1.89 g/cm^3

TIME Sec.	Ux (mm)	Ux2 (mm)	Ux1 (mm)	V (mm)	Tau-x (kPa)	Sig-n (kPa)	T/S
0	0	0.004	-0.004	0	0	499.2	0
5	0.00	0.01	0.00	0.00	4.8	500.1	0.01
10	0.00	0.01	-0.01	0.00	10.2	499.2	0.02
15	0.01	0.01	0.00	0.00	14.2	499.2	0.03
20	0.01	0.01	0.00	0.00	18.9	499.2	0.04
25	0.01	0.02	-0.01	0.00	25.7	500.1	0.05
30	0.02	0.01	0.01	0.00	34.5	500.1	0.07
35	0.03	0.01	0.03	0.00	43.9	500.1	0.09
40	0.04	0.01	0.04	0.00	54.0	499.2	0.11
45	0.06	0.01	0.05	-0.01	64.8	499.2	0.13
50	0.08	0.01	0.07	-0.01	74.9	499.2	0.15
55	0.09	0.00	0.09	-0.01	85.1	499.2	0.17
60	0.11	0.01	0.11	-0.01	94.5	497.2	0.19
65	0.14	0.01	0.13	-0.02	103.3	498.2	0.21
70	0.16	0.01	0.15	-0.03	112.0	498.2	0.22
75	0.19	0.01	0.18	-0.03	120.8	497.2	0.24
80	0.21	0.01	0.21	-0.03	128.9	497.2	0.26
85	0.25	0.01	0.24	-0.04	137.0	498.2	0.28
90	0.27	0.01	0.27	-0.05	144.4	498.2	0.29
95	0.31	0.01	0.30	-0.05	150.5	498.2	0.30
100	0.34	0.01	0.34	-0.05	157.9	498.2	0.32
105	0.38	0.01	0.37	-0.06	164.7	497.2	0.33
110	0.41	0.00	0.41	-0.06	170.1	498.2	0.34
115	0.45	0.01	0.45	-0.06	176.1	498.2	0.35
120	0.50	0.00	0.49	-0.06	182.2	498.2	0.37
125	0.54	0.00	0.54	-0.06	187.6	497.2	0.38
130	0.59	0.00	0.58	-0.06	192.3	497.2	0.39
135	0.63	0.00	0.63	-0.07	198.4	497.2	0.40
140	0.68	0.00	0.67	-0.07	201.8	497.2	0.41
145	0.72	0.00	0.72	-0.07	206.5	497.2	0.42
150	0.78	0.00	0.77	-0.07	209.9	497.2	0.42

155	0.83	0.00	0.83	-0.07	213.9	497.2	0.43
160	0.88	0.00	0.88	-0.07	217.3	497.2	0.44
165	0.93	0.00	0.93	-0.07	222.0	498.2	0.45
170	0.98	0.00	0.98	-0.07	226.1	497.2	0.45
175	1.04	0.00	1.04	-0.07	228.1	498.2	0.46
180	1.12	0.00	1.11	-0.07	228.8	497.2	0.46
185	1.19	0.00	1.18	-0.07	230.8	497.2	0.46
190	1.25	0.00	1.25	-0.07	233.5	497.2	0.47
195	1.32	0.00	1.31	-0.07	235.5	499.2	0.47
200	1.38	0.00	1.37	-0.07	239.6	499.2	0.48
205	1.44	0.00	1.44	-0.07	241.6	500.1	0.48
210	1.50	0.00	1.50	-0.07	245.0	500.1	0.49
215	1.58	0.00	1.57	-0.07	245.6	500.1	0.49
220	1.64	0.00	1.64	-0.07	248.3	501.1	0.50
225	1.72	0.00	1.72	-0.06	248.3	502.1	0.49
230	1.79	0.00	1.78	-0.06	249.7	501.1	0.50
235	1.87	0.00	1.86	-0.06	251.0	502.1	0.50
240	1.95	0.00	1.95	-0.06	251.0	502.1	0.50
245	2.03	0.00	2.03	-0.06	251.7	502.1	0.50
250	2.10	0.00	2.09	-0.05	253.7	502.1	0.51
255	2.18	0.00	2.17	-0.06	253.1	502.1	0.50
260	2.26	0.01	2.25	-0.06	253.7	501.1	0.51
265	2.35	0.00	2.34	-0.06	253.1	502.1	0.50
270	2.42	0.00	2.42	-0.05	253.1	502.1	0.50
275	2.50	0.00	2.50	-0.05	253.1	502.1	0.50
280	2.58	0.00	2.58	-0.05	253.7	502.1	0.51
285	2.67	0.00	2.66	-0.05	252.4	502.1	0.50
290	2.74	0.00	2.74	-0.05	254.4	502.1	0.51
295	2.81	0.00	2.81	-0.05	256.4	502.1	0.51
300	2.84	0.00	2.84	-0.05	258.5	502.1	0.51
305	2.98	0.00	2.98	-0.05	257.1	502.1	0.51
310	3.06	0.01	3.05	-0.05	257.1	503.1	0.51
315	3.14	0.00	3.14	-0.05	257.8	502.1	0.51
320	3.23	0.00	3.22	-0.05	256.4	502.1	0.51
325	3.32	0.00	3.32	-0.05	255.1	502.1	0.51
330	3.40	0.00	3.40	-0.05	256.4	502.1	0.51
335	3.48	0.00	3.48	-0.04	259.1	503.1	0.52
340	3.56	0.00	3.56	-0.04	257.1	502.1	0.51
345	3.64	0.01	3.64	-0.04	257.1	502.1	0.51
350	3.74	0.01	3.73	-0.04	254.4	502.1	0.51
355	3.82	0.00	3.82	-0.04	256.4	502.1	0.51
360	3.90	0.00	3.90	-0.04	257.8	502.1	0.51
365	4.00	0.00	3.99	-0.04	257.1	501.1	0.51
370	4.08	0.01	4.07	-0.04	258.5	501.1	0.52
375	4.16	0.00	4.16	-0.04	257.8	502.1	0.51
380	4.24	0.00	4.23	-0.04	260.5	502.1	0.52
385	4.32	0.00	4.31	-0.04	261.8	503.1	0.52
390	4.42	0.00	4.42	-0.04	255.8	502.1	0.51
395	4.49	0.00	4.49	-0.04	259.8	502.1	0.52
400	4.57	0.00	4.57	-0.04	260.5	502.1	0.52

405	4.66	0.00	4.65	-0.04	260.5	502.1	0.52
410	4.75	0.00	4.75	-0.04	257.8	501.1	0.51
415	4.83	0.00	4.83	-0.04	260.5	502.1	0.52
420	4.93	0.00	4.92	-0.04	258.5	501.1	0.52
425	5.00	0.00	5.00	-0.04	259.1	502.1	0.52
430	5.09	0.00	5.09	-0.04	259.1	502.1	0.52
435	5.17	0.01	5.17	-0.04	259.1	501.1	0.52
440	5.25	0.00	5.25	-0.04	262.5	502.1	0.52
445	5.34	0.00	5.33	-0.04	260.5	502.1	0.52
450	5.43	0.00	5.42	-0.04	259.1	501.1	0.52
455	5.50	0.00	5.50	-0.04	261.8	502.1	0.52
460	5.59	0.00	5.59	-0.04	259.8	502.1	0.52
465	5.68	0.00	5.68	-0.04	259.8	502.1	0.52
470	5.78	0.00	5.77	-0.04	257.1	502.1	0.51
475	5.86	0.00	5.85	-0.04	257.8	502.1	0.51
480	5.95	0.00	5.95	-0.04	255.8	502.1	0.51

Table B7: 2-D Monotonic test on dense sand σ_n = 50 kPa

Date of testing: 7/05/1996
Tested by: Alain Mabia
Type of sample: Dense clean sand
Plate: sand-blasted steel plate
Density: 1.89g/cm3

TIME Sec.	Ux (mm)	Ux2 (mm)	Ux1 (mm)	V (mm)	Tau-x (kPa)	Sig-n (kPa)	T/S
	0.00	0.01	0.00	0.00	0.0	50.3	0.00
5	0.00	0.01	-0.01	-0.01	0.0	50.3	0.00
10	0.00	0.01	-0.01	-0 01	2 7	50 3	0 05
15	0.00	0.01	0.00	-0.01	4.7	50.3	0.09
20	0.01	0.01	0.01	-0.01	8.1	50.3	0.16
25	0.02	0.01	0.01	-0.02	10.8	50.3	0.21
30	0.03	0.01	0.01	-0.02	13.5	50.3	0.27
35	0.04	0.01	0.03	-0.03	16.8	50.3	0.33
40	0.05	0.01	0.04	-0.03	18.9	50.3	0.38
45	0.06	0.01	0.06	-0.04	21.6	50.3	0.43
50	0.08	0.01	0.07	-0.04	23.6	50.3	0.47
55	0.10	0.01	0.09	-0.04	24.9	50.3	0.50
60	0.12	0.01	0.11	-0.04	27.6	51.3	0.54
65	0.14	0.01	0.14	-0.04	29.0	50.3	0.58
70	0.21	0.00	0.21	-0.03	31.0	50.3	0.62
75	0.20	0.01	0.19	-0.03	31.7	50.3	0.63
80	0.23	0.01	0.22	-0.02	33.0	51.3	0.64
85	0.26	0.01	0.25	-0.01	35.0	51.3	0.68
90	0.31	0.01	0.30	0.00	36.4	52.3	0.70
95	0.36	0.01	0.35	0.01	37.7	52.3	0.72
100	0.42	0.01	0.41	0.02	39.8	51.3	0.78
105	0.48	0.01	0.48	0.03	40.4	52.3	0.77
110	0.55	0.01	0.55	0.04	41.1	52.3	0.79
115	0.63	0.01	0.62	0.06	40.4	52.3	0.77
120	0.71	0.00	0.70	0.07	41.1	52.3	0.79
125	0.79	0.00	0.79	0.09	40.4	53.2	0.76
130	0.88	0.00	0.88	0.10	41.1	52.3	0.79
135	0.96	0.00	0.95	0.11	40.4	53.2	0.76
140	1.05	0.00	1.05	0.13	39.8	52.3	0.76
145	1.13	0.00	1.13	0.14	39.1	53.2	0.73
150	1.22	0.00	1.22	0.16	39.1	53.2	0.73

155	1.31	0.00	1.31	0.17	38.4	53.2	0.72
160	1.40	0.00	1.40	0.18	38.4	52.3	0.73
165	1.50	0.01	1.49	0.19	37.1	52.3	0.71
170	1.58	0.00	1.58	0.20	36.4	52.3	0.70
175	1.67	0.00	1.67	0.21	37.1	52.3	0.71
180	1.76	0.00	1.75	0.22	37.1	52.3	0.71
185	1.85	0.00	1.84	0.23	37.1	52.3	0.71
190	1.93	0.00	1.93	0.24	36.4	53.2	0.68
195	2.02	0.00	2.02	0.25	36.4	53.2	0.68
200	2.11	0.00	2.10	0.26	37.1	52.3	0.71
205	2.19	0.00	2.19	0.26	35.7	52.3	0.68
210	2.28	0.00	2.27	0.27	35.7	53.2	0.67
215	2.36	0.00	2.36	0.28	35.7	53.2	0.67
220	2.45	0.00	2.45	0.28	35.0	52.3	0.67
225	2.54	0.00	2.53	0.29	35.7	52.3	0.68
230	2.62	0.00	2.62	0.30	35.7	52.3	0.68
235	2.71	0.00	2.70	0.31	35.7	52.3	0.68
240	2.79	0.00	2.79	0.32	35.7	52.3	0.68
245	2.89	0.00	2.88	0.33	35.0	53.2	0.66
250	2.96	0.00	2.96	0.33	35.7	53.2	0.67
255	3.06	0.01	3.05	0.34	35.7	52.3	0.68
260	3.14	0.00	3.14	0.34	35.0	53.2	0.66
265	3.23	0.00	3.22	0.35	35.0	52.3	0.67
270	3.31	0.01	3.31	0.36	34.4	53.2	0.65
275	3.40	0.00	3.40	0.37	33.7	52.3	0.64
280	3.50	0.00	3.49	0.37	33.7	52.3	0.64
285	3.58	0.00	3.58	0.37	33.7	52.3	0.64
290	3.67	0.00	3.66	0.38	33.0	53.2	0.62
295	3.76	0.00	3.75	0.38	33.0	52.3	0.63
300	3.84	0.00	3.84	0.39	33.7	52.3	0.64
305	3.98	0.00	3.98	0.39	33.0	52.3	0.63
310	4.01	0.00	4.01	0.39	33.7	52.3	0.64
315	4.10	0.00	4.10	0.40	33.0	53.2	0.62
320	4.19	0.00	4.19	0.40	33.0	53.2	0.62
325	4.27	0.00	4.27	0.41	33.7	53.2	0.63
330	4.36	0.01	4.36	0.41	33.0	52.3	0.63
335	4.45	0.00	4.45	0.42	33.0	52.3	0.63
340	4.53	0.00	4.53	0.42	33.0	53.2	0.62
345	4.62	0.00	4.62	0.42	33.0	53.2	0.62
350	4.71	0.00	4.71	0.43	33.0	53.2	0.62
355	4.80	0.00	4.79	0.43	33.0	53.2	0.62
360	4.89	0.00	4.89	0.43	32.3	52.3	0.62
365	4.98	0.00	4.98	0.44	31.7	52.3	0.61
370	5.06	0.00	5.06	0.44	31.7	52.3	0.61
375	5.14	0.00	5.14	0.44	32.3	52.3	0.62
380	5.23	0.00	5.23	0.44	31.7	53.2	0.60
385	5.31	0.00	5.31	0.45	31.7	53.2	0.60
390	5.40	0.00	5.40	0.45	32.3	53.2	0.61
395	5.49	0.01	5.48	0.46	32.3	53.2	0.61
400	5.58	0.01	5.57	0.45	32.3	52.3	0.62

405	5.66	0.00	5.66	0.46	32.3	53.2	0.61
410	5.75	0.00	5.75	0.46	31.7	53.2	0.60
415	5.84	0.00	5.84	0.46	31.7	52.3	0.61
420	5.93	0.00	5.92	0.47	33.0	53.2	0.62

Table B8: 2-D Monotonic test on dense sand σ_n =500 kPa

Date of testing: 7/05/1996
Tested by: Alain Mabia
Type of sample: Oil contaminated dense sand
Plate: sand-blasted steel plate
Density: 1.89 g/cm^3

TIME Sec.	Ux (mm)	Ux2 (mm)	Ux1 (mm)	V (mm)	Tau-x (kPa)	Sig-n (kPa)	T/S
	0.00	0.00	0.00	0.00	0.0	49.3	0.00
5	0.00	0.00	0.00	0.00	3.3	49.3	0.07
10	0.01	0.00	0.01	0.00	6.7	48.3	0.14
15	0.02	0.00	0.02	0.00	8.7	49.3	0.18
20	0.04	0.00	0.04	0.00	11.4	48.3	0.24
25	0.07	0.00	0.06	-0.01	13.5	48.3	0.28
30	0.11	0.00	0.11	-0.01	14.8	48.3	0.31
35	0.17	0.00	0.17	-0.02	16.8	48.3	0.35
40	0.25	0.00	0.24	-0.03	17.5	48.3	0.36
45	0.31	0.00	0.31	-0.03	18.9	48.3	0.39
50	0.39	0.00	0.39	-0.03	18.9	48.3	0.39
55	0.47	0.00	0.47	-0.03	19.5	47.3	0.41
60	0.55	0.00	0.54	-0.04	20.2	48.3	0.42
65	0.63	0.00	0.62	-0.03	20.2	47.3	0.43
70	0.71	0.00	0.70	-0.04	20.9	48.3	0.43
75	0.79	0.00	0.79	-0.04	21.6	48.3	0.45
80	0.87	0.00	0.87	-0.04	21.6	48.3	0.45
85	0.95	0.00	0.95	-0.04	22.2	48.3	0.46
90	1.03	0.00	1.02	-0.04	22.9	48.3	0.47
95	1.11	0.00	1.11	-0.04	22.9	48.3	0.47
100	1.19	0.00	1.19	-0.04	22.9	48.3	0.47
105	1.28	0.00	1.28	-0.04	22.9	48.3	0.47
110	1.36	0.00	1.36	-0.04	23.6	48.3	0.49
115	1.45	0.00	1.45	-0.04	23.6	48.3	0.49
120	1.53	0.00	1.53	-0.03	23.6	48.3	0.49
125	1.62	0.00	1.61	-0.03	24.9	49.3	0.51
130	1.70	0.00	1.70	-0.03	24.9	49.3	0.51
135	1.78	0.00	1.78	-0.03	24.9	49.3	0.51
140	1.87	0.00	1.86	-0.03	24.3	49.3	0.49
145	1.95	0.00	1.95	-0.03	26.3	49.3	0.53

150	2.04	0.00	2.04	-0.02	25.6	48.3	0.53
155	2.13	0.00	2.12	-0.02	25.6	48.3	0.53
160	2.21	0.00	2.21	-0.02	26.3	48.3	0.54
165	2.30	0.00	2.30	-0.01	26.3	49.3	0.53
170	2.38	0.00	2.38	-0.01	26.3	48.3	0.54
175	2.47	0.00	2.46	-0.01	26.3	49.3	0.53
180	2.56	0.00	2.55	-0.01	26.3	49.3	0.53
185	2.64	0.00	2.64	-0.01	25.6	49.3	0.52
190	2.73	0.00	2.73	-0.01	25.6	49.3	0.52
195	2.81	0.00	2.81	-0.01	24.9	49.3	0.51
200	2.89	0.00	2.89	0.00	24.9	49.3	0.51
205	2.98	0.00	2.97	0.00	26.3	49.3	0.53
210	3.07	0.00	3.06	0.00	25.6	49.3	0.52
215	3.15	0.00	3.15	0.00	26.3	49.3	0.53
220	3.24	0.00	3.23	0.00	26.3	49.3	0.53
225	3.33	0.00	3.33	0.00	26.3	50.3	0.52
230	3.41	0.00	3.41	0.01	26.3	49.3	0.53
235	3.50	0.00	3.50	0.00	26.3	49.3	0.53
240	3.58	0.00	3.58	0.01	25.6	50.3	0.51
245	3.67	0.00	3.67	0.01	26.3	50.3	0.52
250	3.75	0.00	3.75	0.01	26.3	49.3	0.53
255	3.84	0.00	3.84	0.01	26.3	49.3	0.53
260	3.93	0.00	3.93	0.01	24.9	49.3	0.51
265	4.02	0.00	4.01	0.01	25.6	50.3	0.51
270	4.10	0.00	4.10	0.01	26.3	50.3	0.52
275	4.18	0.00	4.18	0.02	25.6	49.3	0.52
280	4.27	0.00	4.26	0.02	27.0	50.3	0.54
285	4.36	0.00	4.35	0.02	26.3	49.3	0.53
290	4.45	0.00	4.44	0.02	27.0	49.3	0.55
295	4.53	0.00	4.53	0.03	26.3	50.3	0.52
300	4.62	0.00	4.62	0.03	26.3	50.3	0.52
305	4.70	0.00	4.70	0.03	27.0	50.3	0.54
310	4.79	0.00	4.78	0.03	27.0	49.3	0.55
315	4.88	0.00	4.88	0.03	26.3	49.3	0.53
320	4.96	0.00	4.96	0.03	27.0	50.3	0.54
325	5.05	0.00	5.05	0.03	27.0	49.3	0.55
330	5.14	0.00	5.14	0.04	27.6	50.3	0.55
335	5.22	0.00	5.22	0.04	27.0	50.3	0.54
340	5.31	0.00	5.31	0.03	26.3	49.3	0.53
345	5.40	0.00	5.40	0.04	27.0	50.3	0.54
350	5.49	0.00	5.49	0.04	26.3	49.3	0.53
355	5.58	0.00	5.58	0.04	27.0	50.3	0.54
360	5.66	0.00	5.66	0.04	25.6	49.3	0.52
365	5.75	0.00	5.75	0.04	27.0	50.3	0.54
370	5.83	0.00	5.83	0.04	26.3	49.3	0.53
375	5.92	0.00	5.92	0.05	27.0	50.3	0.54

Table B9: 2-D Monotonic test on loose sand σ_n = 50 kPa

Date of testing: 26/04/1996
Tested by: Alain Mabia
Type of sample: Loose clean sand
Plate: sand-blasted steel plate
Density = 1.445 g/cm^3

TIME Sec.	Ux (mm)	Ux2 (mm)	Ux1 (mm)	V (mm)	Tau-x (kPa)	Sig-n (kPa)	T/S
	0.00	0.00	0.04	0.00	0.0	48.3	0.00
5	0.00	0.00	0.04	0.00	4.1	49.3	0.08
10	0.00	0.00	0.03	0.00	8.1	48.3	0.17
15	0.00	0.00	0.02	-0.01	10.2	48.3	0.21
20	0.01	0.00	0.01	-0.02	10.8	48.3	0.22
25	0.01	0.00	0.01	-0.03	13.5	48.3	0.28
30	0.04	0.00	0.04	-0.04	14.9	48.3	0.31
35	0.08	0.00	0.07	-0.06	16.2	48.3	0.34
40	0.12	0.00	0.12	-0.07	18.3	48.3	0.38
45	0.17	0.00	0.16	-0.08	18.9	48.3	0.39
50	0.22	0.00	0.22	-0.09	21.0	48.3	0.43
55	0.27	0.00	0.27	-0.10	21.6	48.3	0.45
60	0.32	0.00	0.32	-0.11	22.3	48.3	0.46
65	0.38	0.00	0.38	-0.12	23.0	47.3	0.49
70	0.45	0.00	0.44	-0.13	24.3	48.3	0.50
75	0.50	0.00	0.50	-0.13	24.3	48.3	0.50
80	0.57	0.01	0.56	-0.15	25.0	48.3	0.52
85	0.63	0.00	0.63	-0.15	25.7	48.3	0.53
90	0.69	0.00	0.69	-0.15	26.4	48.3	0.55
95	0.76	0.00	0.75	-0.15	26.4	48.3	0.55
100	0.83	0.00	0.82	-0.15	26.4	48.3	0.55
105	0.90	0.00	0.89	-0.15	27.0	48.3	0.56
110	0.96	0.00	0.96	-0.16	28.4	48.3	0.59
115	1.04	0.00	1.04	-0.16	28.4	49.3	0.58
120	1.12	0.00	1.11	-0.16	29.1	49.3	0.59
125	1.20	0.00	1.19	-0.16	29.1	48.3	0.60
130	1.28	0.00	1.28	-0.16	30.4	48.3	0.63
135	1.36	0.00	1.36	-0.16	30.4	48.3	0.63
140	1.43	0.00	1.43	-0.16	31.1	49.3	0.63
145	1.51	0.00	1.51	-0.16	31.8	48.3	0.66

150	1.59	0.00	1.59	-0.16	32.4	49.3	0.66
155	1.67	0.00	1.67	-0.16	31.8	49.3	0.65
160	1.76	0.01	1.75	-0.15	32.4	48.3	0.67
165	1.84	0.00	1.84	-0.15	33.1	48.3	0.69
170	1.93	0.00	1.93	-0.15	32.4	49.3	0.66
175	2.01	0.00	2.01	-0.15	33.1	48.3	0.69
180	2.10	0.00	2.09	-0.15	32.4	49.3	0.66
185	2.18	0.00	2.18	-0.15	33.1	49.3	0.67
190	2.27	0.00	2.26	-0.14	33.1	49.3	0.67
195	2.35	0.00	2.35	-0.14	33.5	49.3	0.70
200	2.44	0.00	2.43	-0.14	33.8	49.3	0.69
205	2.53	0.00	2.52	-0.14	33.1	49.3	0.67
210	2.60	0.01	2.59	-0.14	33.1	49.3	0.67
215	2.69	0.00	2.69	-0.14	33.8	49.3	0.69
220	2.72	0.00	2.72	-0.14	33.8	49.3	0.69
225	2.85	0.00	2.85	-0.13	33.1	50.3	0.66
230	2.94	0.00	2.94	-0.13	33.1	50.3	0.69
235	3.04	0.00	3.04	-0.13	33.1	50.3	0.66
240	3.11	0.00	3.11	-0.12	33.1	50.3	0.69
245	3.20	0.00	3.20	-0.12	33.8	50.3	0.67
250	3.29	0.00	3.29	-0.12	33.8	50.3	0.67
255	3.37	0.01	3.37	-0.12	33.8	49.3	0.69
260	3.46	0.00	3.46	-0.12	33.8	50.3	0.67
265	3.55	0.00	3.54	-0.11	33.8	50.3	0.67
270	3.64	0.00	3.64	-0.11	33.8	50.3	0.67
275	3.72	0.00	3.72	-0.11	33.8	50.3	0.66
280	3.81	0.00	3.81	-0.11	33.8	50.3	0.67
285	3.90	0.00	3.89	-0.11	33.8	50.3	0.67
290	3.99	0.00	3.98	-0.11	33.8	50.3	0.64
295	4.07	0.00	4.07	-0.11	33.8	50.3	0.66
300	4.16	0.00	4.16	-0.10	33.8	50.3	0.67
305	4.25	0.00	4.25	-0.10	33.8	50.3	0.67
310	4.34	0.00	4.34	-0.10	33.8	50.3	0.66
315	4.42	0.00	4.42	-0.10	33.8	50.3	0.64
320	4.52	0.00	4.52	-0.10	33.1	50.3	0.66
325	4.60	0.00	4.60	-0.10	33.8	50.3	0.67
330	4.69	0.00	4.69	-0.10	33.8	50.3	0.67
335	4.78	0.01	4.77	-0.10	33.1	51.3	0.65
340	4.86	0.00	4.86	-0.10	33.1	50.3	0.64
345	4.94	0.00	4.94	-0.10	33.1	50.3	0.66
350	5.04	0.00	5.03	-0.09	33.1	50.3	0.66
355	5.12	0.00	5.12	-0.09	33.1	50.3	0.66
360	5.21	0.00	5.20	-0.09	32.4	50.3	0.64
365	5.30	0.00	5.30	-0.09	32.4	50.3	0.64
370	5.39	0.00	5.38	-0.09	32.4	50.3	0.64
375	5.47	0.00	5.47	-0.09	32.4	50.3	0.64
380	5.56	0.00	5.56	-0.09	31.8	50.3	0.63
385	5.64	0.00	5.64	-0.09	31.8	50.3	0.63
390	5.72	0.00	5.72	-0.09	31.8	51.3	0.63
395	5.82	0.00	5.82	-0.09	31.8	50.3	0.63

400	5.90	0.00	5.89	-0.09	31.8	50.3	0.63
405	5.99	0.00	5.98	-0.09	31.8	50.3	0.64

Table B10: 2-D Monotonic test on loose sand σ_n = 100 kPa

Date of testing: 26/04/1996
Tested by: Alain Mabia
Type of sample: Loose clean sand
Plate: sand-blasted steel plate
Density = 1.445 g/cm^3

TIME Sec.	Ux (mm)	Ux2 (mm)	Ux1 (mm)	V (mm)	Tau-x (kPa)	Sig-n (kPa)	T/S
0	0.01	0.00	0.00	0.00	0.0	100.5	0.00
5	0.01	0.00	0.00	0.00	0.7	100.5	0.01
10	0.00	0.00	0.00	0.00	2.0	100.5	0.02
15	0.00	0.00	0.00	0.00	4.0	100.5	0.04
20	0.00	0.00	0.00	0.00	7.4	100.5	0.07
25	0.01	0.00	0.01	-0.01	11.4	99.5	0.11
30	0.03	0.01	0.02	-0.01	16.8	99.5	0.17
35	0.05	0.00	0.04	-0.03	20.9	99.5	0.21
40	0.08	0.00	0.08	-0.04	24.9	98.5	0.25
45	0.12	0.00	0.12	-0.06	29.0	98.5	0.29
50	0.17	0.00	0.17	-0.07	32.3	98.5	0.33
55	0.22	0.00	0.22	-0.08	35.0	98.5	0.36
60	0.28	0.01	0.27	-0.09	37.1	98.5	0.38
65	0.34	0.00	0.34	-0.11	39.8	98.5	0.40
70	0.40	0.00	0.40	-0.11	41.8	99.5	0.42
75	0.46	0.00	0.46	-0.12	43.1	98.5	0.44
80	0.53	0.00	0.52	-0.13	44.5	97.5	0.46
85	0.59	0.00	0.58	-0.13	46.5	99.5	0.47
90	0.66	0.00	0.65	-0.14	47.9	99.5	0.48
95	0.72	0.00	0.72	-0.14	49.2	98.5	0.50
100	0.79	0.00	0.79	-0.15	49.9	98.5	0.51
105	0.86	0.00	0.86	-0.16	51.2	98.5	0.52
110	0.94	0.00	0.93	-0.16	53.3	98.5	0.54
115	1.01	0.00	1.00	-0.16	51.9	98.5	0.53
120	1.08	0.00	1.07	-0.17	53.9	98.5	0.55
125	1.15	0.00	1.14	-0.17	54.6	98.5	0.55
130	1.22	0.00	1.22	-0.17	54.6	99.5	0.55
135	1.30	0.00	1.29	-0.17	55.3	98.5	0.56
140	1.37	0.00	1.37	-0.17	56.0	98.5	0.57
145	1.45	0.00	1.44	-0.17	56.0	98.5	0.57
150	1.53	0.00	1.52	-0.17	58.0	99.5	0.58

155	1.61	0.00	1.61	-0.17	58.0	98.5	0.59
160	1.69	0.00	1.68	-0.17	57.3	98.5	0.58
165	1.77	0.01	1.76	-0.17	58.0	98.5	0.59
170	1.85	0.00	1.85	-0.17	58.7	98.5	0.60
175	1.93	0.00	1.93	-0.17	60.0	99.5	0.60
180	2.00	0.00	2.00	-0.17	60.7	99.5	0.61
185	2.09	0.00	2.08	-0.17	60.0	99.5	0.60
190	2.16	0.00	2.16	-0.17	60.7	99.5	0.61
195	2.25	0.00	2.25	-0.17	61.4	99.5	0.62
200	2.34	0.00	2.33	-0.17	60.7	99.5	0.61
205	2.42	0.01	2.41	-0.17	60.7	99.5	0.61
210	2.51	0.00	2.51	-0.17	61 4	98.5	0.62
215	2.59	0.00	2.59	-0.16	60.7	99.5	0.61
220	2.68	0.00	2.68	-0.16	60.0	100.5	0.60
225	2.77	0.00	2.76	-0.16	60.0	100.5	0.60
230	2.86	0.00	2.85	-0.16	60.0	99.5	0.60
235	2.94	0.00	2.93	-0.16	60.7	99.5	0.61
240	3.02	0.00	3.02	-0.15	60.0	100.5	0.60
245	3.11	0.00	3.11	-0.15	60.0	100.5	0.60
250	3.19	0.01	3.19	-0.15	60.0	100.5	0.60
255	3.28	0.00	3.28	-0.15	60.0	99.5	0.60
260	3.36	0.01	3.35	-0.15	60.0	100.5	0.60
265	3.45	0.00	3.44	-0.15	60.7	100.5	0.60
270	3.54	0.00	3.53	-0.15	60.7	100.5	0.60
275	3.62	0.00	3.62	-0.15	60.0	100.5	0.60
280	3.71	0.00	3.70	-0.15	60.7	100.5	0.60
285	3.79	0.00	3.79	-0.14	60.7	100.5	0.60
290	3.87	0.00	3.87	-0.14	61.4	100.5	0.61
295	3.96	0.00	3.96	-0.14	61.4	100.5	0.61
300	4.05	0.00	4.04	-0.14	62.0	100.5	0.62
305	4.14	0.00	4.14	-0.14	60.7	100.5	0.60
310	4.22	0.00	4.22	-0.14	60.7	100.5	0.60
315	4.31	0.00	4.31	-0.14	60.0	101.5	0.59
320	4.40	0.00	4.40	-0.14	59.3	99.5	0.60
325	4.48	0.00	4.48	-0.13	60.7	100.5	0.60
330	4.57	0.00	4.57	-0.13	60.0	101.5	0.59
335	4.66	0.00	4.65	-0.13	60.0	101.5	0.59
340	4.75	0.01	4.74	-0.13	59.3	100.5	0.59
345	4.84	0.00	4.83	-0.13	58.7	101.5	0.58
350	4.93	0.00	4.93	-0.13	57.3	100.5	0.57
355	5.01	0.00	5.01	-0.13	58.0	100.5	0.58
360	5.10	0.00	5.10	-0.13	57.3	99.5	0.58
365	5.19	0.00	5.18	-0.13	57.3	99.5	0.58
370	5.27	0.00	5.27	-0.13	57.3	99.5	0.58
375	5.36	0.00	5.35	-0.13	58.0	100.5	0.58
380	5.45	0.00	5.45	-0.14	58.0	99.5	0.58
385	5.53	0.00	5.53	-0.13	57.3	99.5	0.58
390	5.62	0.01	5.62	-0.13	58.7	98.5	0.60
395	5.71	0.01	5.70	-0.13	58.0	99.5	0.58
400	5.80	0.00	5.79	-0.13	58.0	99.5	0.58

405	5.89	0.00	5.88	-0.13	58.7	99.5	0.59
410	5.98	0.00	5.97	-0.13	58.0	100.5	0.58

Table B11: 2-D Monotonic test on loose clean sand σ_n = 300 kPa

Date of testing: 23/04/1996
Tested by: Alain Mabia
Type of sample: Loose clean sand
Plate: sand-blasted steel plate
Density = 1.431 g/cm^3

TIME Sec.	Ux (mm)	Ux2 (mm)	Ux1 (mm)	V (mm)	Tau-x (kPa)	Sig-n (kPa)	T/S
0	0.00	0.00	0.00	0.00	0.0	299.3	0.00
5	0.00	0.00	0.00	-0.01	2.7	298.3	0.01
10	0.00	0.00	0.00	-0.01	8.1	298.3	0.03
15	0.01	0.00	0.00	0.00	12.9	298.3	0.04
20	0.01	0.00	0.01	0.00	16.9	298.3	0.06
25	0.02	0.00	0.01	0.00	21.0	298.3	0.07
30	0.03	0.00	0.02	-0.01	27.7	298.3	0.09
35	0.04	0.00	0.04	-0.01	36.5	298.3	0.12
40	0.06	0.00	0.05	-0.01	45.2	298.3	0.15
45	0.08	0.00	0.07	-0.02	53.3	298.3	0.18
50	0.10	0.00	0.10	-0.03	61.4	298.3	0.21
55	0.13	0.00	0.13	-0.04	70.2	298.3	0.24
60	0.16	0.00	0.16	-0.05	77.6	298.3	0.26
65	0.20	0.00	0.20	-0.06	84.4	298.3	0.28
70	0.23	0.00	0.23	-0.07	91.1	298.3	0.31
75	0.27	0.00	0.27	-0.08	97.2	297.4	0.33
80	0.31	0.00	0.31	-0.09	103.9	298.3	0.35
85	0.36	0.00	0.36	-0.09	110.0	298.3	0.37
90	0.41	0.01	0.40	-0.10	114.7	297.4	0.39
95	0.46	0.00	0.46	-0.11	120.1	298.3	0.40
100	0.51	0.01	0.50	-0.13	125.5	298.3	0.42
105	0.56	0.00	0.56	-0.13	130.3	298.3	0.44
110	0.62	0.00	0.62	-0.13	133.6	297.4	0.45
115	0.68	0.00	0.68	-0.14	137.7	298.3	0.46
120	0.75	0.00	0.74	-0.14	141.1	298.3	0.47
125	0.81	0.01	0.80	-0.15	144.4	298.3	0.48
130	0.87	0.00	0.87	-0.16	147.8	298.3	0.50
135	0.95	0.00	0.94	-0.16	149.8	298.3	0.50
140	1.02	0.00	1.01	-0.16	152.5	298.3	0.51
145	1.09	0.00	1.09	-0.17	154.6	297.4	0.52
150	1.16	0.00	1.16	-0.17	156.6	297.4	0.53

155	1.24	0.00	1.23	-0.18	158.6	298.3	0.53
160	1.31	0.00	1.31	-0.18	160.6	297.4	0.54
165	1.38	0.00	1.38	-0.18	162.7	297.4	0.55
170	1.46	0.01	1.45	-0.18	163.3	298.3	0.55
175	1.53	0.01	1.52	-0.18	165.4	297.4	0.56
180	1.61	0.00	1.61	-0.18	166.7	297.4	0.56
185	1.69	0.00	1.68	-0.18	167.4	297.4	0.56
190	1.77	0.00	1.77	-0.18	167.4	297.4	0.56
195	1.85	0.00	1.84	-0.18	169.4	298.3	0.57
200	1.93	0.01	1.92	-0.18	170.7	297.4	0.57
205	2.01	0.00	2.01	-0.18	169.4	297.4	0.57
210	2.09	0.00	2.09	-0.19	171.4	297.4	0.58
215	2.17	0.00	2.17	-0.19	172.1	298.3	0.58
220	2.26	0.00	2.26	-0.19	170.7	297.4	0.57
225	2.34	0.00	2.33	-0.19	172.8	297.4	0.58
230	2.41	0.00	2.41	-0.19	174.1	298.3	0.58
235	2.50	0.00	2.49	-0.18	174.1	298.3	0.58
240	2.58	0.00	2.58	-0.19	173.4	298.3	0.58
245	2.67	0.00	2.67	-0.19	173.4	298.3	0.58
250	2.75	0.02	2.73	-0.19	173.4	298.3	0.58
255	2.84	0.00	2.84	-0.19	172.8	298.3	0.58
260	2.93	0.00	2.93	-0.19	172.8	298.3	0.58
265	3.01	0.00	3.01	-0.19	173.4	298.3	0.58
270	3.10	0.00	3.10	-0.19	172.1	297.4	0.58
275	3.19	0.00	3.19	-0.19	171.4	297.4	0.58
280	3.28	0.00	3.28	-0.19	170.7	298.3	0.57
285	3.36	0.01	3.35	-0.19	172.1	298.3	0.58
290	3.44	0.00	3.43	-0.18	173.4	297.4	0.58
295	3.52	0.00	3.52	-0.18	173.4	297.4	0.58
300	3.61	0.00	3.60	-0.18	174.8	298.3	0.59
305	3.69	0.00	3.68	-0.18	175.5	297.4	0.59
310	3.78	0.00	3.77	-0.18	176.1	298.3	0.59
315	3.88	0.00	3.87	-0.18	174.1	298.3	0.58
320	3.97	0.00	3.96	-0.18	172.8	298.3	0.58
325	4.05	0.00	4.04	-0.18	175.5	298.3	0.59
330	4.14	0.00	4.14	-0.18	173.4	297.4	0.58
335	4.22	0.01	4.22	-0.18	173.4	298.3	0.58
340	4.31	0.00	4.31	-0.19	172.1	298.3	0.58
345	4.40	0.00	4.40	-0.19	172.8	297.4	0.58
350	4.49	0.00	4.49	-0.19	171.4	298.3	0.57
355	4.59	0.00	4.58	-0.18	170.1	298.3	0.57
360	4.68	0.00	4.67	-0.19	171.4	298.3	0.57
365	4.75	0.00	4.75	-0.19	172.8	298.3	0.58
370	4.86	0.00	4.86	-0.19	167.4	297.4	0.56
375	4.94	0.00	4.94	-0.19	169.4	298.3	0.57
380	5.03	0.00	5.03	-0.19	168.0	298.3	0.56
385	5.11	0.00	5.11	-0.19	168.7	297.4	0.57
390	5.20	0.00	5.20	-0.19	168.7	297.4	0.57
395	5.29	0.00	5.28	-0.18	170.1	298.3	0.57
400	5.36	0.00	5.35	-0.19	169.4	297.4	0.57

405	5.45	0.01	5.45	-0.19	170.1	297.4	0.57
410	5.53	0.00	5.53	-0.19	170.1	298.3	0.57
415	5.62	0.00	5.62	-0.19	170.7	298.3	0.57
420	5.71	0.01	5.71	-0.19	170.1	298.3	0.57
425	5.81	0.00	5.81	-0.19	168	298.3	0.56
430	5.89	0.00	5.89	-0.19	169.4	297.4	0.57
435	5.98	0.00	5.98	-0.19	168.7	298.3	0.57

Table B12: 2-D Monotonic test on loose sand σ_n = 50 kPa

Date of testing: 2/05/1996
Tested by: Alain Mabia
Type of sample: Oil contaminated loose sand
Plate: sand-blasted steel plate
Density = 1.431 g/cm^3

TIME Sec.	Ux (mm)	Ux2 (mm)	Ux1 (mm)	V (mm)	Tau-x (kPa)	Sig-n (kPa)	T/S
0	0.01	0.00	0.00	0.00	0.0	50.3	0.01
5	0.01	0.00	0.00	0.00	1.3	49.3	0.03
10	0.00	0.00	0.00	0.00	4.0	50.3	0.08
15	0.01	0.00	0.00	0.00	6.0	49.3	0.12
20	0.01	0.00	0.01	-0.02	8.7	49.3	0.18
25	0.05	0.00	0.04	-0.03	10.1	49.3	0.20
30	0.10	0.00	0.09	-0.06	11.4	49.3	0.23
35	0.15	0.00	0.14	-0.08	12.1	48.3	0.25
40	0.19	0.00	0.19	-0.10	13.5	50.3	0.27
45	0.25	0.00	0.25	-0.12	14.1	48.3	0.29
50	0.31	0.00	0.31	-0.14	15.5	48.3	0.32
55	0.37	0.01	0.36	-0.16	16.8	48.3	0.35
60	0.43	0.01	0.43	-0.18	16.8	48.3	0.35
65	0.50	0.00	0.49	-0.19	16.8	49.3	0.34
70	0.56	0.00	0.56	-0.22	18.2	49.3	0.37
75	0.63	0.00	0.63	-0.22	18.2	49.3	0.37
80	0.70	0.01	0.69	-0.24	18.9	49.3	0.38
85	0.77	0.00	0.77	-0.25	19.5	49.3	0.40
90	0.84	0.00	0.84	-0.26	19.5	49.3	0.40
95	0.92	0.01	0.91	-0.27	20.2	49.3	0.41
100	1.03	0.00	1.02	-0.28	20.9	49.3	0.42
105	1.07	0.00	1.06	-0.29	20.9	49.3	0.42
110	1.14	0.01	1.14	-0.30	20.9	49.3	0.42
115	1.21	0.00	1.21	-0.31	21.6	49.3	0.44
120	1.29	0.00	1.29	-0.31	22.9	48.3	0.47
125	1.38	0.00	1.38	-0.32	22.2	49.3	0.45
130	1.46	0.00	1.46	-0.32	22.9	48.3	0.47
135	1.54	0.00	1.54	-0.33	22.9	49.3	0.46
140	1.63	0.01	1.62	-0.34	22.9	49.3	0.46
145	1.71	0.00	1.70	-0.34	22.9	49.3	0.46
150	1.79	0.00	1.78	-0.35	23.6	48.3	0.49

155	1.87	0.01	1.86	-0.36	23.6	49.3	0.48
160	1.95	0.01	1.94	-0.35	23.6	49.3	0.48
165	2.03	0.00	2.03	-0.36	23.6	48.3	0.49
170	2.12	0.00	2.12	-0.36	23.6	49.3	0.48
175	2.20	0.00	2.20	-0.37	24.3	49.3	0.49
180	2.29	0.01	2.28	-0.37	23.6	48.3	0.49
185	2.37	0.00	2.37	-0.37	23.6	48.3	0.49
190	2.45	0.00	2.45	-0.37	24.3	48.3	0.50
195	2.54	0.00	2.54	-0.37	24.9	48.3	0.52
200	2.62	0.00	2.62	-0.37	24.9	49.3	0.51
205	2.71	0.00	2.70	-0.37	24.9	49.3	0.51
210	2.78	0.00	2.78	-0.37	24.9	48.3	0.52
215	2.86	0.01	2.85	-0.38	24.9	49.3	0.51
220	2.95	0.00	2.94	-0.38	25.6	49.3	0.52
225	3.03	0.00	3.02	-0.38	24.9	49.3	0.51
230	3.12	0.00	3.11	-0.38	24.3	49.3	0.49
235	3.20	0.01	3.20	-0.38	24.9	48.3	0.52
240	3.29	0.00	3.28	-0.38	24.9	49.3	0.51
245	3.37	0.00	3.37	-0.38	25.6	49.3	0.52
250	3.46	0.00	3.45	-0.38	24.9	48.3	0.52
255	3.54	0.01	3.53	-0.38	24.9	49.3	0.51
260	3.63	0.00	3.62	-0.39	24.9	49.3	0.51
265	3.71	0.00	3.70	-0.39	24.9	48.3	0.52
270	3.79	0.01	3.79	-0.39	25.6	49.3	0.52
275	3.88	0.00	3.88	-0.39	25.6	48.3	0.53
280	3.96	0.00	3.96	-0.39	24.9	49.3	0.51
285	4.05	0.00	4.05	-0.39	24.9	48.3	0.52
290	4.13	0.00	4.13	-0.39	25.6	49.3	0.52
295	4.22	0.00	4.22	-0.39	24.9	49.3	0.51
300	4.31	0.00	4.31	-0.39	24.9	49.3	0.51
305	4.40	0.01	4.39	-0.39	24.9	49.3	0.51
310	4.48	0.00	4.47	-0.39	25.6	48.3	0.53
315	4.57	0.01	4.56	-0.39	25.6	48.3	0.53
320	4.65	0.00	4.64	-0.39	26.3	48.3	0.54
325	4.73	0.01	4.73	-0.40	25.6	48.3	0.53
330	4.83	0.01	4.82	-0.39	26.3	49.3	0.53
335	4.90	0.00	4.90	-0.39	25.6	49.3	0.52
340	4.99	0.00	4.99	-0.40	25.6	49.3	0.52
345	5.07	0.01	5.06	-0.39	25.6	49.3	0.52
350	5.16	0.00	5.16	-0.40	26.3	49.3	0.53
355	5.24	0.00	5.24	-0.39	25.6	49.3	0.52
360	5.33	0.00	5.33	-0.40	25.6	49.3	0.52
365	5.42	0.00	5.41	-0.39	26.3	49.3	0.53
370	5.50	0.01	5.49	-0.39	26.3	49.3	0.53
375	5.59	0.00	5.58	-0.40	25.6	48.3	0.53
380	5.67	0.00	5.67	-0.39	25.6	49.3	0.52
385	5.76	0.01	5.75	-0.39	25.6	49.3	0.52
390	5.84	0.01	5.83	-0.39	25.6	50.3	0.51
395	5.92	0.00	5.92	-0.40	25.6	49.3	0.52

Table B13: 2-D Monotonic test on loose sand σ_n =100 kPa

Date of testing: 2/05/1996
Tested by: Alain Mabia
Type of sample: Oil contaminated loose sand
Plate: sand-blasted steel plate
Density = 1.431 g/cm^3

TIME Sec.	Ux (mm)	Ux2 (mm)	Ux1 (mm)	V (mm)	Tau-x (kPa)	Sig-n (kPa)	T/S
0	0.01	0.01	0.01	0.00	0.7	100.5	0.01
5	0.02	0.00	0.01	0.00	4.1	101.5	0.04
10	0.03	0.00	0.02	0.01	8.1	100.5	0.08
15	0.04	0.00	0.04	0.00	11.5	100.5	0.11
20	0.05	0.00	0.05	-0.01	14.2	100.5	0.14
25	0.08	0.00	0.07	-0.02	17.6	100.5	0.18
30	0.11	0.00	0.11	-0.04	20.3	100.5	0.20
35	0.16	0.01	0.15	-0.05	23.0	100.5	0.23
40	0.21	0.01	0.20	-0.07	25.7	100.5	0.26
45	0.27	0.01	0.26	-0.09	27.7	100.5	0.28
50	0.34	0.00	0.33	-0.11	29.7	100.5	0.30
55	0.40	0.00	0.40	-0.13	31.8	100.5	0.32
60	0.47	0.01	0.46	-0.14	33.8	100.5	0.34
65	0.54	0.00	0.54	-0.16	35.1	100.5	0.35
70	0.61	0.00	0.61	-0.17	36.5	100.5	0.36
75	0.69	0.00	0.69	-0.19	37.1	100.5	0.37
80	0.76	0.00	0.75	-0.20	38.5	100.5	0.38
85	0.83	0.00	0.83	-0.21	39.8	100.5	0.40
90	0.91	0.00	0.91	-0.22	40.5	99.5	0.41
95	0.99	0.00	0.98	-0.23	41.9	100.5	0.42
100	1.06	0.00	1.06	-0.24	43.2	100.5	0.43
105	1.14	0.00	1.14	-0.24	43.9	100.5	0.44
110	1.22	0.00	1.22	-0.25	44.6	99.5	0.45
115	1.30	0.01	1.30	-0.26	45.2	100.5	0.45
120	1.38	0.01	1.38	-0.26	45.2	99.5	0.45
125	1.47	0.00	1.47	-0.28	45.9	100.5	0.46
130	1.55	0.01	1.55	-0.28	45.9	99.5	0.46
135	1.63	0.00	1.63	-0.28	46.6	99.5	0.47
140	1.72	0.00	1.72	-0.29	47.3	99.5	0.48
145	1.80	0.01	1.79	-0.29	46.6	99.5	0.47
150	1.88	0.00	1.88	-0.30	47.3	100.5	0.47

155	1.96	0.01	1.96	-0.30	47.9	99.5	0.48
160	2.05	0.01	2.04	-0.30	49.3	99.5	0.50
165	2.13	0.00	2.13	-0.30	49.3	100.5	0.49
170	2.22	0.00	2.21	-0.31	49.3	99.5	0.50
175	2.31	0.00	2.30	-0.31	49.3	99.5	0.50
180	2.39	0.00	2.39	-0.31	49.3	100.5	0.49
185	2.47	0.00	2.47	-0.31	49.3	99.5	0.50
190	2.56	0.01	2.55	-0.31	49.3	100.5	0.49
195	2.64	0.01	2.64	-0.31	49.3	100.5	0.49
200	2.72	0.01	2.72	-0.31	50.0	99.5	0.50
205	2.81	0.01	2.80	-0.31	50.6	100.5	0.50
210	2.90	0.00	2.90	-0.32	50.6	100.5	0.50
215	2.98	0.01	2.98	-0.32	49.3	100.5	0.49
220	3.07	0.00	3.06	-0.32	50.0	100.5	0.50
225	3.15	0.00	3.15	-0.32	50.6	100.5	0.50
230	3.24	0.00	3.23	-0.32	50.6	99.5	0.51
235	3.33	0.00	3.32	-0.32	50.6	100.5	0.50
240	3.41	0.01	3.41	-0.32	50.6	100.5	0.50
245	3.50	0.00	3.50	-0.32	51.3	101.5	0.51
250	3.59	0.01	3.58	-0.33	50.6	100.5	0.50
255	3.67	0.00	3.67	-0.33	51.3	100.5	0.51
260	3.75	0.00	3.75	-0.33	52.0	100.5	0.52
265	3.84	0.00	3.84	-0.33	51.3	101.5	0.51
270	3.93	0.00	3.93	-0.33	50.6	101.5	0.50
275	4.02	0.00	4.01	-0.33	51.3	100.5	0.51
280	4.11	0.01	4.10	-0.33	50.6	100.5	0.50
285	4.20	0.01	4.19	-0.33	51.3	100.5	0.51
290	4.28	0.01	4.27	-0.33	51.3	100.5	0.51
295	4.37	0.01	4.37	-0.33	50.6	100.5	0.50
300	4.46	0.00	4.46	-0.33	50.6	99.5	0.51
305	4.55	0.00	4.54	-0.33	51.3	100.5	0.51
310	4.63	0.01	4.63	-0.33	52.0	100.5	0.52
315	4.72	0.00	4.72	-0.33	52.0	100.5	0.52
320	4.80	0.01	4.80	-0.33	50.6	99.5	0.51
325	4.89	0.01	4.88	-0.33	50.6	99.5	0.51
330	4.98	0.01	4.97	-0.33	51.3	99.5	0.52
335	5.07	0.00	5.06	-0.33	50.6	100.5	0.50
340	5.16	0.01	5.15	-0.33	50.6	100.5	0.50
345	5.25	0.00	5.24	-0.33	51.3	100.5	0.51
350	5.33	0.00	5.33	-0.33	51.3	100.5	0.51
355	5.38	0.00	5.38	-0.33	51.3	100.5	0.51
360	5.50	0.01	5.49	-0.33	51.3	100.5	0.51
365	5.56	0.01	5.55	-0.33	52.0	100.5	0.52
370	5.68	0.00	5.67	-0.33	51.3	100.5	0.51
375	5.77	0.00	5.76	-0.33	52.0	100.5	0.52
380	5.84	0.00	5.84	-0.33	52.7	100.5	0.52
385	5.93	0.01	5.93	-0.33	52.7	100.5	0.52

Table B14: 2-D Monotonic test on loose sand σ_n =300 kPa

Date of testing: 2/05/1996
Tested by: Alain Mabia
Type of sample: Oil contaminated loose sand
Plate: sand-blasted steel plate
Density = 1.431 g/cm^3

TIME Sec.	Ux (mm)	Ux2 (mm)	Ux1 (mm)	V (mm)	Tau-x (kPa)	Sig-n (kPa)	T/S
0	0.01	0.01	0.00	0.00	0.0	301.3	0.00
5	0.00	0.01	0.00	-0.01	1.3	301.3	0.00
10	0.00	0.01	-0.01	-0.01	5.4	300.3	0.02
15	0.00	0.01	-0.01	-0.01	7.4	301.3	0.02
20	0.00	0.01	0.00	-0.01	12.8	300.3	0.04
25	0.05	0.01	0.04	-0.01	21.6	300.3	0.07
30	0.03	0.01	0.02	-0.02	32.3	301.3	0.11
35	0.05	0.01	0.04	-0.03	41.8	300.3	0.14
40	0.08	0.01	0.08	-0.05	51.2	301.3	0.17
45	0.12	0.01	0.11	-0.06	58.7	300.3	0.20
50	0.15	0.01	0.14	-0.07	66.8	301.3	0.22
55	0.21	0.01	0.20	-0.08	72.8	300.3	0.24
60	0.25	0.01	0.24	-0.10	78.2	301.3	0.26
65	0.30	0.01	0.30	-0.11	84.3	300.3	0.28
70	0.36	0.01	0.35	-0.13	89.0	301.3	0.30
75	0.41	0.01	0.40	-0.14	93.8	300.3	0.31
80	0.47	0.01	0.46	-0.15	96.4	301.3	0.32
85	0.53	0.01	0.52	-0.16	101.8	301.3	0.34
90	0.59	0.01	0.58	-0.17	105.2	300.3	0.35
95	0.66	0.01	0.66	-0.18	107.9	300.3	0.36
100	0.72	0.01	0.71	-0.19	112.0	300.3	0.37
105	0.79	0.01	0.78	-0.21	114.0	300.3	0.38
110	0.86	0.01	0.85	-0.21	117.4	300.3	0.39
115	0.93	0.01	0.92	-0.23	119.4	300.3	0.40
120	1.00	0.00	1.00	-0.23	120.7	299.3	0.40
125	1.08	0.00	1.07	-0.24	122.8	299.3	0.41
130	1.15	0.00	1.14	-0.24	124.8	299.3	0.42
135	1.23	0.01	1.22	-0.25	126.1	299.3	0.42
140	1.30	0.01	1.30	-0.26	128.2	299.3	0.43
145	1.38	0.00	1.38	-0.26	129.5	298.3	0.43
150	1.46	0.00	1.46	-0.26	130.2	299.3	0.43

155	1.54	0.00	1.53	-0.27	132.2	300.3	0.44
160	1.62	0.00	1.62	-0.27	132.9	298.3	0.45
165	1.70	0.00	1.70	-0.27	133.6	299.3	0.45
170	1.79	0.00	1.78	-0.28	133.6	299.3	0.45
175	1.87	0.00	1.86	-0.28	134.9	299.3	0.45
180	1.94	0.00	1.94	-0.28	136.3	299.3	0.46
185	2.03	0.00	2.02	-0.29	136.9	299.3	0.46
190	2.11	0.00	2.10	-0.29	137.6	299.3	0.46
195	2.19	0.01	2.19	-0.29	137.6	299.3	0.46
200	2.28	0.00	2.27	-0.29	136.9	299.3	0.46
205	2.36	0.00	2.36	-0.30	137.6	299.3	0.46
210	2.44	0.00	2.44	-0.29	139.0	299.3	0.46
215	2.53	0.00	2.53	-0.30	139.0	299.3	0.46
220	2.61	0.00	2.61	-0.30	139.0	298.3	0.47
225	2.70	0.00	2.70	-0.31	139.0	299.3	0.46
230	2.78	0.00	2.78	-0.31	140.3	299.3	0.47
235	2.87	0.00	2.86	-0.31	139.6	299.3	0.47
240	2.95	0.01	2.95	-0.31	139.0	298.3	0.47
245	3.04	0.00	3.03	-0.31	139.6	300.3	0.46
250	3.12	0.00	3.12	-0.32	139.6	299.3	0.47
255	3.21	0.00	3.21	-0.31	139.0	299.3	0.46
260	3.29	0.00	3.28	-0.32	139.6	299.3	0.47
265	3.38	0.00	3.37	-0.32	139.6	299.3	0.47
270	3.46	0.00	3.46	-0.32	139.6	299.3	0.47
275	3.55	0.01	3.54	-0.32	140.3	299.3	0.47
280	3.64	0.01	3.64	-0.32	139.6	299.3	0.47
285	3.73	0.00	3.73	-0.32	139.6	299.3	0.47
290	3.82	0.01	3.81	-0.32	141.0	299.3	0.47
295	3.90	0.00	3.90	-0.32	140.3	299.3	0.47
300	3.99	0.01	3.98	-0.33	140.3	299.3	0.47
305	4.08	0.00	4.07	-0.32	139.6	299.3	0.47
310	4.16	0.00	4.16	-0.33	140.3	299.3	0.47
315	4.24	0.01	4.23	-0.33	140.3	299.3	0.47
320	4.34	0.00	4.33	-0.33	139.6	299.3	0.47
325	4.43	0.01	4.42	-0.33	139.6	298.3	0.47
330	4.52	0.01	4.51	-0.33	139.0	299.3	0.46
335	4.61	0.01	4.60	-0.33	139.0	300.3	0.46
340	4.69	0.00	4.68	-0.33	139.6	299.3	0.47
345	4.78	0.00	4.78	-0.33	139.0	299.3	0.46
350	4.87	0.00	4.86	-0.33	139.0	299.3	0.46
355	4.95	0.00	4.95	-0.33	139.6	299.3	0.47
360	5.04	0.00	5.04	-0.33	139.6	300.3	0.46
365	5.13	0.00	5.12	-0.33	138.3	300.3	0.46
370	5.21	0.01	5.21	-0.33	140.3	300.3	0.47
375	5.29	0.00	5.29	-0.34	140.3	300.3	0.47
380	5.39	0.00	5.38	-0.34	139.0	300.3	0.46
385	5.47	0.00	5.47	-0.34	139.6	300.3	0.46
390	5.56	0.01	5.55	-0.34	139.0	300.3	0.46
395	5.64	0.01	5.64	-0.34	139.0	300.3	0.46
400	5.73	0.00	5.72	-0.34	139.6	300.3	0.46

405	5.82	0.00	5.81	-0.34	140.3	300.3	0.47
410	5.90	0.01	5.89	-0.34	139.6	300.3	0.46

Table B15: 2-D Monotonic test on dense sand σ_n =30 kPa

Date of testing: 7/05/1996
Tested by: Alain Mabia
Type of sample: Oil contaminated dense sand
Plate: sand-blasted steel plate
Density: 1.89 g/cm^3

TIME Sec.	Ux (mm)	Ux2 (mm)	Ux1 (mm)	V (mm)	Tau-x (kPa)	Sig-n (kPa)	T/S
0	0.00	0.00	0.00	0.00	1.4	28.6	0.05
5	0.01	0.00	0.00	0.00	3.4	28.6	0.12
10	0.02	0.00	0.02	0.00	6.1	27.6	0.22
15	0.05	0.00	0.05	0.00	6.8	28.6	0.24
20	0.08	0.00	0.08	-0.02	9.5	28.6	0.33
25	0.12	0.00	0.12	-0.02	10.2	27.6	0.37
30	0.16	0.00	0.16	-0.03	10.8	27.6	0.39
35	0.22	0.00	0.22	-0.03	11.5	27.6	0.42
40	0.27	0.00	0.27	-0.04	12.2	27.6	0.44
45	0.32	0.00	0.32	-0.04	12.2	27.6	0.44
50	0.37	0.00	0.37	-0.04	12.9	27.6	0.47
55	0.44	0.00	0.43	-0.04	12.9	27.6	0.47
60	0.51	0.00	0.51	-0.04	12.9	28.6	0.45
65	0.57	0.00	0.57	-0.04	13.5	28.6	0.47
70	0.64	0.00	0.64	-0.04	14.2	27.6	0.51
75	0.72	0.00	0.71	-0.05	14.2	28.6	0.50
80	0.79	0.00	0.79	-0.05	14.2	28.6	0.50
85	0.86	0.00	0.86	-0.05	14.2	28.6	0.50
90	0.92	0.00	0.92	-0.04	14.9	27.6	0.54
95	1.00	0.00	1.00	-0.05	14.9	28.6	0.52
100	1.08	0.00	1.08	-0.05	14.9	27.6	0.54
105	1.15	0.00	1.15	-0.05	15.6	27.6	0.56
110	1.21	0.00	1.21	-0.05	14.9	28.6	0.52
115	1.28	0.00	1.28	-0.04	16.2	27.6	0.59
120	1.35	0.00	1.35	-0.04	16.2	27.6	0.59
125	1.41	0.00	1.41	-0.04	16.9	28.6	0.59
130	1.50	0.00	1.50	-0.04	16.9	28.6	0.59
135	1.58	0.00	1.58	-0.04	16.9	28.6	0.59
140	1.66	0.00	1.66	-0.04	16.9	28.6	0.59
145	1.73	0.00	1.73	-0.04	17.6	28.6	0.61

150	1.80	0.00	1.80	-0.04	18.3	28.6	0.64
155	1.89	0.00	1.89	-0.04	17.6	28.6	0.61
160	1.96	0.00	1.96	-0.04	17.6	28.6	0.61
165	2.05	0.00	2.05	-0.04	17.6	28.6	0.61
170	2.13	0.00	2.13	-0.04	18.3	28.6	0.64
175	2.21	0.00	2.21	-0.04	18.3	28.6	0.64
180	2.30	0.00	2.30	-0.04	18.3	28.6	0.64
185	2.37	0.00	2.37	-0.04	18.3	29.6	0.62
190	2.45	0.00	2.45	-0.03	18.3	28.6	0.64
195	2.54	0.00	2.54	-0.03	18.9	28.6	0.66
200	2.62	0.00	2.62	-0.03	18.9	29.6	0.64
205	2.71	0.00	2.71	-0.03	18.3	28.6	0.64
210	2.78	0.00	2.78	-0.03	18.9	29.6	0.64
215	2.86	0.00	2.86	-0.03	18.9	29.6	0.64
220	2.95	0.00	2.95	-0.03	18.3	29.6	0.62
225	3.03	0.00	3.03	-0.03	18.3	29.6	0.62
230	3.11	0.00	3.11	-0.03	18.3	29.6	0.62
235	3.20	0.00	3.20	-0.02	18.3	29.6	0.62
240	3.28	0.00	3.28	-0.02	18.9	29.6	0.64
245	3.36	0.00	3.36	-0.02	18.9	29.6	0.64
250	3.45	0.00	3.45	-0.02	18.3	27.6	0.66
255	3.53	0.00	3.53	-0.02	18.9	29.6	0.64
260	3.61	0.00	3.61	-0.02	18.9	29.6	0.64
265	3.70	0.00	3.69	-0.02	18.9	29.6	0.64
270	3.78	0.00	3.78	-0.02	19.6	29.6	0.66
275	3.87	0.00	3.87	-0.01	19.6	29.6	0.66
280	3.95	0.00	3.95	-0.01	18.9	29.6	0.64
285	4.03	0.00	4.03	-0.01	18.9	29.6	0.64
290	4.11	0.00	4.11	-0.01	18.9	29.6	0.64
295	4.20	0.00	4.20	-0.01	18.9	29.6	0.64
300	4.29	0.00	4.29	-0.01	19.6	29.6	0.66
305	4.37	0.00	4.37	-0.01	19.6	29.6	0.66
310	4.46	0.00	4.46	-0.01	19.6	29.6	0.66
315	4.55	0.00	4.55	-0.01	18.9	29.6	0.64
320	4.63	0.00	4.63	-0.01	19.6	30.6	0.64
325	4.72	0.00	4.72	-0.01	18.9	29.6	0.64
330	4.80	0.00	4.80	-0.01	19.6	29.6	0.66
335	4.89	0.00	4.89	0.00	18.9	29.6	0.64
340	4.97	0.00	4.97	0.00	19.6	28.6	0.68
345	5.06	0.00	5.06	0.00	19.6	29.6	0.66
350	5.14	0.00	5.14	0.00	18.9	29.6	0.64
355	5.23	0.00	5.23	0.00	19.6	30.6	0.64
360	5.31	0.00	5.31	0.00	18.9	30.6	0.62
365	5.40	0.00	5.40	0.00	18.9	29.6	0.64
370	5.50	0.00	5.50	0.00	18.9	29.6	0.64
375	5.58	0.00	5.58	0.00	19.6	29.6	0.66
380	5.67	0.00	5.66	0.00	19.6	29.6	0.66
385	5.75	0.00	5.75	0.00	19.6	29.6	0.66
390	5.84	0.00	5.84	0.00	19.6	29.6	0.66
395	5.92	0.00	5.92	0.00	18.9	29.6	0.64

Table B16: 2-D Monotonic test on dense sand σ_n = 40 kPa

Date of testing: 7/05/1996
Tested by: Alain Mabia
Type of sample: Oil contaminated dense sand
Plate: sand-blasted steel plate
Density: 1.89 g/cm^3

TIME Sec.	Ux (mm)	Ux2 (mm)	Ux1 (mm)	V (mm)	Tau-x (kPa)	Sig-n (kPa)	T/S
0	0.00	0.01	-0.01	0.00	0.0	39.5	0.00
5	0.00	0.01	-0.01	-0.01	1.4	38.5	0.02
10	0.00	0.01	0.00	-0.01	3.3	38.5	0.09
15	0.01	0.01	0.00	-0.01	6.0	39.5	0.15
20	0.04	0.01	0.03	-0.02	8.7	38.5	0.23
25	0.07	0.01	0.06	-0.03	10.8	39.5	0.27
30	0.13	0.01	0.11	-0.05	12.8	38.5	0.33
35	0.19	0.01	0.18	-0.06	15.5	38.5	0.40
40	0.26	0.01	0.25	-0.07	16.2	39.5	0.41
45	0.34	0.01	0.33	-0.08	18.2	38.5	0.47
50	0.41	0.01	0.41	-0.09	18.9	38.5	0.49
55	0.49	0.01	0.48	-0.09	19.5	39.5	0.49
60	0.57	0.01	0.56	-0.10	20.2	39.5	0.51
65	0.65	0.01	0.64	-0.10	20.9	39.5	0.53
70	0.73	0.01	0.72	-0.11	20.9	39.5	0.53
75	0.81	0.01	0.80	-0.11	21.6	39.5	0.55
80	0.90	0.01	0.90	-0.11	20.9	38.5	0.51
85	1.00	0.01	0.99	-0.12	20.9	38.5	0.51
90	1.09	0.01	1.09	-0.12	20.9	38.5	0.45
95	1.17	0.01	1.17	-0.12	20.8	38.5	0.45
100	1.26	0.01	1.26	-0.12	20.8	39.5	0.46
105	1.35	0.01	1.34	-0.12	20.8	38.5	0.49
110	1.43	0.01	1.43	-0.12	20.7	38.5	0.49
115	1.52	0.01	1.51	-0.12	20.7	38.5	0.49
120	1.60	0.00	1.59	-0.12	20.7	39.5	0.48
125	1.68	0.00	1.68	-0.12	20.6	38.5	0.51
130	1.77	0.01	1.76	-0.12	20.3	39.5	0.49
135	1.85	0.01	1.84	-0.12	20.2	39.5	0.51
140	1.93	0.01	1.93	-0.12	20.2	39.5	0.51
145	2.02	0.01	2.01	-0.12	20.9	38.5	0.54
150	2.10	0.00	2.10	-0.12	20.9	38.5	0.54

155	2.19	0.01	2.18	-0.12	20.9	39.5	0.53
160	2.28	0.01	2.27	-0.12	20.9	39.5	0.53
165	2.36	0.01	2.36	-0.11	20.9	39.5	0.53
170	2.45	0.00	2.45	-0.12	20.9	39.5	0.53
175	2.53	0.00	2.53	-0.12	20.9	38.5	0.54
180	2.62	0.01	2.61	-0.11	20.9	39.5	0.53
185	2.70	0.01	2.69	-0.12	20.9	39.5	0.53
190	2.79	0.00	2.79	-0.11	20.9	39.5	0.53
195	2.88	0.00	2.87	-0.11	20.9	39.5	0.53
200	2.96	0.01	2.96	-0.11	20.9	39.5	0.53
205	3.05	0.00	3.05	-0.11	21.6	39.5	0.55
210	3.14	0.00	3.13	-0.11	21.6	39.5	0.55
215	3.22	0.01	3.21	-0.11	21.6	39.5	0.55
220	3.31	0.00	3.31	-0.11	21.6	39.5	0.55
225	3.40	0.00	3.40	-0.11	22.2	39.5	0.56
230	3.48	0.01	3.47	-0.11	22.2	39.5	0.56
235	3.57	0.00	3.56	-0.11	21.6	38.5	0.56
240	3.65	0.00	3.65	-0.11	22.2	39.5	0.56
245	3.73	0.00	3.73	-0.11	22.2	38.5	0.58
250	3.82	0.00	3.82	-0.11	22.2	38.5	0.58
255	3.91	0.01	3.90	-0.10	22.2	39.5	0.56
260	3.99	0.00	3.99	-0.10	22.2	40.4	0.55
265	4.08	0.00	4.08	-0.10	22.2	39.5	0.56
270	4.17	0.00	4.17	-0.10	22.2	40.4	0.55
275	4.26	0.00	4.26	-0.10	22.2	39.5	0.56
280	4.35	0.00	4.35	-0.10	21.6	39.5	0.55
285	4.43	0.00	4.43	-0.10	21.6	39.5	0.55
290	4.52	0.00	4.51	-0.10	22.2	39.5	0.56
295	4.60	0.00	4.59	-0.10	22.2	39.5	0.56
300	4.68	0.00	4.68	-0.10	22.2	39.5	0.56
305	4.77	0.00	4.77	-0.10	21.6	39.5	0.55
310	4.85	0.00	4.85	-0.09	22.2	39.5	0.56
315	4.94	0.00	4.94	-0.10	22.2	39.5	0.56
320	5.03	0.00	5.03	-0.09	22.9	40.4	0.57
325	5.11	0.00	5.11	-0.09	22.2	40.4	0.55
330	5.20	0.00	5.20	-0.09	22.9	39.5	0.58
335	5.29	0.00	5.29	-0.09	22.9	39.5	0.58
340	5.37	0.00	5.37	-0.09	22.9	40.4	0.57
345	5.46	0.00	5.46	-0.09	22.9	39.5	0.58
350	5.55	0.00	5.55	-0.09	22.9	40.4	0.57
355	5.63	0.00	5.63	-0.09	22.9	40.4	0.57
360	5.72	0.01	5.71	-0.09	22.9	39.5	0.58
365	5.81	0.01	5.80	-0.09	22.9	39.5	0.58
370	5.89	0.00	5.89	-0.09	22.2	39.5	0.56
375	5.98	0.00	5.98	-0.09	22.9	40.4	0.57

Table B17: 2-D Monotonic test on loose sand $\sigma_n = 40$ kPa

Date of testing: 7/05/1996
Tested by: Alain Mabia
Type of sample: Oil contaminated loose sand
Plate: sand-blasted steel plate
Density: 1.43g/cm3

TIME Sec.	Ux (mm)	Ux2 (mm)	Ux1 (mm)	V (mm)	Tau-x (kPa)	Sig-n (kPa)	T/S
0	0.00	0.01	-0.01	0.01	0.7	40.4	0.02
5	0.01	0.01	0.00	0.01	2.7	39.5	0.07
10	0.02	0.01	0.01	0.01	6.1	39.5	0.15
15	0.05	0.01	0.04	0.01	7.5	39.5	0.19
20	0.10	0.01	0.09	0.01	9.5	39.5	0.24
25	0.15	0.01	0.14	0.01	10.8	38.5	0.28
30	0.21	0.01	0.20	0.01	11.5	38.5	0.30
35	0.27	0.01	0.27	0.01	12.2	39.5	0.31
40	0.34	0.01	0.34	0.01	13.5	38.5	0.35
45	0.41	0.01	0.40	0.01	13.5	39.5	0.34
50	0.49	0.01	0.48	0.01	14.2	38.5	0.37
55	0.57	0.01	0.56	0.01	14.2	38.5	0.37
60	0.64	0.01	0.63	0.01	15.6	39.5	0.40
65	0.72	0.01	0.71	0.01	15.6	38.5	0.41
70	0.80	0.01	0.79	0.01	16.2	39.5	0.41
75	0.88	0.01	0.87	0.01	16.2	39.5	0.41
80	0.96	0.01	0.95	0.01	16.9	38.5	0.44
85	1.04	0.01	1.03	0.01	16.9	39.5	0.43
90	1.11	0.01	1.11	0.01	17.6	39.5	0.45
95	1.20	0.01	1.20	0.01	16.9	39.5	0.43
100	1.28	0.01	1.27	0.01	17.6	38.5	0.46
105	1.37	0.01	1.36	0.01	18.3	39.5	0.46
110	1.45	0.01	1.44	0.01	18.3	37.5	0.49
115	1.53	0.01	1.52	0.01	18.3	39.5	0.46
120	1.62	0.01	1.62	0.01	19.6	37.5	0.52
125	1.71	0.01	1.70	0.01	19.6	37.5	0.52
130	1.79	0.00	1.79	0.01	19.6	38.5	0.51
135	1.87	0.01	1.87	0.01	19.6	37.5	0.52
140	1.96	0.00	1.95	0.01	20.3	38.5	0.53
145	2.05	0.01	2.04	0.01	18.9	37.5	0.50
150	2.13	0.01	2.13	0.01	19.6	37.5	0.52

155	2.22	0.01	2.21	0.01	19.6	38.5	0.51
160	2.31	0.01	2.30	0.01	19.6	37.5	0.52
165	2.39	0.01	2.38	0.01	19.6	37.5	0.52
170	2.48	0.01	2.47	0.01	19.6	37.5	0.52
175	2.57	0.01	2.56	0.01	20.3	37.5	0.54
180	2.65	0.01	2.64	0.01	20.3	37.5	0.54
185	2.73	0.00	2.73	0.01	20.3	38.5	0.53
190	2.82	0.01	2.81	0.01	20.3	38.5	0.53
195	2.90	0.01	2.89	0.01	19.6	38.5	0.51
200	2.99	0.01	2.98	0.01	20.3	38.5	0.53
205	3.07	0.01	3.06	0.01	21.0	37.5	0.56
210	3.16	0.00	3.16	0.01	20.3	37.5	0.54
215	3.25	0.01	3.24	0.01	20.3	37.5	0.54
220	3.34	0.01	3.33	0.01	20.3	37.5	0.54
225	3.42	0.00	3.42	0.01	20.3	37.5	0.54
230	3.51	0.01	3.50	0.01	20.3	37.5	0.54
235	3.59	0.01	3.58	0.01	20.3	37.5	0.54
240	3.68	0.00	3.68	0.01	21.0	37.5	0.56
245	3.77	0.00	3.77	0.01	21.0	37.5	0.56
250	3.86	0.00	3.86	0.01	20.3	37.5	0.54
255	3.94	0.00	3.94	0.01	19.6	37.5	0.52
260	4.03	0.00	4.03	0.01	20.3	37.5	0.54
265	4.11	0.00	4.11	0.01	20.3	37.5	0.54
270	4.20	0.00	4.20	0.01	20.3	38.5	0.53
275	4.29	0.00	4.28	0.01	20.3	38.5	0.53
280	4.38	0.00	4.38	0.01	19.6	38.5	0.51
285	4.47	0.01	4.46	0.01	20.3	38.5	0.53
290	4.56	0.00	4.56	0.01	21.0	38.5	0.55
295	4.65	0.00	4.64	0.01	19.6	38.5	0.51
300	4.73	0.00	4.73	0.01	20.3	37.5	0.54
305	4.82	0.00	4.82	0.01	20.3	37.5	0.54
310	4.90	0.00	4.90	0.01	20.3	38.5	0.53
315	4.99	0.00	4.99	0.01	20.3	37.5	0.54
320	5.08	0.00	5.07	0.01	20.3	38.5	0.53
325	5.16	0.00	5.16	0.01	20.3	37.5	0.54
330	5.25	0.00	5.25	0.01	20.3	37.5	0.54
335	5.34	0.00	5.34	0.01	21.0	37.5	0.56
340	5.43	0.00	5.42	0.01	20.3	37.5	0.54
345	5.52	0.00	5.51	0.01	20.3	37.5	0.54
350	5.61	0.00	5.61	0.01	21.0	37.5	0.56
355	5.70	0.00	5.69	0.01	19.6	37.5	0.52
360	5.78	0.00	5.78	0.01	20.3	38.5	0.53
365	5.87	0.00	5.87	0.01	20.3	37.5	0.54
370	5.96	0.00	5.96	0.01	20.3	37.5	0.54

Table B18: 2-D Monotonic test on loose sand σ_n = 30 kPa

Date of testing: 7/05/1996
Tested by: Alain Mabia
Type of sample: Oil contaminated loose sand
Plate: sand-blasted steel plate
Density: 1.43g/cm3

TIME Sec.	Ux (mm)	Ux2 (mm)	Ux1 (mm)	V (mm)	Tau-x (kPa)	Sig-n (kPa)	T/S
0	0.00	0.01	-0.01	0.00	0.0	29.6	0.00
5	0.00	0.01	-0.01	0.00	1.4	29.6	0.02
10	0.02	0.01	0.01	-0.01	4.0	29.6	0.14
15	0.06	0.01	0.05	-0.03	5.4	30.6	0.18
20	0.10	0.01	0.09	-0.05	6.0	29.6	0.20
25	0.16	0.01	0.15	-0.07	6.7	28.6	0.23
30	0.23	0.01	0.22	-0.09	7.4	28.6	0.26
35	0.30	0.01	0.29	-0.11	7.4	29.6	0.25
40	0.37	0.01	0.37	-0.14	8.1	29.6	0.27
45	0.45	0.01	0.43	-0.16	9.4	29.6	0.32
50	0.52	0.01	0.51	-0.17	9.4	29.6	0.32
55	0.59	0.01	0.58	-0.19	9.4	28.6	0.33
60	0.66	0.01	0.65	-0.21	10.1	29.6	0.34
65	0.73	0.01	0.72	-0.24	10.8	28.6	0.38
70	0.81	0.01	0.80	-0.23	11.4	28.6	0.40
75	0.89	0.01	0.88	-0.25	11.4	28.6	0.40
80	0.97	0.01	0.96	-0.26	10.1	28.6	0.35
85	1.05	0.01	1.04	-0.27	11.4	28.6	0.40
90	1.13	0.01	1.12	-0.28	11.4	28.6	0.40
95	1.21	0.01	1.20	-0.29	12.1	28.6	0.42
100	1.29	0.01	1.29	-0.30	11.4	28.6	0.40
105	1.38	0.01	1.37	-0.31	12.1	28.6	0.42
110	1.47	0.01	1.46	-0.31	12.8	28.6	0.45
115	1.54	0.01	1.53	-0.32	12.1	28.6	0.42
120	1.63	0.01	1.62	-0.33	12.8	29.6	0.43
125	1.71	0.01	1.70	-0.33	12.8	28.6	0.45
130	1.79	0.01	1.78	-0.33	12.8	28.6	0.45
135	1.87	0.01	1.87	-0.34	12.8	28.6	0.45
140	1.96	0.01	1.95	-0.34	12.8	28.6	0.45
145	2.05	0.01	2.04	-0.35	12.8	29.6	0.43
150	2.13	0.00	2.13	-0.35	12.8	28.6	0.45

155	2.22	0.01	2.21	-0.35	14.1	27.6	0.51
160	2.30	0.01	2.29	-0.36	12.8	28.6	0.45
165	2.38	0.01	2.38	-0.37	12.8	28.6	0.45
170	2.47	0.01	2.46	-0.37	13.5	28.6	0.47
175	2.56	0.01	2.55	-0.37	12.8	28.6	0.45
180	2.64	0.01	2.63	-0.37	13.5	28.6	0.47
185	2.73	0.01	2.72	-0.37	13.5	28.6	0.47
190	2.81	0.01	2.80	-0.38	12.8	28.6	0.45
195	2.89	0.01	2.89	-0.38	13.5	28.6	0.47
200	2.98	0.00	2.98	-0.38	13.5	28.6	0.47
205	3.07	0.01	3.06	-0.38	12.8	28.6	0.45
210	3.15	0.00	3.15	-0.38	13.5	28.6	0.47
215	3.24	0.01	3.24	-0.39	13.5	28.6	0.47
220	3.33	0.01	3.32	-0.39	12.8	28.6	0.45
225	3.41	0.01	3.41	-0.39	13.5	28.6	0.47
230	3.50	0.01	3.49	-0.39	13.5	28.6	0.47
235	3.58	0.00	3.58	-0.39	13.5	28.6	0.47
240	3.67	0.01	3.66	-0.39	12.8	27.6	0.46
245	3.76	0.01	3.75	-0.40	14.1	27.6	0.51
250	3.84	0.00	3.84	-0.40	12.1	27.6	0.44
255	3.93	0.01	3.92	-0.40	12.8	26.7	0.48
260	4.01	0.01	4.00	-0.40	12.1	27.6	0.44
265	4.10	0.01	4.09	-0.40	13.5	27.6	0.49
270	4.19	0.01	4.18	-0.40	12.8	27.6	0.46
275	4.27	0.01	4.27	-0.41	12.8	27.6	0.46
280	4.36	0.01	4.35	-0.40	13.5	27.6	0.49
285	4.44	0.01	4.43	-0.40	13.5	27.6	0.49
290	4.53	0.00	4.53	-0.41	12.8	27.6	0.46
295	4.61	0.00	4.61	-0.41	12.8	27.6	0.46
300	4.70	0.00	4.69	-0.41	12.1	26.7	0.45
305	4.78	0.01	4.78	-0.41	12.1	27.6	0.44
310	4.87	0.01	4.87	-0.41	12.1	27.6	0.44
315	4.96	0.01	4.95	-0.41	12.8	28.6	0.45
320	5.05	0.01	5.05	-0.41	13.5	27.6	0.49
325	5.14	0.01	5.13	-0.42	12.8	27.6	0.46
330	5.22	0.01	5.22	-0.42	12.8	27.6	0.46
335	5.31	0.01	5.30	-0.42	13.5	27.6	0.49
340	5.40	0.01	5.38	-0.42	13.5	28.6	0.47
345	5.48	0.01	5.47	-0.42	12.8	26.7	0.48
350	5.57	0.01	5.56	-0.42	12.8	27.6	0.46
355	5.66	0.01	5.65	-0.42	13.5	27.6	0.49
360	5.74	0.00	5.74	-0.42	14.1	28.6	0.49
365	5.83	0.00	5.82	-0.42	13.5	28.6	0.47
370	5.91	0.00	5.91	-0.42	12.8	28.6	0.45

Table B19: 2-D Monotonic test on dense sand σ_n = 30 kPa

Date of testing: 7/05/1996
Tested by: Alain Mabia
Type of sample: Dense clean sand
Plate: sand-blasted steel plate
Density: 1.89g/cm3

TIME Sec.	Ux (mm)	Ux2 (mm)	Ux1 (mm)	V (mm)	Tau-x (kPa)	Sig-n (kPa)	T/S
0	0.00	0.00	0.00	0.00	0.0	28.6	0.00
5	0.01	0.00	0.00	0.00	3.4	28.6	0.12
10	0.02	0.00	0.02	0.00	6.1	27.6	0.22
15	0.05	0.00	0.05	0.00	6.8	28.6	0.24
20	0.08	0.00	0.08	-0.02	9.5	28.6	0.33
25	0.12	0.00	0.12	-0.02	10.2	27.6	0.37
30	0.16	0.00	0.16	-0.03	10.8	27.6	0.39
35	0.22	0.00	0.22	-0.03	11.5	27.6	0.42
40	0.27	0.00	0.27	-0.04	12.2	27.6	0.44
45	0.32	0.00	0.32	-0.04	12.2	27.6	0.44
50	0.37	0.00	0.37	-0.04	12.9	27.6	0.47
55	0.44	0.00	0.43	-0.05	12.9	27.6	0.47
60	0.51	0.00	0.51	-0.04	12.9	28.6	0.45
65	0.57	0.00	0.57	-0.04	13.5	28.6	0.47
70	0.64	0.00	0.64	-0.04	14.2	27.6	0.51
75	0.72	0.00	0.71	-0.05	14.2	28.6	0.50
80	0.79	0.00	0.79	-0.05	14.2	28.6	0.50
85	0.86	0.00	0.86	-0.05	14.2	28.6	0.50
90	0.92	0.00	0.92	-0.04	14.9	27.6	0.54
95	1.00	0.00	1.00	-0.04	14.9	28.6	0.52
100	1.08	0.00	1.08	-0.05	14.9	27.6	0.54
105	1.15	0.00	1.15	-0.05	15.6	27.6	0.56
110	1.21	0.00	1.21	-0.05	14.9	28.6	0.52
115	1.28	0.00	1.28	-0.04	16.2	27.6	0.59
120	1.35	0.00	1.35	-0.04	16.2	27.6	0.59
125	1.41	0.00	1.41	-0.04	16.9	28.6	0.59
130	1.50	0.00	1.50	-0.04	16.9	28.6	0.59
135	1.58	0.00	1.58	-0.04	16.9	28.6	0.59
140	1.66	0.00	1.66	-0.04	16.9	28.6	0.59
145	1.73	0.00	1.73	-0.04	17.6	28.6	0.61
150	1.80	0.00	1.80	-0.04	18.3	28.6	0.64

155	1.89	0.00	1.89	-0.04	17.6	28.6	0.61
160	1.96	0.00	1.96	-0.04	17.6	28.6	0.61
165	2.05	0.00	2.05	-0.04	17.6	28.6	0.61
170	2.13	0.00	2.13	-0.04	18.3	28.6	0.64
175	2.21	0.00	2.21	-0.04	18.3	28.6	0.64
180	2.30	0.00	2.30	-0.04	18.3	28.6	0.64
185	2.37	0.00	2.37	-0.04	18.3	29.6	0.62
190	2.45	0.00	2.45	-0.03	18.3	28.6	0.64
195	2.54	0.00	2.54	-0.03	18.9	28.6	0.66
200	2.62	0.00	2.62	-0.03	18.9	29.6	0.64
205	2.71	0.00	2.71	-0.03	18.3	28.6	0.64
210	2.78	0.00	2.78	-0.03	18.9	29.6	0.64
215	2.86	0.00	2.86	-0.03	18.9	29.6	0.64
220	2.95	0.00	2.95	-0.03	18.3	29.6	0.62
225	3.03	0.00	3.03	-0.03	18.3	29.6	0.62
230	3.11	0.00	3.11	-0.03	18.3	29.6	0.62
235	3.20	0.00	3.20	-0.02	18.3	29.6	0.62
240	3.28	0.00	3.28	-0.02	18.9	29.6	0.64
245	3.36	0.00	3.36	-0.03	18.9	29.6	0.64
250	3.45	0.00	3.45	-0.02	18.3	27.6	0.66
255	3.53	0.00	3.53	-0.02	18.9	29.6	0.64
260	3.61	0.00	3.61	-0.03	18.9	29.6	0.64
265	3.70	0.00	3.69	-0.02	18.9	29.6	0.64
270	3.78	0.00	3.78	-0.02	19.6	29.6	0.66
275	3.87	0.00	3.87	-0.01	19.6	29.6	0.66
280	3.95	0.00	3.95	-0.01	18.9	29.6	0.64
285	4.03	0.00	4.03	-0.02	18.9	29.6	0.64
290	4.11	0.00	4.11	-0.01	18.9	29.6	0.64
295	4.20	0.00	4.20	-0.01	18.9	29.6	0.64
300	4.29	0.00	4.29	-0.01	19.6	29.6	0.66
305	4.37	0.00	4.37	-0.01	19.6	29.6	0.66
310	4.46	0.00	4.46	-0.01	19.6	29.6	0.66
315	4.55	0.00	4.55	-0.01	18.9	29.6	0.64
320	4.63	0.00	4.63	-0.01	19.6	30.6	0.64
325	4.72	0.00	4.72	-0.01	18.9	29.6	0.64
330	4.80	0.00	4.80	-0.01	19.6	29.6	0.66
335	4.89	0.00	4.89	0.00	18.9	29.6	0.64
340	4.97	0.00	4.97	0.00	19.6	28.6	0.68
345	5.06	0.00	5.06	0.00	19.6	29.6	0.66
350	5.14	0.00	5.14	0.00	18.9	29.6	0.64
355	5.23	0.00	5.23	0.00	19.6	30.6	0.64
360	5.31	0.00	5.31	0.00	18.9	30.6	0.62
365	5.40	0.00	5.40	0.00	18.9	29.6	0.64
370	5.50	0.00	5.50	0.00	18.9	29.6	0.64
375	5.58	0.00	5.58	0.00	19.6	29.6	0.66
380	5.67	0.00	5.66	0.00	19.6	29.6	0.66
385	5.75	0.00	5.75	0.00	19.6	29.6	0.66
390	5.84	0.00	5.84	0.00	19.6	29.6	0.66
395	5.92	0.00	5.92	0.00	18.9	29.6	0.64

Table B20: 2-D Monotonic test on loose sand σ_n = 30 kPa

Date of testing: 7/05/1996
Tested by: Alain Mabia
Type of sample: Loose clean sand
Plate: sand-blasted steel plate
Density: 1.43g/cm3

TIME Sec.	Ux (mm)	Ux2 (mm)	Ux1 (mm)	V (mm)	Tau-x (kPa)	Sig-n (kPa)	T/S
0	0.00	0.01	0.00	0.00	0.0	28.6	0.02
5	0.00	0.00	0.00	0.00	0.7	28.6	0.02
10	0.00	0.00	0.00	0.00	2.0	28.6	0.07
15	0.02	0.01	0.01	-0.01	4.7	28.6	0.16
20	0.04	0.00	0.04	-0.03	6.0	28.6	0.21
25	0.06	0.00	0.06	-0.04	7.4	27.6	0.27
30	0.10	0.01	0.09	-0.05	8.7	27.6	0.31
35	0.14	0.00	0.14	-0.07	8.1	28.6	0.28
40	0.19	0.01	0.18	-0.08	9.4	26.7	0.35
45	0.27	0.00	0.27	-0.09	10.8	27.6	0.39
50	0.29	0.00	0.29	-0.11	10.8	27.6	0.39
55	0.35	0.00	0.35	-0.12	12.1	27.6	0.44
60	0.41	0.00	0.41	-0.13	11.4	28.6	0.40
65	0.48	0.00	0.48	-0.14	12.1	28.6	0.42
70	0.54	0.00	0.54	-0.14	12.8	28.6	0.45
75	0.62	0.00	0.61	-0.15	12.8	28.6	0.45
80	0.68	0.01	0.68	-0.16	13.5	28.6	0.47
85	0.75	0.01	0.74	-0.17	13.5	27.6	0.49
90	0.81	0.00	0.81	-0.17	14.1	28.6	0.49
95	0.89	0.00	0.89	-0.17	14.1	27.6	0.51
100	0.96	0.00	0.96	-0.18	14.8	28.6	0.52
105	1.04	0.00	1.04	-0.18	14.8	28.6	0.52
110	1.13	0.01	1.12	-0.18	15.5	28.6	0.54
115	1.20	0.01	1.20	-0.19	14.8	28.6	0.52
120	1.28	0.00	1.27	-0.18	15.5	27.6	0.56
125	1.34	0.00	1.34	-0.19	14.8	27.6	0.54
130	1.41	0.00	1.41	-0.19	15.5	27.6	0.56
135	1.50	0.00	1.50	-0.19	14.8	27.6	0.54
140	1.57	0.00	1.57	-0.19	15.5	27.6	0.56
145	1.63	0.00	1.63	-0.19	15.5	28.6	0.54
150	1.70	0.00	1.70	-0.20	16.2	27.6	0.59

155	1.78	0.00	1.78	-0.19	15.5	28.6	0.54
160	1.86	0.00	1.86	-0.19	16.2	27.6	0.59
165	1.94	0.00	1.94	-0.19	16.8	27.6	0.61
170	2.02	0.00	2.02	-0.19	16.8	27.6	0.61
175	2.10	0.00	2.10	-0.19	16.8	28.6	0.59
180	2.19	0.00	2.19	-0.20	17.5	27.6	0.63
185	2.27	0.00	2.27	-0.19	17.5	27.6	0.63
190	2.35	0.00	2.35	-0.19	17.5	28.6	0.61
195	2.42	0.00	2.42	-0.19	17.5	28.6	0.61
200	2.50	0.00	2.50	-0.19	17.5	28.6	0.61
205	2.58	0.00	2.58	-0.19	18.2	28.6	0.64
210	2.66	0.00	2.66	-0.19	18.9	28.6	0.66
215	2.75	0.00	2.74	-0.19	18.2	28.6	0.64
220	2.82	0.00	2.82	-0.19	18.2	27.6	0.66
225	2.90	0.00	2.90	-0.19	18.2	28.6	0.64
230	2.98	0.00	2.98	-0.19	18.9	27.6	0.68
235	3.07	0.00	3.06	-0.19	18.2	27.6	0.66
240	3.15	0.00	3.15	-0.19	18.2	28.6	0.64
245	3.24	0.00	3.23	-0.19	18.2	28.6	0.64
250	3.32	0.00	3.32	-0.18	18.2	27.6	0.66
255	3.41	0.00	3.41	-0.18	18.2	28.6	0.64
260	3.49	0.00	3.49	-0.19	18.2	28.6	0.64
265	3.57	0.00	3.57	-0.18	18.2	28.6	0.64
270	3.65	0.00	3.65	-0.18	18.2	28.6	0.64
275	3.74	0.00	3.74	-0.18	18.2	28.6	0.64
280	3.82	0.00	3.82	-0.18	18.2	28.6	0.64
285	3.91	0.00	3.91	-0.18	18.2	28.6	0.64
290	4.00	0.00	3.99	-0.18	16.8	28.6	0.59
295	4.08	0.00	4.08	-0.18	18.2	28.6	0.64
300	4.16	0.00	4.16	-0.18	18.2	27.6	0.66
305	4.25	0.00	4.24	-0.18	18.2	28.6	0.64
310	4.33	0.00	4.33	-0.18	18.2	28.6	0.64
315	4.41	0.00	4.41	-0.18	18.2	27.6	0.66
320	4.50	0.00	4.50	-0.18	17.5	28.6	0.61
325	4.59	0.00	4.59	-0.18	17.5	28.6	0.61
330	4.67	0.00	4.66	-0.18	17.5	29.6	0.59
335	4.75	0.00	4.75	-0.18	18.2	28.6	0.64
340	4.84	0.00	4.84	-0.18	17.5	28.6	0.61
345	4.93	0.00	4.93	-0.18	17.5	29.6	0.59
350	5.01	0.00	5.01	-0.17	17.5	28.6	0.61
355	5.10	0.00	5.10	-0.18	17.5	27.6	0.63
360	5.19	0.00	5.19	-0.18	17.5	28.6	0.61
365	5.28	0.00	5.28	-0.17	16.8	28.6	0.59
370	5.36	0.00	5.36	-0.18	17.5	28.6	0.61
375	5.45	0.00	5.45	-0.18	18.2	28.6	0.64
380	5.53	0.00	5.53	-0.18	17.5	28.6	0.61
385	5.62	0.00	5.62	-0.17	17.5	28.6	0.61
390	5.71	0.00	5.71	-0.18	17.5	29.6	0.59
395	5.79	0.00	5.79	-0.17	18.2	28.6	0.64
400	5.88	0.00	5.88	-0.17	17.5	28.6	0.61

Table B21: 2-D Monotonic test on dense sand σ_n = 40 kPa

Date of testing: 7/05/1996
Tested by: Alain Mabia
Type of sample: Dense clean sand
Plate: sand-blasted steel plate
Density: 1.89 g/cm3

TIME Sec.	Ux (mm)	Ux2 (mm)	Ux1 (mm)	V (mm)	Tau-x (kPa)	Sig-n (kPa)	T/S
0	0.01	0.01	0.00	0.01	1.4	40.4	0.03
5	0.00	0.01	-0.01	0.01	0.7	40.4	0.02
10	0.00	0.01	0.00	0.01	2.7	40.4	0.07
15	0.01	0.01	0.00	0.01	5.4	40.4	0.13
20	0.01	0.01	0.00	0.01	8.1	40.4	0.20
25	0.03	0.01	0.01	0.01	10.8	40.4	0.27
30	0.04	0.01	0.04	0.01	12.1	40.4	0.30
35	0.07	0.01	0.06	0.01	15.5	40.4	0.38
40	0.09	0.01	0.09	0.01	18.2	40.4	0.45
45	0.12	0.01	0.11	0.01	19.5	40.4	0.48
50	0.15	0.01	0.14	0.01	20.9	41.4	0.50
55	0.17	0.01	0.16	0.01	22.2	40.4	0.55
60	0.25	0.01	0.24	0.01	22.9	40.4	0.57
65	0.25	0.01	0.24	0.01	24.9	42.4	0.59
70	0.27	0.01	0.26	0.01	24.9	42.4	0.59
75	0.31	0.01	0.30	0.01	26.3	41.4	0.63
80	0.35	0.01	0.35	0.01	27.0	42.4	0.64
85	0.38	0.01	0.37	0.01	27.0	42.4	0.64
90	0.43	0.01	0.42	0.01	27.6	42.4	0.65
95	0.47	0.01	0.46	0.01	29.0	42.4	0.68
100	0.52	0.01	0.52	0.01	29.7	43.4	0.68
105	0.57	0.01	0.56	0.01	29.7	42.4	0.70
110	0.62	0.01	0.61	0.01	30.3	43.4	0.70
115	0.68	0.01	0.67	0.01	30.3	42.4	0.71
120	0.73	0.00	0.73	0.01	31.7	43.4	0.73
125	0.80	0.00	0.80	0.01	31.7	42.4	0.75
130	0.87	0.00	0.87	0.01	32.3	42.4	0.76
135	0.95	0.00	0.95	0.01	32.3	43.4	0.74
140	1.03	0.00	1.03	0.01	32.3	43.4	0.74
145	1.11	0.00	1.10	0.01	33.0	43.4	0.76
150	1.19	0.00	1.19	0.01	33.0	42.4	0.78

155	1.27	0.00	1.27	0.01	33.0	43.4	0.76
160	1.36	0.00	1.36	0.01	33.0	43.4	0.76
165	1.44	0.00	1.44	0.01	32.3	42.4	0.76
170	1.53	0.00	1.53	0.01	32.3	43.4	0.74
175	1.61	0.00	1.61	0.01	32.3	42.4	0.76
180	1.69	0.00	1.69	0.01	32.3	43.4	0.74
185	1.79	0.00	1.78	0.01	31.7	43.4	0.73
190	1.87	0.00	1.87	0.01	31.7	43.4	0.73
195	1.96	0.00	1.95	0.01	31.7	42.4	0.75
200	2.04	0.00	2.04	0.01	31.7	43.4	0.73
205	2.13	0.00	2.13	0.01	31.0	43.4	0.71
210	2.22	0.00	2.21	0.01	31.7	43.4	0.73
215	2.30	0.00	2.30	0.01	30.3	43.4	0.70
220	2.39	0.00	2.39	0.01	31.0	43.4	0.71
225	2.48	0.00	2.48	0.01	29.7	43.4	0.68
230	2.57	0.00	2.57	0.01	30.3	43.4	0.70
235	2.65	0.00	2.65	0.01	29.7	43.4	0.68
240	2.74	0.00	2.74	0.01	30.3	43.4	0.70
245	2.83	0.00	2.83	0.01	29.7	42.4	0.70
250	2.92	0.00	2.91	0.01	29.7	42.4	0.70
255	3.00	0.00	3.00	0.01	29.0	44.4	0.65
260	3.10	0.00	3.10	0.01	29.0	43.4	0.67
265	3.18	0.00	3.18	0.01	29.0	43.4	0.67
270	3.27	0.00	3.27	0.01	29.0	43.4	0.67
275	3.36	0.00	3.35	0.01	29.0	43.4	0.67
280	3.44	0.00	3.44	0.01	29.0	42.4	0.68
285	3.53	0.01	3.52	0.01	29.7	43.4	0.68
290	3.61	0.00	3.61	0.01	29.0	43.4	0.67
295	3.71	0.00	3.70	0.01	28.3	43.4	0.65
300	3.79	0.00	3.79	0.01	28.3	43.4	0.65
305	3.89	0.00	3.88	0.01	28.3	43.4	0.65
310	3.97	0.00	3.97	0.01	29.0	43.4	0.67
315	4.07	0.00	4.07	0.01	27.0	42.4	0.64
320	4.15	0.00	4.15	0.01	27.6	43.4	0.64
325	4.24	0.00	4.24	0.01	27.6	44.4	0.62
330	4.33	0.00	4.32	0.01	27.6	44.4	0.62
335	4.41	0.00	4.41	0.01	27.6	43.4	0.64
340	4.50	0.00	4.50	0.01	27.6	43.4	0.64
345	4.58	0.00	4.58	0.01	27.6	43.4	0.64
350	4.67	0.00	4.67	0.01	27.6	43.4	0.64
355	4.76	0.00	4.75	0.01	27.6	43.4	0.64
360	4.85	0.00	4.85	0.01	28.3	44.4	0.64
365	4.93	0.00	4.93	0.01	28.3	44.4	0.64
370	5.03	0.00	5.02	0.01	28.3	44.4	0.64
375	5.11	0.00	5.11	0.01	27.6	44.4	0.62
380	5.20	0.00	5.20	0.01	28.3	44.4	0.64
385	5.29	0.00	5.29	0.01	27.6	43.4	0.64
390	5.38	0.00	5.38	0.01	27.6	44.4	0.62
395	5.47	0.00	5.47	0.01	27.6	44.4	0.62
400	5.55	0.00	5.55	0.01	27.6	43.4	0.64

405	5.64	0.00	5.64	0.01	27.0	44.4	0.61
410	5.73	0.00	5.73	0.01	27.0	44.4	0.61
415	5.82	0.00	5.81	0.01	27.6	44.4	0.62
420	5.91	0.00	5.91	0.01	27.0	44.4	0.61

Table B22: 2-D Monotonic test on loose sand σ_n = 40 kPa

Date of testing: 26/04/1996
Tested by: Alain Mabia
Type of sample: Loose clean sand
Plate: sand-blasted steel plate
Density = 1.445 g/cm^3

TIME Sec.	Ux (mm)	Ux2 (mm)	Ux1 (mm)	V (mm)	Tau-x (kPa)	Sig-n (kPa)	T/S
0	0.00	0.01	0.00	0.00	0.0	41.4	0.00
5	0.01	0.00	0.00	0.00	2.7	41.4	0.07
10	0.01	0.00	0.01	0.00	6.8	40.4	0.17
15	0.05	0.01	0.04	-0.02	8.8	40.4	0.22
20	0.09	0.00	0.08	-0.03	10.8	40.4	0.27
25	0.13	0.00	0.12	-0.04	12.9	40.4	0.32
30	0.17	0.01	0.16	-0.05	12.9	40.4	0.32
35	0.23	0.01	0.22	-0.07	14.2	40.4	0.35
40	0.29	0.01	0.28	-0.08	16.2	40.4	0.40
45	0.36	0.00	0.35	-0.09	17.6	40.4	0.44
50	0.42	0.01	0.42	-0.10	18.3	41.4	0.44
55	0.50	0.00	0.49	-0.11	18.9	39.5	0.48
60	0.57	0.01	0.57	-0.12	19.6	40.4	0.48
65	0.65	0.00	0.65	-0.13	20.3	39.5	0.51
70	0.73	0.00	0.73	-0.13	21.0	39.5	0.53
75	0.82	0.00	0.81	-0.13	21.0	40.4	0.52
80	0.89	0.00	0.89	-0.14	21.0	40.4	0.52
85	0.97	0.01	0.96	-0.14	21.6	40.4	0.53
90	1.05	0.01	1.04	-0.14	23.0	39.5	0.58
95	1.13	0.01	1.12	-0.14	23.0	41.4	0.56
100	1.21	0.01	1.20	-0.14	23.7	40.4	0.59
105	1.29	0.00	1.28	-0.14	23.0	41.4	0.56
110	1.38	0.01	1.37	-0.15	23.0	40.4	0.57
115	1.46	0.00	1.46	-0.14	23.7	39.5	0.60
120	1.54	0.00	1.54	-0.14	24.3	40.4	0.60
125	1.63	0.00	1.63	-0.15	25.0	39.5	0.63
130	1.71	0.00	1.71	-0.15	25.0	39.5	0.63
135	1.80	0.00	1.80	-0.14	25.7	40.4	0.64
140	1.88	0.00	1.88	-0.14	25.7	40.4	0.64
145	1.96	0.00	1.96	-0.14	25.7	39.5	0.65
150	2.05	0.00	2.05	-0.14	25.7	39.5	0.65

155	2.13	0.00	2.13	-0.14	26.4	39.5	0.67
160	2.22	0.00	2.22	-0.14	25.7	39.5	0.65
165	2.30	0.00	2.30	-0.14	27.0	40.4	0.67
170	2.39	0.00	2.38	-0.14	25.7	40.4	0.64
175	2.48	0.00	2.47	-0.14	25.7	40.4	0.64
180	2.56	0.00	2.56	-0.14	26.4	40.4	0.65
185	2.65	0.00	2.65	-0.13	26.4	40.4	0.65
190	2.74	0.00	2.74	-0.13	26.4	40.4	0.65
195	2.83	0.00	2.82	-0.13	26.4	40.4	0.65
200	2.91	0.00	2.91	-0.13	26.4	40.4	0.65
205	2.99	0.00	2.99	-0.13	26.4	40.4	0.65
210	3.08	0.00	3.08	-0.13	25.7	40.4	0.64
215	3.17	0.00	3.17	-0.13	26.4	41.4	0.64
220	3.26	0.00	3.25	-0.12	25.7	39.5	0.65
225	3.35	0.00	3.35	-0.12	26.4	41.4	0.64
230	3.43	0.00	3.43	-0.12	26.4	41.4	0.64
235	3.52	0.00	3.52	-0.12	26.4	40.4	0.65
240	3.61	0.00	3.61	-0.12	25.7	41.4	0.62
245	3.70	0.00	3.70	-0.12	25.7	40.4	0.64
250	3.79	0.00	3.78	-0.12	25.0	40.4	0.62
255	3.88	0.00	3.88	-0.12	25.0	40.4	0.62
260	3.96	0.00	3.96	-0.11	25.7	40.4	0.64
265	4.04	0.00	4.04	-0.12	26.4	40.4	0.65
270	4.13	0.00	4.13	-0.12	25.0	40.4	0.62
275	4.22	0.00	4.22	-0.11	25.7	39.5	0.65
280	4.31	0.00	4.30	-0.12	25.7	40.4	0.64
285	4.40	0.00	4.39	-0.11	25.0	41.4	0.60
290	4.48	0.00	4.48	-0.11	25.7	40.4	0.64
295	4.57	0.00	4.57	-0.11	26.4	40.4	0.65
300	4.66	0.00	4.66	-0.11	25.7	41.4	0.62
305	4.71	0.00	4.70	-0.11	26.4	40.4	0.65
310	4.84	0.00	4.84	-0.11	25.0	41.4	0.60
315	4.93	0.00	4.93	-0.11	25.0	41.4	0.60
320	5.01	0.00	5.00	-0.11	25.0	40.4	0.62
325	5.09	0.00	5.09	-0.11	25.7	41.4	0.62
330	5.18	0.00	5.18	-0.11	25.7	41.4	0.62
335	5.26	0.00	5.26	-0.11	25.0	41.4	0.60
340	5.35	0.00	5.35	-0.11	25.7	39.5	0.65
345	5.44	0.00	5.44	-0.11	25.7	40.4	0.64
350	5.53	0.00	5.53	-0.11	25.0	41.4	0.60
355	5.62	0.00	5.62	-0.11	25.7	41.4	0.62
360	5.71	0.00	5.71	-0.11	25.0	41.4	0.60
365	5.80	0.00	5.80	-0.11	25.0	40.4	0.62
370	5.89	0.00	5.89	-0.11	25.0	41.4	0.60
375	5.97	0.00	5.97	-0.11	25.7	40.4	0.64

APPENDIX C

OIL MIGRATION RESULTS

Table C1: Data collected before the soil was fully contaminated.

Date	initial reservoir level (ml)	final reservoir level (ml)	amount of oil added (ml)	water collected (ml)	distance traveled (cm)	Time (days)	Average velocity (cm/day)
19/08/94	640	640	0	0	0	0	0.0
23/08/94	640	291	349	0	14	4	3.5
24/08/94	291	251	40	0	28	5	5.6
25/08/94	251	194	57	5	31	6	5.2
26/08/94	194	121	73	15	33.2	7	4.7
29/08/94	640	426	214	20	38.2	10	3.8
30/08/94	426	365	61	55	52.4	11	4.8
31/08/94	365	296	69	15	55.8	12	4.7
1/9/94	296	229	67	15	59.2	13	4.6
2/9/94	229	174	55	20	62.6	14	4.5
3/9/94	644	518	126	15	65.3	15	4.4
4/9/94	518	456	62	20	69.4	16	4.3
6/9/94	456	342	113	15	73.3	18	4.1
7/9/94	342	288	54	30	79.4	19	4.2
9/9/94	288	181	107	20	82.4	21	3.9
10/9/94	640	564	77	15	88.9	22	4.0
12/9/94	564	456	108	25	92.4	24	3.9
13/9/1994	456	410	46	15	97.5	25	3.9
14/9/1994	410	359	51	15	100.1	26	3.9
15/9/1994	359	315	44	10	102.5	27	3.8
19/9/1994	315	102	213	50	104.9	31	3.4
20/9/1994	640	604	36	10	114.4	32	3.6
22/9/1994	604	509	95	20	116	34	3.4
25/9/1994	509	356	153	45	120.5	37	3.3
27/9/1994	356	275	81	15	127	39	3.3
28/9/1994	275	238	38	10	131	40	3.3
3/10/94	238	37	201	50	133.1	45	3.0
10/10/94	640	383	257	45	142.9	52	2.7
20/10/1994	383	53	330	65	157	62	2.5
24/10/1994	640	514	126	20	171	72	2.4
31/10/94	514	342	172	20	180.7	76	2.4
6/11/94	342	184	158	15	198.7	83	2.4
15/11/1994	184	22	162	25	209	89	2.3
					245	98	2.5

Table C2: Data collected after the soil was fully contaminated.

Date	Water-oil-Soil (ml)	Reservoir level (div)	Oil added (ml)
28/12/94	90	40	601.4
2/1/95	100	600	0
3/1/95	120	595	0
10/1/95	130	524	0
13/1/1995	135	487	0
14/1/1995	135	479	0
17/1/1995	145	448	0
19/1/1995	150	442	0
21/1/1995	155	416	0
23/1/1995	160	400	0
23/1/1995	170	380	0
26/1/1995	175	340	0
28/1/1995	180	320	0
2/2/95	200	270	0
6/2/95	205	224	0
7/2/95	210	216	0
9/2/95	220	200	0
14/2/1995	220	170	0
20/2/1995	220	86	0
24/2/1995	230	48	593.64
3/3/95	235	646	0
9/3/95	250	584	0
16/3/1995	250	508	0
6/4/95	250	210	0
8/4/95	250	175	0
16/4/1995	250	60	0
19/4/1995	250	18	0
28/4/1995	250	0	0

Note: 1 div = 0.97 ml

APPENDIX D

RESULTS OF THE TOTAL HEAD DISTRIBUTIONS USING THE FINITE ELEMENT METHOD

```
2-D POTENTIAL DISTRIBUTION IN THE J-TUBE
1,14,12,0,4,2.E-2,2.E-2
1,0.,171.
? 0.,136.8
  J.,102.6
4,0.,68.4
5,0.,0.
6,23.7,0.
7,47.3,0.
8,71.0,0.
9,5.022,171.
10,5.022,136.8
11,5.022,102.6
12,5.022,68.4
13,47.3,5.022
14,71.,5.022
1,2,9,1
2,2,10,9
3,3,10,2
4,3,11,10
5,4,11,3
6,4,12,11
7,5,12,4
8,5,6,12
9,6,13,12
10,6,7,13
11,7,14,13
12,7,8,14
1,191.24
1. 191.24
13,140.4
14,140.4
```

-D POTENTIAL DISTRIBUTION IN THE J-TUBE

PXX = .0

PYY = .0

NEL	NODE NUMBER			X(1)	Y(1)	X(2)	Y(2)	X(3)	Y(3)
1	2	9	1	.00	136.80	5.02	171.00	.00	171.00
2	2	10	9	.00	136.80	5.02	136.80	5.02	171.00
3	3	10	2	.00	102.60	5.02	136.80	.00	136.80
4	3	11	10	.00	102.60	5.02	102.60	5.02	136.80
5	4	11	3	.00	68.40	5.02	102.60	.00	102.60
6	4	12	11	.00	68.40	5.02	68.40	5.02	102.60
7	5	12	4	.00	.00	5.02	68.40	.00	68.40
8	5	6	12	.00	.00	23.70	.00	5.02	68.40
9	6	13	12	23.70	.00	47.30	5.02	5.02	68.40
10	6	7	13	23.70	.00	47.30	.00	47.30	5.02
11	7	14	13	47.30	.00	71.00	5.02	47.30	5.02
12	7	8	14	47.30	.00	71.00	.00	71.00	5.02

PRESCRIBED NODAL VALUES

1	.19124E+03
9	.19124E+03
13	.14040E+03
14	.14040E+03

NODAL VALUES, LOADING CASE 1

1	.19124E+03	2	.17679E+03	3	.16233E+03	4	.14792E+03
5	.14251E+03	6	.14186E+03	7	.14043E+03	8	.14040E+03
9	.19124E+03	10	.17679E+03	11	.16233E+03	12	.14783E+03
13	.14040E+03	14	.14040E+03				

RESULTANT NODAL VALUES

1	.19124E+03
2	.17679E+03
3	.16233E+03
4	.14792E+03
5	.14251E+03
6	.14186E+03
7	.14043E+03
8	.14040E+03
9	.19124E+03
10	.17679E+03
11	.16233E+03
12	.14783E+03
13	.14040E+03
14	.00000E+00

TEST TARGET (QA-3)

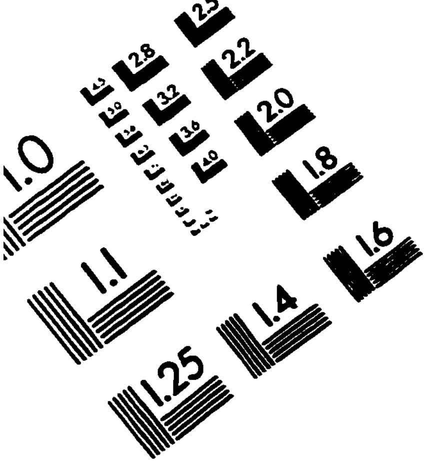

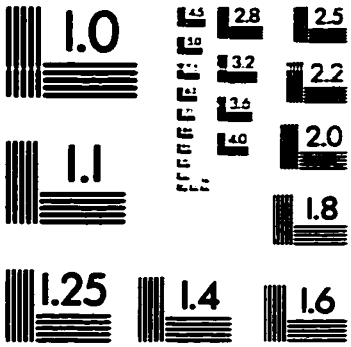

150mm

6"

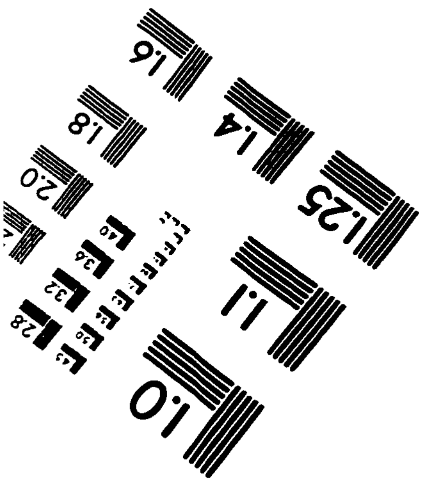

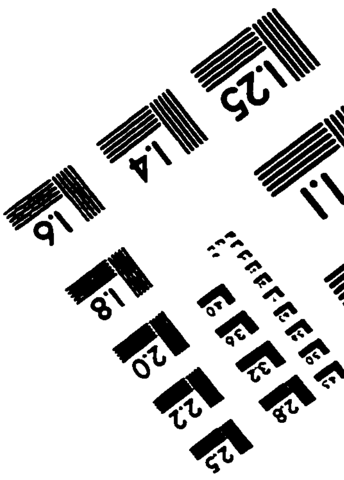

APPLIED IMAGE . Inc
1653 East Main Street
Rochester, NY 14609 USA
Phone: 716/482-0300
Fax: 716/288-5989

© 1993, Applied Image, Inc., All Rights Reserved